Kinetics, Synthesis and Characterization of copolymers containing the bio-renewable monomer γ-methyl-α-methylene-γ-butyrolactone (MeMBL)

By

Robert Alexander Dwight Cockburn

A thesis submitted to the Department of Chemical Engineering
in conformity with the requirements for
the degree of Master of Applied Science

Queen's University
Kingston, Ontario, Canada
April 2011

Abstract

The bio-renewable monomer γ-methyl-α-methylene-γ-butyrolactone (MeMBL) has been thoroughly investigated in this thesis. MeMBL is a relatively unstudied monomer that had received little attention since the early 1980's but has become a subject of renewed interest since a process to produce it from biomass derivatives was developed in 2004. The principle interest with this monomer aside from the "green" potential associated with bio-renewables results from its structure being cyclically analogous to methyl methacrylate (MMA) as well as improved solvent resistance and a high (215^{o}C+) glass transition temperature (T_g) compared to most petroleum sourced acrylics.

There are three major areas of focus in this work, examining polymerization kinetics, synthesis and polymer characterization. The polymerization kinetics of MeMBL were investigated with a variety of petroleum sourced monomers. MeMBL is in all cases preferentially incorporated into copolymers, presenting challenges for composition control. Preliminary investigations of aqueous phase polymerizations of MeMBL were problematic and led to investigations of organic phase polymerizations. The dispersion polymerization method was used to produce copolymers of MeMBL and MMA; during the study we obtained new insight into the mechanisms of particle nucleation and growth. With the acquired knowledge of MeMBL polymerization kinetics, the dispersion technique was used to produce MeMBL/MMA copolymers of controlled composition by semibatch for characterization studies. The addition of MeMBL raises polymer T_g and lowers molecular weight, but due to unexpected difficulties in processing MeMBL copolymers, mechanical properties could not be investigated in this study. Future work may need to revisit other polymerization techniques in order to produce processable polymers to test whether or not MeMBL might be a suitable alternative to petroleum sourced monomers that is capable of extending the range and utility of acrylics.

Acknowledgements

I would like to express my gratitude to my supervisors Dr. Robin Hutchinson and Dr. Timothy McKenna. Without their guidance, enthusiasm and support, this work would not have been possible. I am especially thankful for the wonderful experience of attending the 10th International Workshop on Polymer Reaction Engineering in Hamburg Germany in fall 2010 that they made possible. Their supervision has helped me grow as a researcher and professional.

To my labmates, whose ideas, discussions and assistance have made the lab a great place to conduct research and Kingston a fun place to live over past two years – thank you.

I should also thank my family and friends, whose support, patience and wisdom have helped to educate me throughout my nearly 7 years at Queen's and in Kingston. I have grown much as a person, son, brother and friend because of all of you.

Last but certainly not least, I would also like to thank my wife Jessica for her unconditional and unyielding support and love. Despite all of the fun we have had as students at Queen's, I know we look forward to the day when can both stop paying tuition. If I accomplished nothing else in all of my time at university, finding you has made it worthwhile.

Table of Contents

List of Tables

List of Figures

Chapter 1

Introduction, Background and Literature Review

1.1 Introduction

1.1.1 Motivation

Bio-renewable products are of increasing importance in an era of volatile oil prices and environmental consciousness. Few plant-derived plastics are currently available commercially due to their relatively high cost compared to petroleum analogues.[1] With some researchers suggesting that petroleum resources will be vastly depleted by the end of this century[2] plant derived oils, fats and sugars are likely to be a more economical alternative. Converting processes from fossil fuel to bio-renewable feed stocks is a means of promoting sustainable development and minimizing greenhouse gas emissions;[3] In future, it will be a necessity for the chemical industries who rely primarily on petroleum feed stocks.[1] As such, a variety of new processes utilizing biomass as a feed stock are gaining interest within the chemical industry.[1, 3-5] As will be described in detail in this thesis, one of these biomass utilizing processes[5] is capable of producing a monomer, γ-methyl-α-methylene-γ-butyrolactone (MeMBL), that is a cyclic analogue to Methyl Methacrylate (MMA), a key component in the production of acrylic glasses and as a component of paints and coatings that is currently derived from petrochemical sources.[5-9] Little is known in the open literature about MeMBL, but preliminary studies of it and similar monomers in the early 1980's showed that it may be well suited for similar applications to MMA.[6-11]

The three primary goals of this thesis are related. In order to be able to produce homopolymers and copolymers of MeMBL with well-defined characteristics and tailored physical properties, an improved understanding of its free radical polymerization kinetics is essential. The first aim is to examine the reaction kinetics of MeMBL copolymerizations with petroleum based monomers commonly used in industry (Chapter 2). The next goal sees the development of methods capable of producing MeMBL copolymers and thoroughly investigates the dispersion polymerization process, paying particular attention to particle nucleation mechanisms (Chapter 3). The final objective of this thesis is to produce copolymers of controlled composition and investigate their physical properties to quantify the effects of MeMBL incorporation on MMA based polymers (Chapter 4). Taken together, this thesis aims to test the hypothesis that MeMBL is a bio-renewable monomer that may displace some volume of and extend the operating range and utility of MMA based polymers such as Lucite® and Plexiglas® with potential applications in medical technologies including implants as well as an impact resistant substitute for glass .[12, 13]

1.1.2 A history of Gamma Lactones and background to MeMBL

Lactones are a class of cyclic esters found commonly in plants in nature.[6, 7, 14-17] They are colourless, bitter relatively stable lypophylic constituents that often evoke allergic reactions in humans and are derived chiefly from the *Compositae* (sunflower) and to a lesser extent, *Liliaceae* (Lilly) families of plants.[16] The largest concentrations (0.001-5wt% depending on plant species) of lactones is found in the leaves and flowering heads (phylleries) of plants.[16] Lactones are classified based on the size of their carbocyclic skeleton with prefixes denoting the number of carbons in the ring structure; alpha-lactone (3 carbon), beta-lactone (4 carbon), gamma-lactone (5 carbon) and delta-lactone (6 carbon) are common. Due to their 5 membered structure, which optimizes the bond angles of the ring to their lowest energy orientations, the most stable are gamma-lactones.[18] More complex sesquiterpene lactones incorporate long carbon chains and

ring structures as they commonly build off of the basic α,β-unsaturated lactone structure.[16] Sesquiterpene lactones first generated significant scientific interest owing to their demonstrated cytotoxicity and tumor inhibitory properties;[6, 14-17, 19] a study of 50 compounds conducted in 1969 found that all contained a lactone functional group and further, that all but one was α,β-unsaturated with an exocyclic ethelyenic linkage at the α position in every case.[20] The structure found in all of the cytotoxic sesquiterpenes was identified as early as 1946 and is known as α-methylene γ-butyrolactone, α-MBL.[19] This compound, seen in Figure 1-1, and also known as Tulipalin-A, is the simplest member of a family of naturally occurring gamma-lactones, so named as it is easily isolated from the common tulip, *Tulipa Gesneriania L* (a member of the genus *Tulipa*, belonging to the *Liliaceae* family).[4, 6] Independently from other sesquiterpene lactones, α-MBL received much attention since its simple stereochemistry and functionality were thought to reduce its biological toxicity.[17] The compound is cytotoxic to both gram negative and gram positive bacteria. Its cytotoxicity towards certain types of cells is based on its ability to act as a cysteine scavenger by 1,4 addition to the SH group of L-cysteine.[19, 21] Thus, the first major medical application for α-MBL containing sesquiterpene lactones was as a chemotherapeutic agent potentially useful in the treatment of Leukemia (as lymphoblastic leukemia cells have an absolute requirement for L-cysteine whereas non cancerous cells can form this compound from precursors).[14, 15, 17] A search of more recent literature reveals that drugs containing α-MBL functionality continue to be investigated and used for chemotherapeutic purposes.

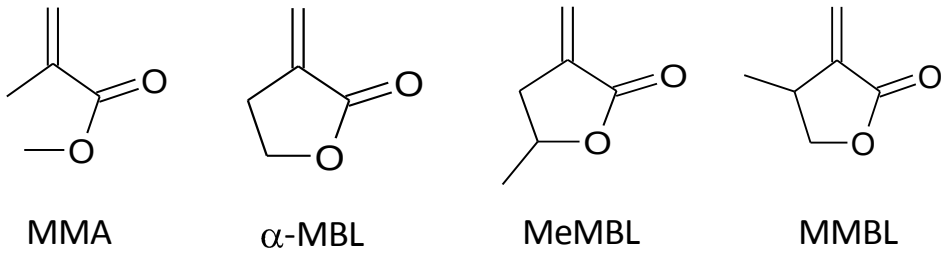

Figure 1-1 - The structures of MMA and gamma lactone monomers α-MBL, MeMBL and MMBL. α -MBL is a cyclic analogue to MMA, while MeMBL and MMBL differ from α -MBL only by the positioning of their exocyclic methylene groups

Although α-MBL was originally studied for medicinal purposes, its structure was also identified as being cyclically analogous to that of the methyl methacrylate (MMA) monomer and thus this chemical also gained the interest of polymer scientists. α-MBL and two other similar monomers MeMBL and β-methyl-α-methylene-γ-butyrolactone (MMBL) are shown in Figure 1-1. The free-radical polymerization behaviour of α-MBL, MeMBL and other gamma lactone monomers was compared to that of MMA in the late 1970s and early 1980s.[6-11] Since the interest of polymer chemists was specific to the α-MBL functionality and not the broader range of naturally derived sesquiterpene lactones, it was during the same period that methods to synthetically prepare these monomers were refined.[22, 23] Typical reaction schemes for the production of α-MBL and MeMBL are shown in Figure 1-2 and Figure 1-3. The reaction scheme for the preparation of α-MBL is much less complex than that of MeMBL, with commercially available γ-butyrolactone used as the starting material. The reaction presented in Figure 1-2 results in yields of less than 60% and takes at least 8 hours to complete. Further specifics (originally developed by Ksander et al.[22]) are succinctly summarized by Akkapeddi.[6] The first study of MeMBL polymerization by Suenaga[8] used a method developed by Martin and Stille[23] to produce their monomer. The process was slow, with the palladium catalyzed step alone taking 2 days for a final yield of 88%.

The other steps used extreme temperatures and hazardous grignard type reactions, the details of which can be found in Martin and Stille.[23]

The monomers thus synthesized were polymerized by a variety of techniques; α-MBL by free radical polymerization in bulk and by solution in DMF and DMSO as well as by anionic polymerization.[6, 7] MeMBL was polymerized anionically, in bulk and in benzene.[8] The α-MBL homopolymer was found to have a significantly higher glass transition temperature than pMMA (T_g of 195 vs. 105 °C), and the related MeMBL monomer produced a polymer with an even higher T_g of 210-220 °C.[6, 8, 11] The enhanced structural rigidity of the polymers due to the ring structure found in the gamma lactone precursors is thought to be the principle reason for the drastic change in T_g.[6, 8] Polymer specimens moulded above these temperatures were clear, hard and brittle with improved solvent resistance, being soluble only in polar aprotic solvents such as DMF and DMSO.[5-9, 11] The physical properties of α-MBL determined by Akkapeddi (tensile strength of 62.7 KPa, elongation of 6.5% and tensile modulus of 2GPa) are close to typical values for MMA polymers. Thus, the evaluated properties of the gamma lactones suggest their polymers may be well suited for a variety of uses, including thermoplastic toughening, dental resins, acrylic glasses and coatings.[12, 24]

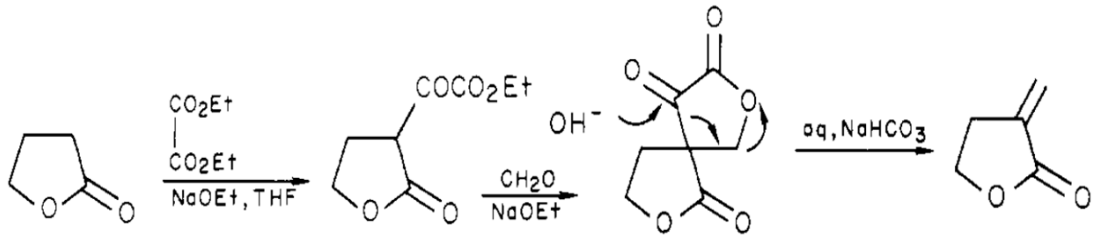

Figure 1-2 – Reaction Schemes for the production of Gamma Lactone monomers: α-MBL from Ksander et al.[22]

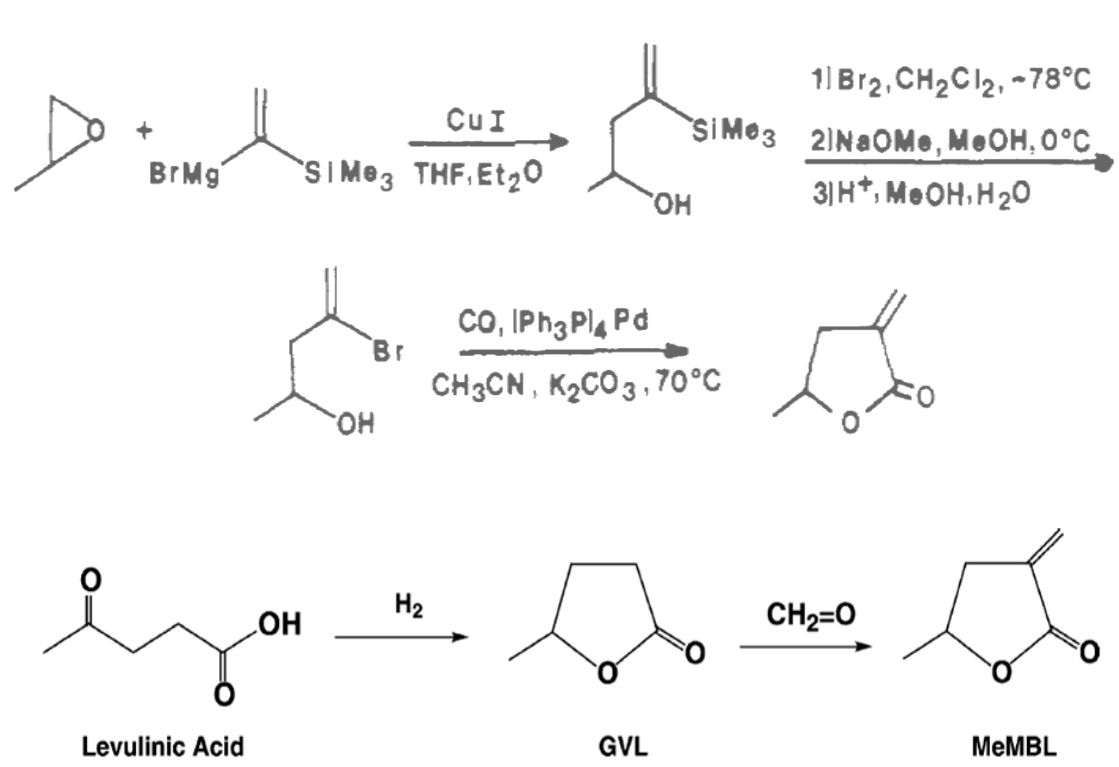

Figure 1-3 – Reaction Schemes for the production of Gamma Lactone monomers: MeMBL from Martin and Stille.[23] (top) compared to the recent catalytic process developed for DuPont by Manzer[5] (bottom).

During the same period as gamma lactone homopolymers were first studied, some copolymers of α-MBL with styrene (ST) and MMA were also investigated.[7, 11] However, little further research on the α-MBL family of monomers took place for a period of about twenty years, largely due to the lack of a large scale and low cost method to synthesize the lactones. More recently, DuPont has developed a potentially commercially viable synthesis technique for the production of MeMBL by a catalytic, two-step process from levulinic acid, a chemical intermediate derived from cellulosic biomass.[5] This process, shown also in Figure 1-3, is much simpler than the method developed by Martin and Stille[23] for the production of the MeMBL monomer. Conversion of levulinic acid to the intermediate, γ-valerolactone (GVL) was accomplished using a 5% Ruthenium (on a carbon support) catalyst with 500 psi (gauge) H_2 for 4 hours, resulting in

near 100% conversion with 97% selectivity for GVL. [5] Barium acetate catalysts were used to react a 37 wt% solution of formalin in water with desired molar ratios of GVL (necessary to prevent reactions of these intermediates) at 340^{o}C, resulting in highly selective MeMBL production (95%) in process that can be run nearly continuously.[5] The process is not fully continuous as it requires a Nitrogen (or air) regeneration cycle at reaction temperature to restore catalyst activity and remove high boiling organics which build up on the catalyst over the course of a reaction. The major impurities include ring opening byproducts of GVL and MeMBL (<2%) and the isomer of MeMBL, which has isomerized the exocyclic double bond internally (double bond is in ring structure and 2 exocyclic methylene groups). The isomer of MeMBL is the thermodynamically favoured product but reaction kinetics dictate which is formed and can be tailored to ensure MeMBL production.[5] The key points are that this process to produce MeMBL avoids the costly raw materials and time-consuming methods used previously[22, 23, 25, 26] that resulted in lower yields, and generates a monomer produced from a bio-renewable source. [5] Further details on DuPont's catalytic production of MeMBL can be found in Manzer et al.[5]

1.1.3 Bio-renewables in Polymer Science

Before the 20th century, most materials were produced from bio-based or inorganic (i.e. metal) materials. Beginning with the industrial revolution, society has developed a reliance on coal, and later oil and natural gas; non-renewable resources.[27, 28] As the developing world rapidly grows in affluence and develops tastes for the same quality and standard of living available to a minority of people in developed nations, the demand in energy is expected to increase by 50% by 2025.[28] Since increasing demands for a finite resource cannot be sustainable, it is imperative that the transition from non-renewable to renewable carbon resources be prepared for. Reliance on fossil fuels is inherently unsustainable as those reserves have taken millions of years to form. A sustainable chemical industry requires that the timescale of feedstock formation match that of

chemical utilization.[27] Scientific interest in renewables was initially sparked by the oil crisis in the 1970s and has since developed into its own field of research.[28] Processes that utilize biomass feedstocks are increasingly of interest[1, 3, 4] as "greener" alternatives are sought as a means to curb the effects of volatile oil prices and greenhouse gas emissions in an era of increased environmental consciousness.[28] Unlike energy production, which has non carbon based alternatives such as nuclear, wind and solar, the development of sustainable alternatives for the modern chemical industry is very much limited by the intrinsic requirement for carbon. Thus, biomass, with its short formation time, must become the feedstock of choice for the industry.[27] Biomass refers to both waste and purpose-grown plant and animal matter that can be converted directly to energy (heat or electricity) or used in the production of bio-fuels, fibres and chemicals. Biomass is widely available and is a relatively inexpensive, sustainable alternative to fossil fuels.[1, 3, 27-29] In addition to biomass, other prevalent renewable feed stocks from purpose grown crops include plant oils, sugars and polysaccharides (mostly cellulose and starch).[3]

Currently, plant oils are among the most widely used renewable resources, having been already used for decades in paint and coatings formulations (notably pioneered by the Glidden company)[30] and flooring materials (such as linoleum, derived from linseed oil as early as 1864)[3]. The term plant/vegetable oil refers to room temperature liquids chiefly composed of triglycerides (long chain fatty acid triesters of glycerol) derived from plant sources.[31] Notable oils that commonly are discussed for their potential in a variety of applications include rapeseed oil (canola), soyabean oil and palm oil, all of which are rich in one or more of the most desirable types of long chain fatty acids (oleic acid, linoleic acid, erucic acid, lauric acid; the composition of the fatty acid chain varies according to crop, growing conditions and season).[3, 31] Plant oils make up 80% of global renewable fats and oils, a percentage that is increasing yearly at the expense of fats and oils of animal origin. Of all plant oils, soybean oil is the most prevalent and

accounts for about 25% of all vegetable oils, followed closely by palm oil.[31, 32] The applications of oils as renewable fuel sources, such as through conversion to bio-diesel, is a major field of research at present.[33] However, polymeric applications of these unprocessed long chain fatty oils is mostly limited to direct crosslinking for applications in coatings and resins.[3]

In order to make an impact to polymer science, more specialized and refined chemical structures than simply extracted long chain fatty acids are required. An interesting point to consider when looking at many modern chemical products is that they have been developed almost by accident, in the sense that there was no pre-identification of a target molecule. Rather, new chemical processes were developed based on "platform" chemicals and the products thus created were explored and marketed based on their properties, further driving the expansion of the chemical industry.[27] The concept of the platform chemical has been the driving source of efficiency in the modern chemical industry.[27, 29] Petrochemical refineries produce mostly fuels, with only about 5% of total outputs going to chemical products.[28] However, the processes that have been developed over the last century (catalytic and thermal cracking, reforming etc) have been tailored to produce ethylene, propylene and benzene above all other chemicals. By processes such as oxidation, alkylation and oligomerization, those three platform chemicals can be transformed into a majority of all of the chemicals used today.[27] An example of the range of products possible from the benzene platform chemical is seen in Figure 1-4.

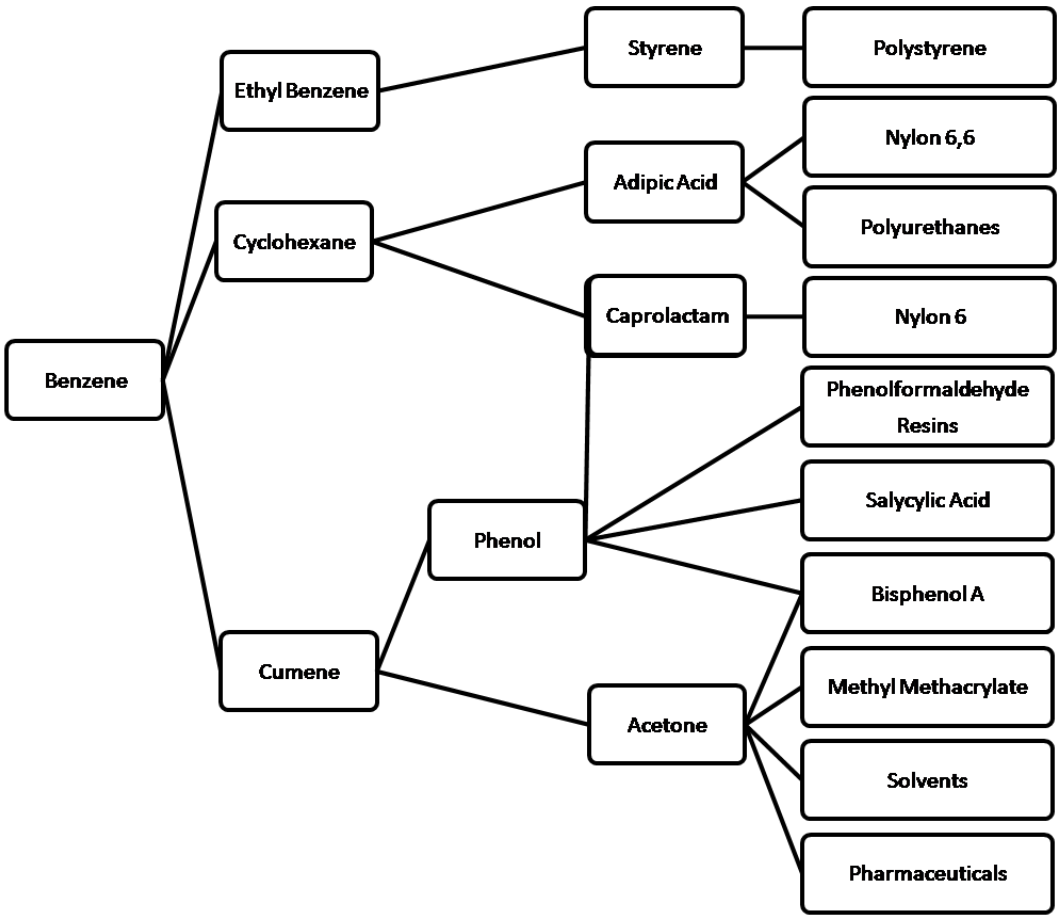

Figure 1-4 – Industrial chemicals produced from the platform chemical benzene. Adapted from Werpy and Peterson.[29]

In order to be efficient, cost effective and successful, the development of bio-based fuels and chemicals may in fact model that of the chemical industry by locating production at bio-refineries, analogous to petrochemical refineries.[27-29] A bio-refinery would take renewable raw materials, and through an array of processes (such as the fermentation of sugars) convert them to a mixture of platform biochemicals, biofuels and energy.[27-29] Potential platform bio-chemicals, shown in Figure 1-5 as adapted from Werpy and Peterson[29] include levulinic acid, the building block used in DuPont's synthesis of MeMBL.[5] In addition to the challenges of developing the industry required to produce them in meaningful quantities, the introduction of bio-based chemicals will face the challenge of being required to fit into the existing chemical market, and

must be developed to fill pre-established needs and meet specific requirements. Bio-based production routes will either provide different methods for creating the same petroleum products currently in use, or new products that functionally replace their petroleum analogues.[27] Those bio-renewable products that would replace petroleum products must have similar, if not improved functionality and properties compared to current alternatives. The investigation of MeMBL in this study explores its potential as a functional replacement for MMA and other acrylics. The potential of bio-renewable resources (such as levulinic acid and MeMBL) is immense and covers many areas of interest to chemical engineers, including refining and polymerization of virtually all major polymer types such polyesters, polyamides, polyurethanes, acrylates and methacrylate derivatives among others.[3] A complete review of the field is beyond the scope of this work however there are some excellent resources available for additional information on this topic.[1, 3, 27-29, 31, 32]

1.2 Polymerization Background

A number of polymerization techniques and terms are discussed in this work. This section provides background information to the relevant methods and key terminology with a major focus on dispersed phase polymerizations which were investigated in great detail over the course of this thesis.

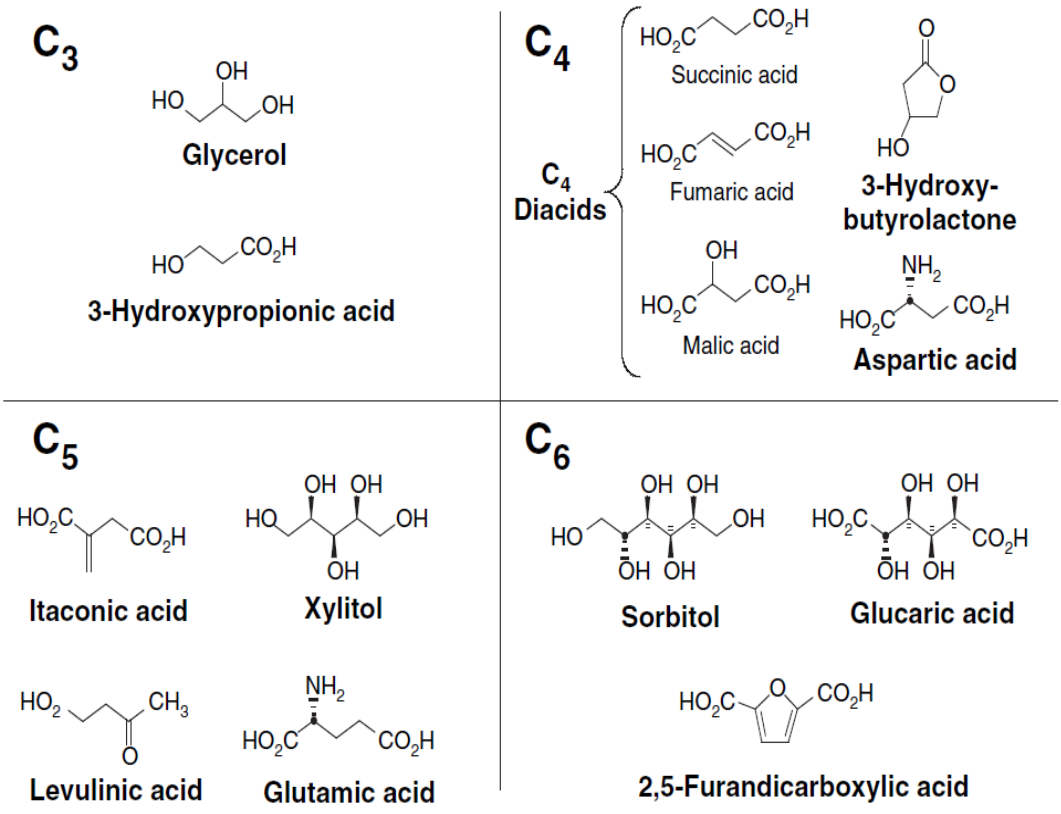

Figure 1-5 – Potential platform chemicals from biomass. Adapted from Werpy and Peterson.[29]

1.2.1 Emulsion and Miniemulsion Polymerization

Emulsion polymerization commonly refers to an oil in water system, where droplets of monomer (oil phase) are emulsified in water with the aid of a surfactant and water soluble initiators.[34] Surfactants are used to reduce the interfacial tension between the oil and water phase, thereby stabilizing the solution by absorbing at the liquid-liquid interface.[34] Sodium Dodecyl Sulfate (SDS) is a surfactant often used in industry. The dispersion of particles in water that results from an emulsion polymerization is referred to as a latex.[34] Polymerization occurs in the latex particles that are formed in the early stages of the reaction. Nucleation is primarily through heterogeneous mechanisms through the formation of micelles. Coagulation is prevented by the surfactant. Miniemulsion polymerization is a special case of emulsion polymerization where

shearing of the two immisible phases of an emulsion polymerization (often by sonication) creates much smaller droplets on the order of 50-500nm.[24, 35] The droplets are small enough that they can be polymerized directly without the need for a specific particle nucleation step. Coalescence and Ostwald ripening are suppressed by the presence of high quantities of stabilizer.[35] Further details on emulsion and miniemulsion polymerization are discussed in the literature.[24, 34-36]

1.2.2 Suspension Polymerization

Suspension polymerization typically involves the dispersion of water insoluble monomers and monomer soluble, free radical initiators in a continuous aqueous phase by means of strong agitation and small amounts of surfactants, such as poly vinyl alcohols, PVA.[36] It is similar to bulk polymerization but polymer growth occurs in the particle rather than in solution.[37-40] Another difference between emulsion and suspension techniques is in the scale of the particle produced. Emulsion polymerizations typically produce particles on the order of hundreds of nanometers whereas particles produced via suspension are often as large as a millimetre.[38, 39] Further details on suspension polymerization are available in the literature. [36-40]

1.2.3 Precipitation Polymerization

A precipitation polymerization differs from other common polymerization techniques such as emulsion and suspension polymerization in that the monomer(s), solvent(s) and stabilizer(s) form a miscible, continuous phase and polymer particles, insoluble in the continuous phase, form during the reaction. The system is initially homogenous but becomes heterogeneous as the reaction proceeds and the polymer produced in solution exceeds its solubility limits (critical chain length).[41] Compared to homogenous polymerizations, precipitations are marked by a notable increase in molecular weight and a marked, autocatalytic rise in the rate of polymerization.[42]

After precipitation, the primary loci of polymerization shifts to the particulate phase from the continuous phase. No surfactant or stabilizer is used in this polymerization technique.[43-45]

1.2.4 Dispersion Polymerization

The dispersion polymerization technique is actually a specialized case of precipitation polymerization where the addition of a surfactant to the recipe prevents flocculation and helps to control the size and distribution of the polymer particles.[41] It was first developed in the 1950's as a single step method for creating a monodisperse, micron sized dispersion of polymer particles for the automotive coatings industry in non-aqueous media.[41] Like precipitation polymerization, the system is initially homogenous but becomes heterogeneous as the reaction proceeds since the continuous phase is a poor solvent for the polymer that is being produced. Dispersion polymerization is usually a rapid process, with the small size of particles formed and the low viscosity of the reaction mixture promoting good heat transfer.[41] Unlike dispersions produced via emulsion (aqueous) polymerization, the rate of reaction does not depend on the number of initial particles formed, but rather is dependent on the concentration of monomer and initiator.[41, 46] Dispersion polymerizations of monomers such as MMA, ST and other acrylics are commonly carried out industrially in organic solvents, especially in alcohols and other water miscible solvents, with monomer soluble free radical initiators and water soluble surfactants.[46, 47]

Since the dispersion polymerization technique employed in Chapter 3 is somewhat unique, it is useful to illustrate a picture of what goes on over the course of a polymerization. Firstly, nucleation in dispersion polymerization will be examined. Later, the various models that have been developed over the past 30 years to examine the dispersion technique are reviewed to help understand what is believed to occur in the polymerization after nucleation. Additionally, the surfactant used in dispersion polymerization is of critical importance, as it creates a reproducible

polymerization system (unlike precipitation polymerization) by providing colloidal stability and helping to control average particle size and size distribution of the polymer created.[42] The mechanisms of particle stabilization employed in dispersion polymerization are quite different than those often employed in emulsion polymerization[36] and because of this, the commonly used surfactant employed in this and many other studies and the mechanism by which it stabilizes dispersions will also be reviewed.

1.2.4.1 Particle Nucleation in Dispersion Polymerization

The nucleation of particles is an important step in the dispersion polymerization process. In general terms, there are two types of particle nucleation: homogenous and heterogeneous nucleation. Homogenous nucleation occurs when oligomers are first formed in the polymerization by the decomposition of initiator and its subsequent reaction with dissolved monomer. As those oligomers grow, they will eventually exceed the chain length at which they are soluble in the reaction media (j_{crit}) and precipitate.[35, 48] The process of heterogeneous nucleation is often associated with micellar nucleation in emulsion polymerization.[35] When micelles are not present in the system, heterogeneous nucleation may occur at phase boundaries where potential energy differences are reduced; these include interfaces such as crevices or surface imperfections on the walls of the reactor where wetting occurs and on particulates found in solution, including particles that are formed via homogenous nucleation which act as sites that promote nucleation. Both forms of particle nucleation may be present in a reaction at the same time. Homogenous nucleation is generally preferable in monomers with high water solubility (such as MMA 1.5g/100g water) whereas heterogeneous nucleation is more commonly encountered with less water soluble monomers, such as styrene (0.045g/100g water).[35] Because the particles formed by both homogenous and heterogeneous nucleation are so small initially (20 nm or less in typical MMA dispersions),[49] it is difficult to stabilize them. Often, the particles initially nucleated are

referred to as precursor particles which are only truly stabilized by growth through polymerization and coagulation, which is a process sometimes referred to as coagulative nucleation.[35, 50]

A schematic representation of the many mechanisms simultaneously involved in dispersion polymerization and a proposed mechanism of particle formation is shown in Figure 1-6. Both heterogeneous and homogenous nucleation processes are thought to occur in dispersion polymerization; however, as will be explained in further detail later in this chapter, the surfactants typically employed are themselves polymers that stabilize the growing polymer particles by grafting and to a lesser extent adsorbing to their surfaces. For this reason, micellar nucleation, prevalent in emulsion polymerizations, is not thought to have as much an influence on non-aqueous dispersions.[49] In a typical dispersion polymerization, the nucleation of the particles is believed to occur at a low overall conversion (less than 2%) and is marked by the precipitation of chains (B) that grew to their critical chain length (j_{crit}) primarily by solution polymerization (homogenous mechanisms, A).[49, 51-53] For the first few minutes of a polymerization, the reaction appears homogeneous and no particles are observed at all. Real time dynamic light scattering (DLS) of MMA dispersion polymerizations was conducted by Shen et al. who saw nuclei of 15-20nm precipitate after 3 to 4 minutes and quickly appear to grow via coagulative nucleation to sizes in excess of 200nm within another 2 minutes.[49] While this data supports that nuclei are formed and appear rapidly in dispersion polymerization, its utility for further measuring nucleation is limited, as the particles that coagulate to large size quickly dominate the system and DLS detector. The overall number of particles found in the dispersion is thought to be set very soon after the initial nucleation occurs (C), and those first few large particles that form by coagulative nucleation are termed primary particles. [49, 53-55] At this point in the polymerization, solution polymerization still dominates the system.[53] How many primary particles form is related

to the efficiency and speed of the chain transfer to steric dispersant (which equates to how fast the surfactant grafts to the polymer), as coagulation will continue until a sufficient amount of stabilizer is fixed to the growing particles.[51, 53] As more primary particles are formed, monomer is able to diffuse into the polymer phase and the primary mode of polymerization shifts to more bulk-like behaviours, similar to those observed in precipitation polymerization.[53] At the same time as bulk-like polymerization within the particle occurs, it is believed that a steady flux of nuclei, which are themselves short lived and unstable, is supplied over the course of the reaction, produced via the same mechanisms as those that are initially detected. Once the population of larger, primary particles is established, it is thought that any nuclei that are formed are swept up by the mature particles by various mechanisms until either the monomer or radical source is depleted (D), leaving only primary particles at the end of the reaction.[43, 49, 51, 53, 55] Thus, the mature particles found at the end of a typical dispersion polymerization are composed of many oligomer and polymer chains. The length of the oligomer chains is a function of their critical chain length, and the number of aggregated oligomers is related to the competition between coagulation of nuclei and stabilization of nuclei by surfactant.[49] This description of the currently held views in the literature on the dispersion polymerization process will become especially relevant to the results and discussions in Chapter 3.

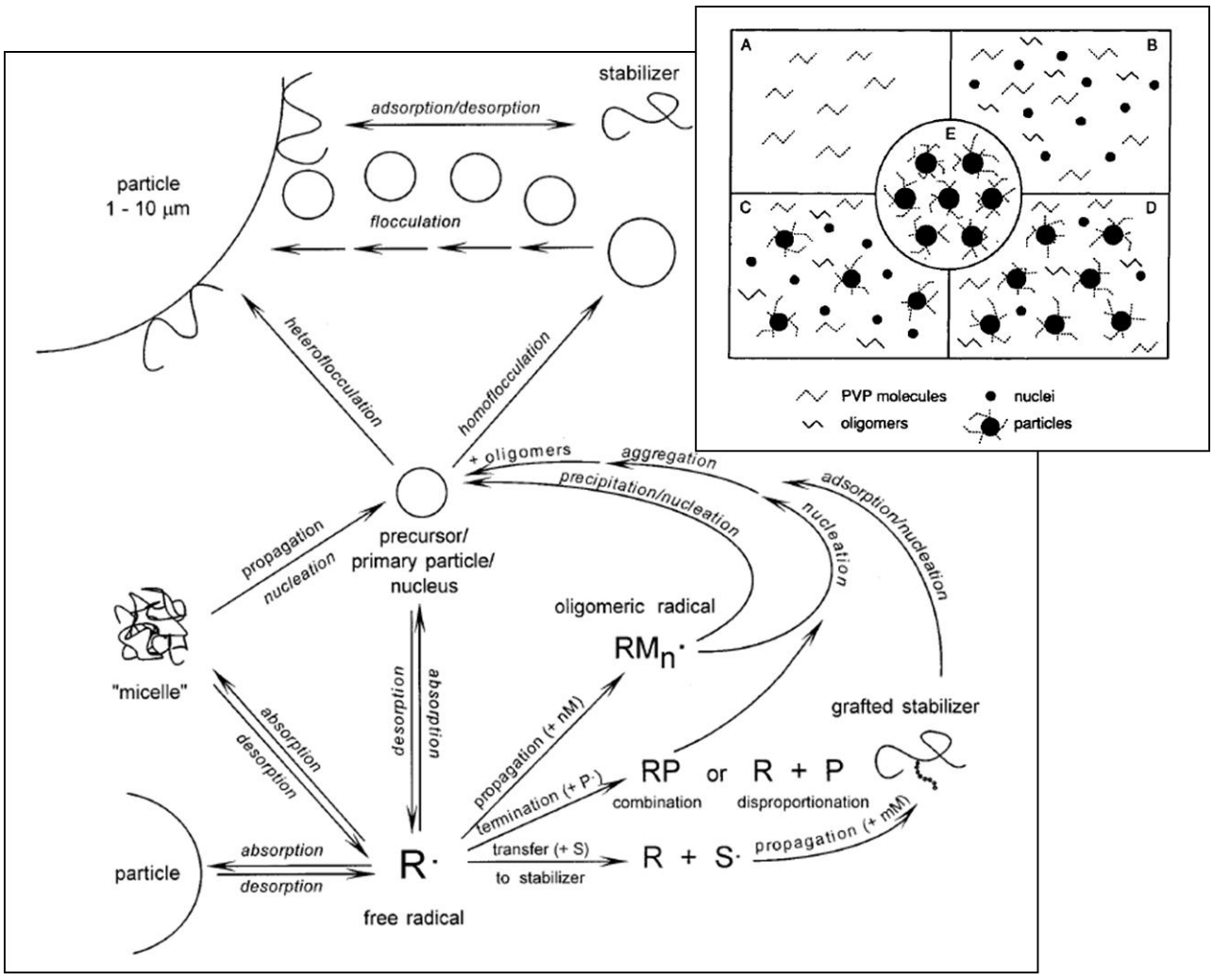

Figure 1-6 – Schematic representation of the mechanisms involved in free radical dispersion polymerization and a proposed mechanism of particle formation (inset). Words in italic represent physical processes. Adapted from Wang et al. and from Shen et al.[49, 55] A) Homogenous system before Polymerization; B) nuclei generated by precipitation of oligomers at j_{crit}; C) Primary particles formed by coagulation and stabilization of nuclei; D) Nuclei and primary particles coexist during particle growth and no new primary particles are formed; E) Only primary particles observed at the end of the reaction.

1.2.4.2 The Basics of Dispersion Polymerization Modeling

Mathematical modeling, coupled with experimental measurements, is a useful method for investigating process mechanisms and their impacts on polymer properties. It is currently an area of growing interest, with a number of publications having been written in the past 5 years which

have revisited older models and challenged some long held assumptions. Those recent works have provided a much better understanding of the processes inherent to dispersion and precipitation polymerization, and have been used to represent a variety of polymer systems with good accuracy, including poly(vinyl chloride),[56] pMMA,[57, 58] poly(vinylidine fluoride)[59] and poly(acrylic acid),[60, 61] among others. Most generally accepted models are based on the 2 phase model first proposed in the 1960's by Talamini et al.[62, 63] which accounts for the two reactive phases, incorporating mass transfer resistance in both phases and equilibrium at the interface. All of the models listed above assume that the number of particles in the reaction is fixed from an early stage in the reaction – a point that will become relevant to the discussion in Chapter 3.

A critical aspect to consider when investigating dispersion and precipitation polymerizations is that the kinetics are predominantly determined by the composition of the phases (monomer, polymer and radical concentrations).[56-58] The precipitated phase consists mostly of polymer molecules and the other reactive phase consists mostly of monomer molecules miscible in a continuous phase; however, the composition of the two phases remains significantly different.[56-58] The miscibility of the monomer molecules in the solvent does however create some added complexity when attempting to model these systems, as the initiator is soluble in both phases, unlike in emulsion polymerization, and radicals are thus formed in both the dispersed and continuous phases.

The location and mobility of radicals in these polymerizations is a key consideration when modeling the reactions. Mueller et al.[57] in 2005 investigated the two most prevalent models then in use when considering the interphase transport of polymer chains. The two models in question, known as the radical segregation model (RS) and radical partitioning model (RP) are quite opposite. The RS model assumes that active chains spend their entire lives in the same phase in which they were created. This corresponds to the case where, in each phase, the characteristic

time required for radical termination is much less than the time required for interphase mass transport and is assumed in many older models. The other model (RP) assumes that the radicals produced in either phase can transfer freely to the other, subject to solubility limits, meaning the rate of mass transport between phases is infinitely fast and thermodynamic equilibrium is always established. This corresponds to the case where the characteristic time for termination is less than the time required for interphase mass transport.

The solubility limit of the polymer chains in the dispersed phase is often represented using a critical chain length (j_{crit})[56-61] above which growing polymer chains are insoluble in the dispersed phase and below which identical rates of transfer between phases is assumed. [56-58] This means that radicals of low chain length may transfer to the monomer rich phase, and radicals of higher molecular weight transfer to the polymer phase, with an overall net transfer of chains to the polymer phase as the reaction proceeds.[56] The net transfer of chains to the polymer phase causes the rate of polymerization to rise, a characteristic effect of this type of polymerization.[41] The result of Mueller's work, since supported by other researchers,[56] showed that while not fully satisfactory, the RP model was much better able to represent real system behaviours and MWDs. Similarly, there had been some question in the literature about the extent of interphase transfer of highly reactive species, such as initiator radicals. It is now widely accepted that these species are too reactive and the time scale of reaction is less than the time scale of transport, thus they do not undergo transfer.[56] Thus, there is growing consensus that any useful model must account for radical as well as initiator and monomer transfer between phases in order to accurately predict these types of polymerizations, as rates of transfer of growing radicals between reactive phases have been shown to significantly affect model predictions for conversion and polymer molar mass distribution. [56-58]

1.2.4.3 Steric Stabilization of Dispersion Polymerizations by Poly-N-vinylpyrrolidone

Poly-N-vinylpyrrolidone (PVP), is the most well known of a class of poly-N-vinylamides.[64] In the past 50 years, PVP has been a subject of great interest to researchers, owing to its unique combination of chemical, physicochemical and biological properties.[64] Beneficial properties of PVP include its film forming and adhesive characteristics, complexing ability, high degree of water solubility and ability to absorb large quantities of water, low toxicity, biological compatibility and the fact that it is temperature-resistant, pH-stable, non-ionic and colorless.[64] Another important property of PVP is its relatively high glass transition temperature, T_g, of 175-180^{o}C. PVP is also soluble in many organic solvents, notably alcohols, amines, acids, chlorinated hydrocarbons, amides and lactams.[64] The structure of PVP is shown below in Figure 1-7.

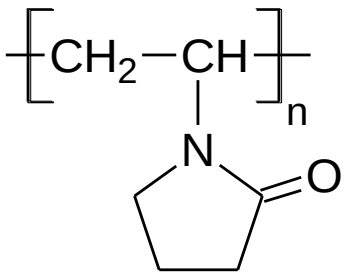

Figure 1-7 – Poly-N-vinylpyrrolidone polymer structure

PVP and other like homopolymers (including poly(acrylic acid) and hydroxyl propyl cellulose) have been successfully used for many years as steric stabilizers in dispersion polymerizations due to their high solubility in water and organic media.[43] An important characteristic of polymeric stabilizers used in dispersion polymerization (including PVP) is that they contain many labile hydrogen atoms. These labile hydrogen atoms are easily abstracted during a reaction, allowing the stabilizer to graft onto the monomer or growing polymer particle, forming a sterically stabilized *in-situ* graft polymer.[43] The grafting of the stabilizer onto the polymer creates a strong, permanent interaction that does not easily allow the stabilizer to be removed.[43-45]

Understanding how and why steric stabilization is able to take place is an important aspect of understanding dispersion polymerization.

To better understand steric stabilization, it is useful to first understand on a general level more about colloidal stability. Colloidal systems are microscopically heterogenous systems characterized by the dispersion of one phase (the dispersed phase), typically on the scale of nanometres to microns, in another phase (the continuous phase). The colloidal particles dispersed in the continuous phase are in constant motion due to Brownian forces and thus frequently collide with each other.[65] The outcome of these collisions is either attractive or repulsive interaction between the particles. To maintain a colloidal system, attractive interactions must be minimized or else particles will flocculate. The primary attractive forces between colloidal particles are Van der Waals forces, of which there are 3 types; Keesom, Debye and London. Keesom forces are related to the orientation of dipolar interaction between two permanent dipoles. Debye forces are interactions between a permanent and an induced dipole. London forces are the most important contributors to overall Van der Waals forces as they represent the interactions of induced dipoles and are present irrespective of the properties of the molecules involved (they do not require a permanent dipole). The distance over which London forces occur (5 to 10 nm) is much greater than that of Keesom and Debye forces and in terms of total interaction energy, Keesom and Debye forces typically contribute 2% or less. Consequently, in order to obtain a stable colloidal system, a sufficiently strong repulsive force is required to counteract the attractive van der Waals forces.[41, 66] The most well known methods able to impart stability on a colloidal system are either to surround the colloidal particle with an electrical double layer (electrostatic or charge stabilization) or with adsorbed or chemically bonded polymeric molecules (steric stabilization.) Electrostatic repulsive forces are generated by the adsorption (by various methods) of charged species (ions) onto the colloidal particle and are commonly employed in emulsion

polymerizations.[36] In an effort to maintain electroneutrality, an equivalent number of counter ions is attracted and forms what is known as the double layer, which has a net neutral charge.[66] It is the mutual repulsion between the double layers surrounding the particle that provides stability.

Steric stabilization refers to the mechanism by which certain polymers and surfactants are able to inhibit coagulation in emulsions, suspensions and dispersions and generally encompasses all aspects of the stabilization of colloidal particles by non-ionic macromolecules.[67] The molecules stabilizing particles in steric stabilization are much larger than most common surfactants and emulsifiers like sodium dodecyl sulphate (SDS). The origins of steric stabilization date back to the very first recorded use of ink and paper in ancient Egypt, 5000 years ago, where carbon black was suspended in water by means of natural steric stabilizers like casein and albumin.[67] The term steric stabilization has no relation to the "steric effects" term commonly used to describe geometric and orientation interactions between functional groups and molecules (which are always repulsive electron-electron and electron-nuclei interactions).[67] The principle need for steric stabilization arises from the fact that charge stabilization is not known to be effective in media of low dielectric constant; media that encompass the majority of organic solvents, inks, paints and plasticizers. [67] As such, a different method is required to prevent flocculation and maintain the dispersed character of the particles in the system. Sterically stabilized systems are known to remain well dispersed when exposed to high salt concentrations and conditions where the zeta potential of the surface is near zero.[66] The common property shared by the polymers and surfactants (stabilizers) involved in steric stabilization is their affinity for the media in which they are dissolved, be it water in the case of emulsions and suspension, or other organics in the case of dispersions.

In sterically stabilized systems, the stabilizer attaches to the surface of the particle by various methods such as adsorption or by grafting as noted for the case of PVP. Like most stabilizers, steric stabilizers, especially copolymer steric stabilizers, have a hydrophilic and hydrophobic section. The hydrophobic end is attracted to the polymer particle as it wants to be as far removed from the solvent as possible. The hydrophilic stabilizer chains extend out into the solvent from the points of adsorption, giving the stabilized particle a large hydrodynamic radius. The best steric stabilizers are typically block or graft copolymers, where one end has an affinity for the solution and the other has an affinity to adsorb to the polymer particle.[66, 67] Polymers like PVP are able to work effectively because they have a great affinity for the solution phase, but are easily made to graft onto the growing polymer chain, providing a stabilizer that has both strong attraction to the particle and solution. Grafting of the stabilizer onto the particle helps to ensure that the stabilizing moieties are not moved or desorbed when in close contact with another particle.[67]

It is important for the stabilizers to be fully solvated by the solvent media, thus the nature of the solvent is therefore of great importance to steric stabilizers. Theta (or better) solvents (i.e. good solvents) are typically required to ensure that the stabilizer is free to fully extend into the medium.[68, 69] In systems where chains are poorly solvated, the hydrodynamic radius of the stabilized particle is reduced, and stabilizer chains are confined to the surface of the particle. The importance of this observation leads to the primary theory used to explain how steric stabilization works, based on the Flory treatment of polymer thermodynamics.[41] When two sterically stabilized particles come into close contact (less than twice the distance of the adsorbed layer), as depicted in Figure 1-8, the hydrophilic stabilizer chains intermingle and compress one another, and lose a degree of freedom that they had in solution. There will be an energy change in the system upon interaction. In terms of thermodynamics, for an isothermal system, the loss of

freedom seen in the system is equivalent to a reduction in entropy. The Gibbs energy of the system is expressed as:

$$\Delta G = \Delta H - T\Delta S \quad (1)$$

where G represents the Gibbs energy, H the enthalpy and S the entropy in the system. If ΔG is negative, flocculation and coagulation may occur in the system and if ΔG is positive, repulsion will result. A reduction in entropy (a system becoming more ordered, a negative change in ΔS) is an unfavourable event, which creates a thermodynamic barrier that prevents further attraction of the particles. Because ΔS is decreasing and the TΔS term is negative, the overall result of a decrease in entropy is an increase in ΔG. A secondary aspect of the accepted theory involves solvency effects. As the adsorbed chains of the stabilized particles intermingle, solvent is forced out from around the particle, leading to an imbalance in concentration.[41, 67-69] The imbalance in concentration produces a concentration gradient which is resisted by osmotic pressure which tends to force the solvent molecules back between the particles and maintains separation. [41, 67-69] Together, contributions of solvency and entropy make up the forces of steric repulsion.

The effect of the addition of a steric stabilizer to a dispersed system can be seen in Figure 1-8. Enhanced repulsion is observed when stabilizers are added to the system. This can be seen in the illustrated shift of the overall potential energy curve. Enhanced steric repulsion dominates the system at close separation, supplanting the effects of van der Waals attractions to create a net repulsive force. Thus, from the prior discussion, the importance of the surfactant to the dispersion technique becomes obvious.

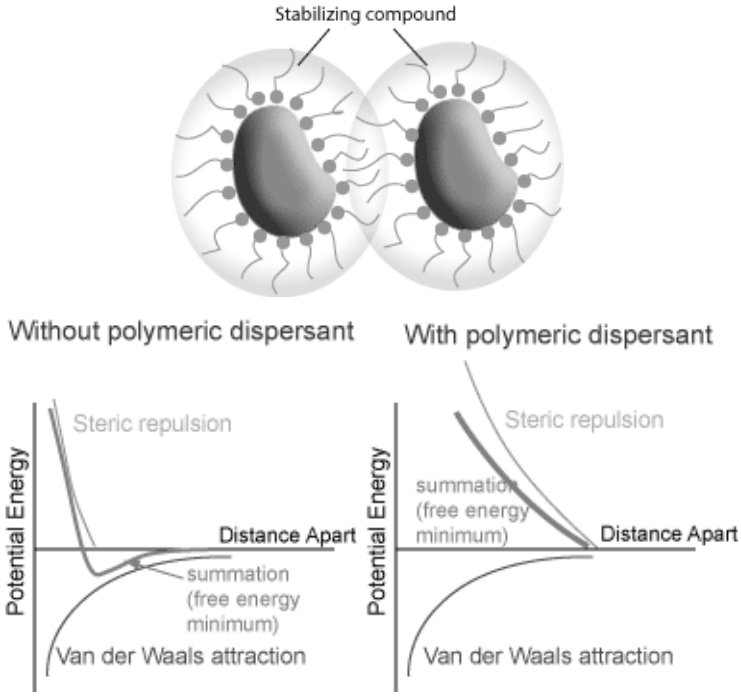

Figure 1-8 – Steric Stabilization of particles (top) and the effects of Steric Stabilization on the Potential Energy Curve (bottom).[70]

1.3 Summary

Having completed a review of the relevant literature, we will now present our findings into the investigations of the bio-renewable MeMBL monomer. Chapter 2 presents the results of pulsed laser polymerization studies on the kinetics of MeMBL homopolymers and copolymers of MeMBL with each of MMA, styrene and *n*-butyl acrylate. Chapter 3 details our examination of the dispersion polymerization technique, which focuses on the effects of a number of parameters on nucleation and particle size control of MMA and MeMBL/MMA copolymers. Chapter 4 completes the study by preparing and testing the physical properties of MeMBL/MMA copolymers with well controlled compositions. Finally, Chapter 5 summarizes and relates the key discoveries of the prior chapters and details a path forwards for future research endeavours related to the study of this monomer.

Chapter 2

A study of the free radical copolymerization kinetics of a bio-renewable monomer γ-methyl-α-methylene-γ-butyrolactone (MeMBL) with Butyl Acrylate, Methyl Metacrylate and Styrene

2.1 Pulsed Laser Polymerization Background

The PLP-SEC technique has been used extensively to study homopolymerizations and copolymerizations of styrene with various methacrylates,[71-79] measuring effective propagation rate coefficients as a function of temperature and composition. The breakdown of a photoinitiator on exposure to intense flashes of UV light generates radicals instantaneously at set intervals. Those radicals that survive the dark period between laser flashes are typically terminated by the next pulse of light to form a significant population of dead polymer chains with a characteristic chain length of L_o.

$$\boldsymbol{L_o = k_{p,cop}[M]t_o} \quad (1)$$

Knowing both the total monomer concentration [M] and flash interval (pulse frequency) t_o, allows for the calculation of the copolymer-averaged propagation rate coefficient $k_{p,cop}$ from experimental determination of L_o by SEC. While radicals that survive the dark period between laser pulses are often terminated with the next flash of light, there is some probability that a radical survives, continuing to propagate and terminating at some other later flash. This has the effect of producing polymer chains of length $2L_o$ or $3L_o$, also observable within the polymer molecular weight distribution. An overview of this technique, which has greatly improved knowledge of free radical polymerization kinetics, is found in a number of reviews such as that by Beuermann and Buback.[80]

Copolymer composition for many two monomer systems containing methacrylates or styrene is often well represented by the terminal model (also known as the Mayo-Lewis equation), where radical reactivity depends only on the terminal unit of the growing chain such that the instantaneous mole fraction of monomer-1 incorporated into the copolymer (F_1^{inst}) is a function of monomer mole fractions (f_1 and f_2) and the monomer reactivity ratios:

$$F_1^{\text{inst}} = \frac{r_1 {f_1}^2 + f_1 f_2}{r_1 {f_1}^2 + 2 f_1 f_2 + r_2 {f_2}^2} \tag{2}$$

where $r_1 = k_{\text{p}11}/k_{\text{p}12}$, $r_2 = k_{\text{p}22}/k_{\text{p}21}$, and $k_{\text{p,ij}}$ is the propagation rate coefficient for addition of monomer-j to radical-i. Although the terminal model is generally a good descriptor for copolymer composition, its predictions of the copolymer-averaged propagation rate coefficient ($k_{\text{p,cop}}$) as a function of monomer composition often deviate significantly from experimental measures.[74-79] The penultimate unit representation was originally developed by Merz et al. to describe $k_{\text{p,cop}}$.[81]

$$k_{\text{p,cop}} = \frac{\overline{r_1} {f_1}^2 + 2 f_1 f_2 + \overline{r_2} {f_2}^2}{\left(\frac{\overline{r_1} f_1}{\overline{k_{11}}}\right) + \left(\frac{\overline{r_2} f_2}{\overline{k_{22}}}\right)} \tag{3}$$

As the terminal model provides an adequate representation of composition, it can be assumed that the penultimate unit does not affect the selectivity of the radicals ($\overline{r_1} = r_1$ and $\overline{r_2} = r_2$). However, according to the Implicit Penultimate Effect (IPUE) model first developed by Fukuda et al.,[82] both terminal and penultimate units affect radical reactivity, such that $\overline{k_{11}}$ and $\overline{k_{22}}$ are expressed as functions of monomer fraction,

$$\overline{k_{11}} = \frac{k_{\text{p}111}(r_1 f_1 + f_2)}{r_1 f_1 + (f_2/s_1)} \quad ; \quad \overline{k_{22}} = \frac{k_{\text{p}222}(r_2 f_2 + f_1)}{r_2 f_2 + (f_1/s_2)} \tag{4}$$

where $k_{\text{p}111}$ and $k_{\text{p}222}$ are homopolymerization propagation rate coefficients, and radical reactivity ratios s_1 and s_2 are defined as $k_{\text{p}211}/k_{\text{p}111}$ and $k_{\text{p}122}/k_{\text{p}222}$, respectively ($k_{\text{p,ijk}}$ is the

propagation rate coefficient for addition of monomer-k to a growing radical-j with unit-i in the penultimate position). This model reduces to the terminal model predicition of $k_{p,cop}$ when $s_1 = s_2 = 1$. Values of the radical reactivity ratios are estimated by fitting the penultimate model to experimental $k_{p,cop}$ vs. monomer composition data, as measured by PLP/SEC techniques.

2.2 Experimental

MMA (99% purity) inhibited with 10-100 ppm of monomethyl ether hydroquinone (MEHQ), styrene (ST, 99% purity) inhibited with 10−15 ppm of 4-*tert*-butylcatechol and BA (99% purity), inhibited with 10-60 ppm MEHQ were purchased from Sigma Aldrich and used as received. The photoinitiator DMPA (2,2-dimethoxy-2-phenylacetophenone, 99% purity) and Chloroform-*d* with 99.8 atom %D were also obtained from Sigma Aldrich and used as received. MeMBL inhibited with 50 ppm of hydroquinone (97.5% purity, major impurity gamma valerolactone, GVL) was obtained from DuPont Central Research Laboratories and used as received. Monomer purification is not necessary for PLP/SEC investigations, as the technique depends on MW analysis to estimate $k_{p,cop}$, not rate measurements.[73]

Low-conversion MeMBL homopolymerizations and copolymerizations of MeMBL/ST, MeMBL/BA and MeMBL/MMA were conducted in a pulsed laser setup consisting of a Spectra-Physics Quanta-Ray 100 Hz Nd:YAG laser that is capable of producing a 355 nm laser pulse of duration 7−10 ns and energy of 1−50 mJ per pulse, with further specifics of the apparatus as described by Wang and Hutchinson.[79] Monomer mixtures in bulk with 5 mmol·L^{-1} DMPA photoinitiator were added to a Hellma QS100 optical sample cell used as the PLP reactor and exposed to laser energy, with temperature controlled to ±1.0°C during pulsing by a circulating oil bath. Experiments were run between 22 and 90 °C at varying frequencies depending on the monomer systems studied (typically 33Hz or 50Hz). The MeMBL mole fraction in the monomer

mixture was systematically varied between 0−100%. Monomer conversions were controlled below 3% to avoid significant compositional drift.

The kinetics of MeMBL/ST, MeMBL/BA and MeMBL/MMA homo and copolymerizations were determined by analyzing polymer molecular weight distributions (MWD) of PLP samples as measured by SEC. The resulting samples from PLP were precipitated in methanol and the solid polymers were isolated by drying under a stream of forced air. The polymers were further dried in a vacuum oven and then redissolved in a solvent; either tetrahydrofuran (THF) or *N*,*N*-Dimethylacetamide (DMAc) depending on the SEC setup used. MeMBL/MMA and MeMBL/BA copolymers with greater than 50 and 60 mol% MeMBL, respectively, are not THF-soluble, where MeMBL/ST is soluble up to 80 mol% MeMBL. All samples of all copolymers from 0 mol% to 100 mol% MeMBL are soluble in DMAc and so samples spanning the complete composition range were analyzed in a SEC setup that uses this eluent at the University of Potsdam in Germany.

THF SEC analyses were performed at 35 °C using a Waters 2960 separation module with Styragel packed columns HR 0.5, HR 1, HR 3, HR 4, and HR 5E (Waters Division Millipore). THF was used as the eluent at a flow rate of 1 $mL \cdot min^{-1}$ and detection was provided by a Waters 410 differential refractometer (DRI detector) and a Wyatt Instruments Dawn EOS 690 nm laser photometer multiangle light scattering (LS) unit.[78, 79] Calibration of the RI detector was established using 8 linear narrow polystyrene standards with narrow dispersity over a molecular weight range of 890 to 3.55×10^5 $g \cdot mol^{-1}$.

DMAc SEC analysis were performed using an Agilent 1200 isocratic pump, an Agilent 1200 differential refractive index detector, a WEG Dr. Bures ETA 2010 online viscosity detector, and three PSS analytical GRAM columns (8 x 300 mm, particle size 10 μm, pore sizes 100 Å and 2 x 3000 Å). DMAc containing 0.1 % LiBr at 45 ^{o}C at a flow rate of 1 mL·min^{-1} was used as eluent. The SEC setup was calibrated against 11 pST standards of narrow dispersity with molecular weights between 500 and 1 x 10 ^{6} g·mol^{-1}. With online viscosity detector data a universal calibration curve was created.

In order to analyze the outputs from the DMAc SEC, Mark-Houwink (MH) parameters are needed to transform the data from the relative polystyrene calibration. While MH parameters for ST and MMA are easily known from MH plots derived from coupled RI and online viscosity measurements of many narrow polymer standards, no narrow polymer standards for BA and MeMBL are commercially available. To rectify this, broad homopolymer samples of BA and MeMBL were analyzed by viscometry in DMAc to determine the appropriate constants. Samples analyzed to determine the Mark Houwink parameters for MeMBL included polymer produced via PLP at 50 and 70^{o}C and by precipitation polymerization in organic media at 70^{o}C (Discussed in Chapter 3).[83] Polymer samples for BA were produced at the University of Potsdam by 100 Hz PLP experiments at 10 °C with 1 vol.% *n*-dodecyl mercaptan as CTA to reduce branching. The samples were purified three times by dissolving the polymer in acetone and precipitation in methanol. Three samples of the polymer produced at each condition were each injected at least twice. For each polymer sample the variation of intrinsic viscosity with the elution volume, V_e, is derived on the basis of the precisely known polymer concentration. By using the aforementioned universal calibration curve and the measured intrinsic viscosity the absolute molecular weight at every elution volume and thus the MH plot are available. Taking the slopes and y-intercepts of the individual lines of log(intrinsic viscosity) vs. log(MW) in Figure 2-1 provides an estimate for

the a and K Mark Houwink parameters, respectively; final estimates were obtained by averaging the values for each respective condition. When MeMBL homopolymer k_p values were calculated with both PLP and precipitation Mark Houwink constants, it was found that the difference between the highest values predicted (precipitation polymerization constants) and the lowest values predicted (50°C PLP constants) was 12-13%, a typical uncertainty range for SEC. The various Mark Houwink parameters for MeMBL in DMAc were compared with poly(MeMBL/ST) THF results[84] and the data sets were found to be most consistent using the calibration from pMeMBL produced by precipitation polymerization; this calibration was used for all of the MWD analysis in this work

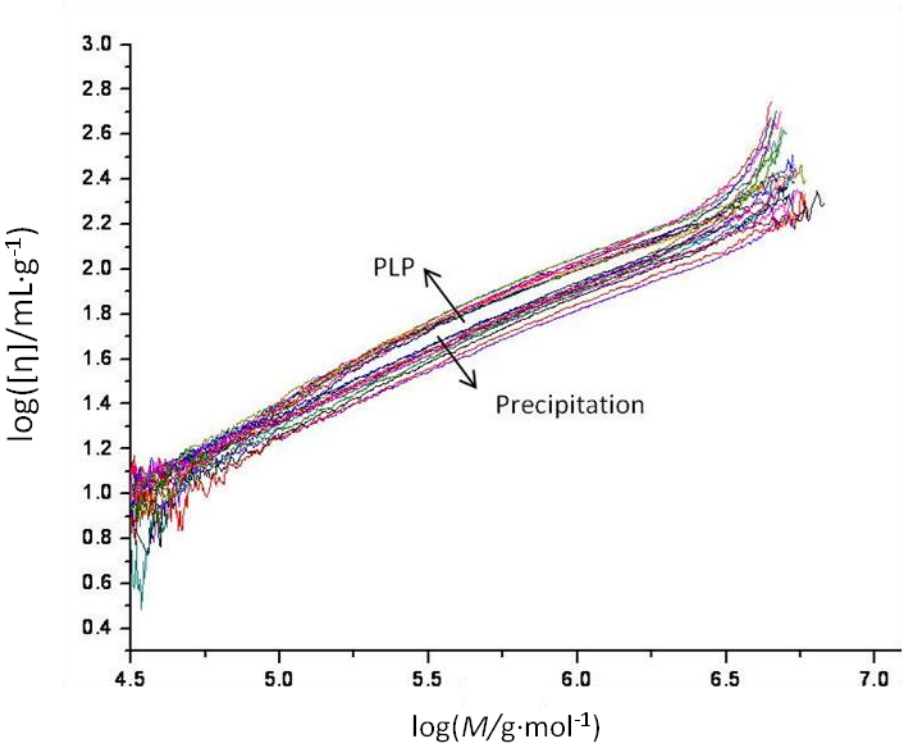

Figure 2-1 - Plot of log of viscosity vs. log of MW for MeMBL polymers in DMAc. Data is shown for MeMBL polymer produced via PLP (upper) and precipitation (lower) polymerization techniques.

Another piece of information, the refractive index (d*n*/d*c*) of the polymer in THF is required to process the data from the LS detector and was measured by a Wyatt Optilab DSP refractometer at 30 °C and 690 nm, calibrated with sodium chloride. Samples between 1 and 10 $mg \cdot mL^{-1}$ were prepared in THF for each polymer and injected sequentially to construct curves with slope d*n*/d*c*. As homopolymers of MeMBL cannot be dissolved in THF, d*n*/d*c* values for ST and MMA homopolymers and copolymers of MeMBL/ST and MeMBL/MMA produced from monomer mixtures containing 0.1 to 0.8 and 0.1 to 0.5 mole fractions MeMBL, respectively, were measured as shown in Figure 2-2. The values varied linearly with copolymer composition as found for various ST/methacrylate copolymers.[74, 78, 79] Thus, the curves could be extrapolated to estimate a value for the MeMBL homopolymer. The two extrapolated values of 0.094 $mL \cdot g^{-1}$ and 0.102 $mL \cdot g^{-1}$ have been averaged to provide an estimate for the MeMBL homopolymer d*n*/d*c* value of 0.098 $mL \cdot g^{-1}$. Copolymer d*n*/d*c* values for analysis of LS results were calculated assuming linear relationships between the two homopolymer values. The approximately 4% uncertainty in the d*n*/d*c* value for the MeMBL homopolymer results in a similar uncertainty for the estimated peak positions of the inflection points of the MWDs.

Additionally, Mark-Houwink parameters for the MeMBL homopolymer are required in order to analyze outputs from the RI detector as composition-weighted averages of the homopolymer values.[74, 77-79] As the homopolymer of MeMBL cannot be dissolved in THF, these values have been estimated, with the '*a*' exponent value set to the accepted value for MMA and the '*K*' term adjusted to minimize the discrepancy between the LS and RI MW results for MeMBL/ST and MeMBL/MMA produced with $f_{MeMBL} \leq 0.8$ and $f_{MeMBL} \leq 0.5$, respectively. Estimating Mark-Houwink parameters in this way is by no means ideal, as there is great dependence on the accuracy of the LS results. However, since the LS results are an absolute measurement processed

with experimentally determined d*n*/d*c* values for the copolymers, the RI measurements are used only as a check on SEC operation. Agreement between the two detectors is acceptable, generally within 10%, over a wide range of MW_0 values, between 5×10^3 and 1×10^5 Da.

The polymers isolated from the PLP experiments were also used for composition analysis by proton NMR. Preparation of samples for NMR analysis on a 400 MHz Bruker instrument was conducted in deuterated chloroform as described previously.[79] Determination of poly(MeMBL/ST) copolymer composition was done as described by Qi et al.,[24] using chemical shifts from the phenyl protons in the region of 6.2−7.3 ppm, and from the proton at the gamma carbon (attached to the exocyclic methyl group) of MeMBL in the region of 4.4-4.8 ppm. Composition of MeMBL/MMA copolymers was calculated using the distinct peaks from the MMA methoxy-methyl protons at 3.6−3.7 ppm and from the proton at the gamma carbon (attached to the exocyclic methyl group) of MeMBL in the region of 4.3-4.8 ppm, slightly downshifted from the location seen for the same peak in poly(α-MBL) as published by Akkapeddi.[6] To determine the composition of the MeMBL/BA copolymers, the characteristic peak of MeMBL (from the proton at the gamma carbon of MeMBL in the region of 4.4-4.8 ppm) was compared to the peak in n-butyl acrylate at 4.1ppm, representative of the CH_2 group in the butyl chain closest to the ether linkage.

The same polymer samples isolated from the PLP experiments for NMR analysis were also analyzed by DSC to determine the glass transition temperatures, T_g, of the closely controlled compositions. Samples of 10 to 40 mg were placed into aluminum sample pans and sealed for testing in a TA Instruments DSC Q100 Differential Scanning Calorimeter. The applied heating rate was 10 °C per minute over a range of 50 to 230 °C. Data was collected from the third scan. T_g's were taken as the inflection point between the onset and end point temperatures. Nitrogen

atmosphere was used to minimize thermal degradation of the copolymer. DSC analysis was performed on PLP samples produced at different reaction temperatures, with averaged values presented.

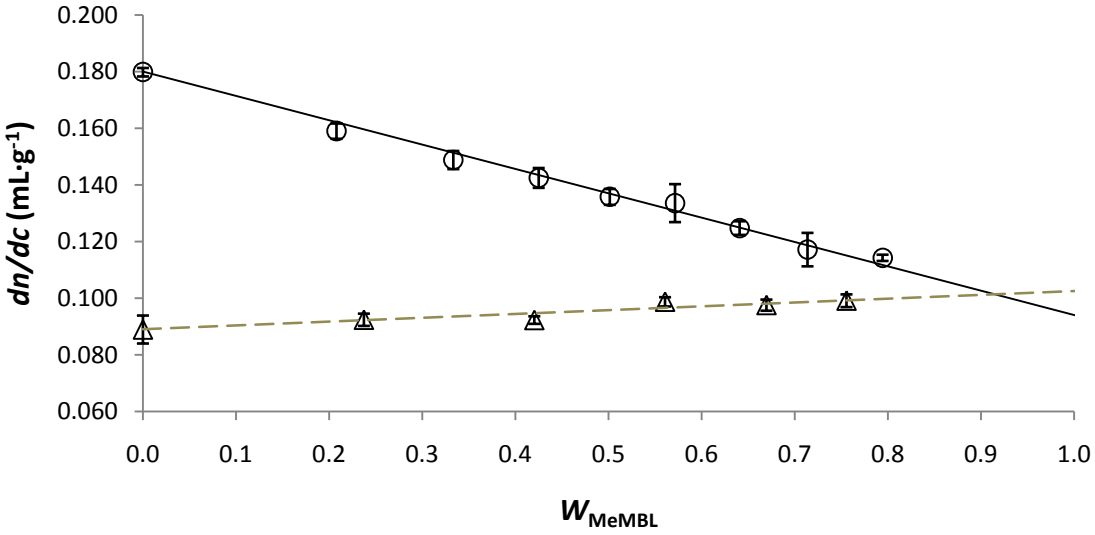

Figure 2-2 - Refractive index (d*n*/d*c*) values for MeMBL/Styrene (○) and MeMBL/MMA (Δ) copolymers in THF at 30 °C, plotted as a function of weight fraction of MeMBL (W_{MeMBL}) in the copolymer, as measured by NMR.

All parameters required to estimate $k_{p,cop}$ from SEC data are summarized in Table 2-1. Monomer densities are calculated as a function of temperature, and the refractive index (d*n*/d*c*) values used in the analysis of LS results were measured as previously discussed. A relationship between density and temperature for the MeMBL monomer has not been published in literature although the density of the monomer at standard conditions is known. For the purposes of this study, the assumption was made that the change in MeMBL density with temperature can be approximated using the known temperature dependency of MMA although the absolute value at 25^{o}C differs. A density function for BA was estimated assuming a linear dependency on temperature and density values at 20 and 60^{o}C.[85] Outputs from RI detectors are transformed to absolute MW values assuming universal calibration and using a composition weighted average of the two

homopolymer calibrations. [74, 77-79] THF LS results are normalized based on known polystyrene calibration standards. Thus, there are as many as three independent estimates of k_p for some samples, from DMAc RI analysis and from THF analysis with RI and LS detectors.

Table 2-1 - Parameters required for calculation of $k_{p,cop}$ from the SEC analysis of PLP-generated copolymer samples of MeMBL with Styrene, BA and MMA.

Monomer	Density Function	Density ρ ($g \cdot mL^{-1}$) at 25 °C	Polymer d*n*/d*c* in THF ($mL \cdot g^{-1}$)	Mark-Houwink Parameters			
				THF		DMAc	
				K ($dL \cdot g^{-1}$) × 10^4	a	K ($dL \cdot g^{-1}$) × 10^4	a
Styrene	0.9193-0.000665*T*/°C[78]	0.903	0.180[77]	1.14[77]	0.716[77]	1.22	0.678
MMA	0.9569 - 1.2129× 10^{-3} *T*/°C + 1.6813× 10^{-6} T^2/°C + 1.0164× 10^{-8} T^3/°C[86]	0.928	0.089[87]	0.944[85]	0.719[85]	1.44	0.663
MeMBL	1.2235 - 1.2129× 10^{-3} *T*/°C + 1.6813× 10^{-6} T^2/°C + 1.0164× 10^{-8} T^3/°C	1.194	0.098[84]	0.5[84]	0.719[84]	2.63	0.579
BA	0.9217-0.0011 *T*/°C[85]	0.894	0.069[87]	1.22[85]	0.700[85]	27.08	0.367

2.3 Results and Discussion

2.3.1 Monomer Reactivity Ratios

Copolymer composition was measured for MeMBL/MMA, MeMBL/BA and MeMBL/ST copolymers over the complete composition range at temperatures of 22, 50, 70 and 90 °C. As described in the Experimental Section, the low conversion samples were generated in the PLP setup and compositions were measured by proton NMR. The full set of experimental conditions and results is summarized in Appendix A. No systematic variation in copolymer composition with temperature was observed, and thus the data were combined into three larger data sets. Figure 2-3 plots MeMBL fraction in the copolymer as a function of monomer composition using an averaged value from the experiments at different temperatures, with error bars indicating the standard deviation. In each case, the Mayo-Lewis terminal model (Equation 2) represents the data well. Nonlinear parameter estimates for monomer reactivity ratios were calculated using the Predici® software package. For the MeMBL/ST system, monomer reactivity ratios of r_{MeMBL} = 0.80±0.04 and r_{ST} = 0.34±0.04 provide the best fit to the experimental data. For the MeMBL/MMA system, monomer reactivity ratios of r_{MeMBL} = 3.0±0.3 and r_{MMA} = 0.33±0.01 were estimated; for the MeMBL/BA system r_{MeMBL} = 7.0±2 and r_{BA} = 0.16±0.03. In all cases, MeMBL is incorporated into the copolymer to a greater extent than MMA; i.e. the curves for MeMBL copolymers lie above the corresponding MMA copolymer curves. The higher reactivity of MeMBL compared with MMA is also reflected in the reactivity rates (Table 2-2). The reactivity ratios determined indicate that MeMBL and MMA form an ideal random copolymer (r_1r_2=0.99) and that MeMBL and BA form a nearly ideal, random copolymer (r_1r_2=1.17). The copolymer of MeMBL and ST will have alternating tendencies as r_1r_2=0.24.

Table 2-2 - Monomer reactivity ratios for copolymerizations of MeMBL with styrene, BA and MMA, and MMA with styrene and BA, where r_1 refers to either MeMBL or the first monomer listed and r_2 to the second monomer listed.

Monomer 1| Monomer 2	r_1	r_2
MMA|ST [74]	0.46	0.52
MMA|BA [88]	2.55±0.35	0.36±0.08
MeMBL|ST This Work	0.80±0.04	0.34±0.04
MeMBL|MMA[84]	3.0±0.3	0.33±0.01
MeMBL|BA This Work	7.3±2.1	0.16±0.03
MeMBL|ST[24]	0.75-0.85	0.33-0.39
α-MBL|ST[6]	0.70	0.09
α-MBL|ST[11]	0.87	0.14
MMBL|ST[89]	0.74	0.22
α-MBL|MMA[6]	1.67	0.60

The monomer reactivity coefficients determined for the MeMBL/ST and MeMBL/MMA systems is compared to other work with gamma lactones and styrenics (MeMBL/ST, [24] α-MBL/MMA,[7] α-MBL/ST,[7, 11] and MMBL/ST copolymer[89]) in Table 2-2. The estimates for MeMBL/ST monomer reactivity ratios are in close agreement to the values determined by Qi et al.[24] at 70 °C who used both the Fineman-Ross (r_{MeMBL} = 0.85 and r_{ST} = 0.39) and Kelen-Tudos (r_{MeMBL} = 0.75 and r_{ST} = 0.33) methods in their analysis. All of the lactone monomers add to a ST radical at a rate faster than MMA monomer, as evidenced by the lower r_{ST} (r_1) values. The order of reactivity towards a ST radical is given by α-MBL>MMBL>MeMBL>MMA>ST. There is no systematic trend evident in the relative rate of ST addition to a lactone radical structure, with all r_2 values between 0.7 and 0.9. These values are, however, significantly higher than the corresponding values of 0.4-0.5 reported for ST-methacrylate systems (0.46 for ST/MMA as in Table 1).[78] Both of these trends (lower r_{ST} and higher $r_{comonomer}$ values) lead to a preferential incorporation of the lactone monomer into the ST copolymer compared to the MMA case, as illustrated in Figure 2-4.

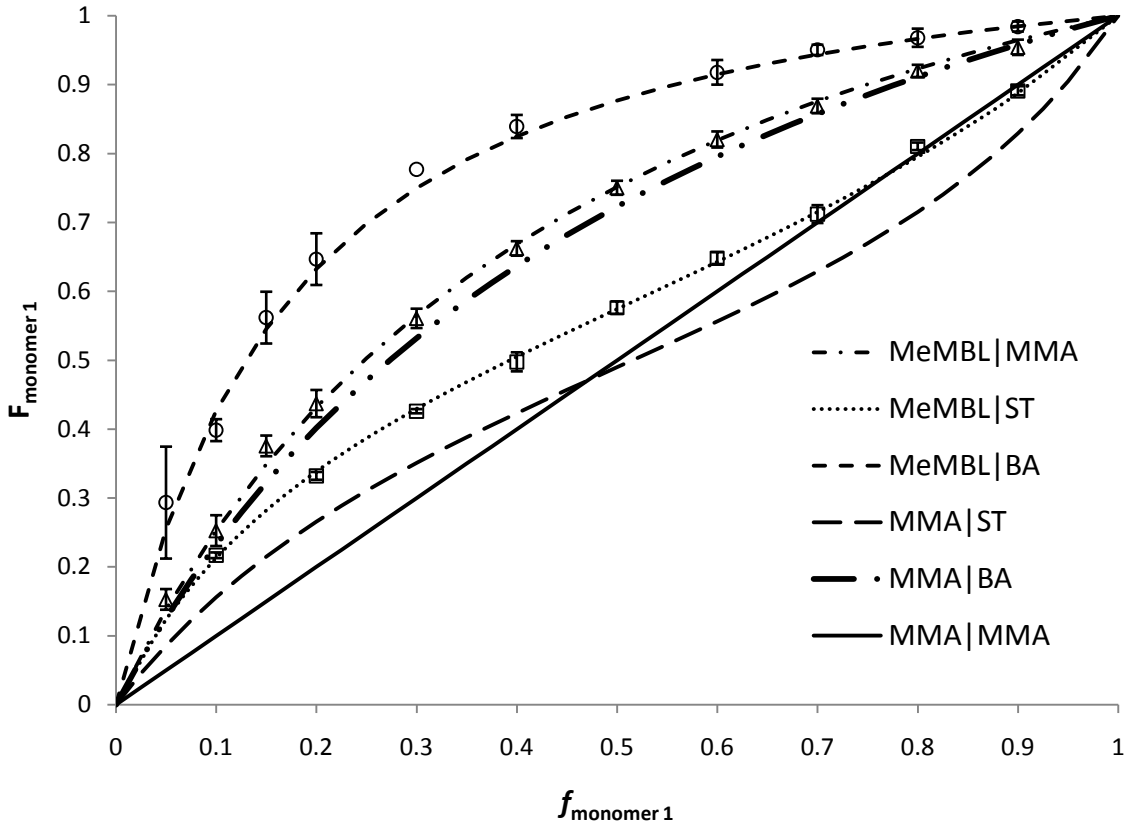

Figure 2-3 - Mole fraction in copolymer ($F_{monomer1}$) as a function of mole fraction in the monomer phase ($f_{monomer1}$) for low-conversion MeMBL/BA (○, – – –), MeMBL/ST (□,• • •) and MeMBL/MMA (Δ, – • –) bulk copolymerizations between 50 and 90 °C. Additionally, curves for MMA/MMA (—), MMA/ST (– •• –) and MMA/BA (— —) from literature are shown. All curves shown are calculated by the terminal model with associated reactivity ratios noted in Table 2-2.

It is also interesting to compare the relative activity of lactone monomers to MMA when copolymerized together. The results from this work indicate that MeMBL monomer addition is preferred over MMA addition to both MeMBL and MMA radicals (r_{MeMBL} = 3.0, r_{MMA} = 0.33). These reactivity ratios deviate from unity more than the corresponding values for α-MBL and MMA (see Table 2-2). Thus, whereas α-MBL/ST copolymers show a greater deviation from the MMA/ST system than do MeMBL/ST copolymers, the opposite is true for MeMBL/MMA copolymers compared to copolymers of α-MBL/MMA (Figure 2-5). Despite the structural similarities of the gamma lactone monomers and MMA it is clear that the rigid ring considerably affects the propagation kinetics, most likely through resonance stabilization and conjugation

effects as suggested by Pittman et al.[89] What is most surprising is the difference in reactivity between MeMBL and α-MBL monomers towards ST or MMA radicals, as the lactone rings differ only by the methyl group in the gamma position. This difference in reactivity might be explored computationally in the future, as has been done recently for polymers of ST with various methacrylates.[78]

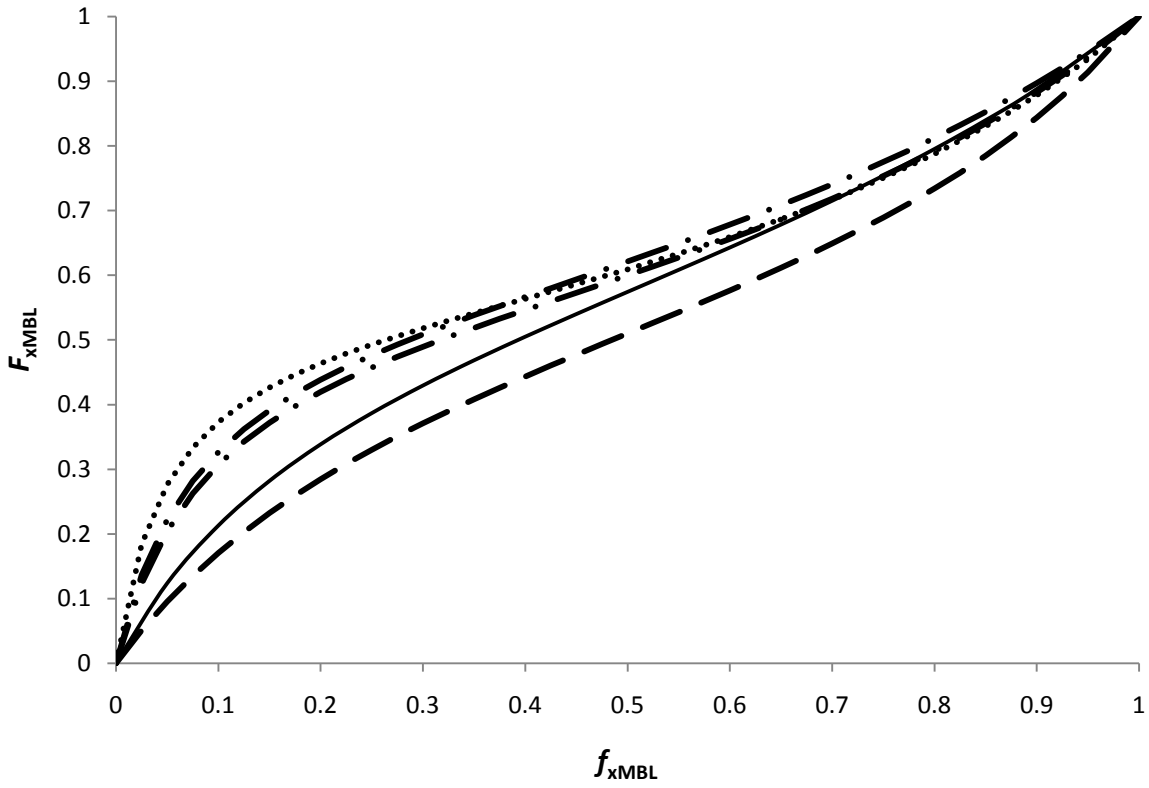

Figure 2-4 - Mole fraction of gamma lactone in copolymer (F_{xMBL}) vs. mole fraction in monomer mixture (f_{xMBL}) for MeMBL/ST **(—)**, MMBL/ST **(• • •),** and α-MBL/ST **(– • –),** with MMA/ST **(– – –)** as a reference, as calculated using the monomer reactivity ratios in Table 2-2.

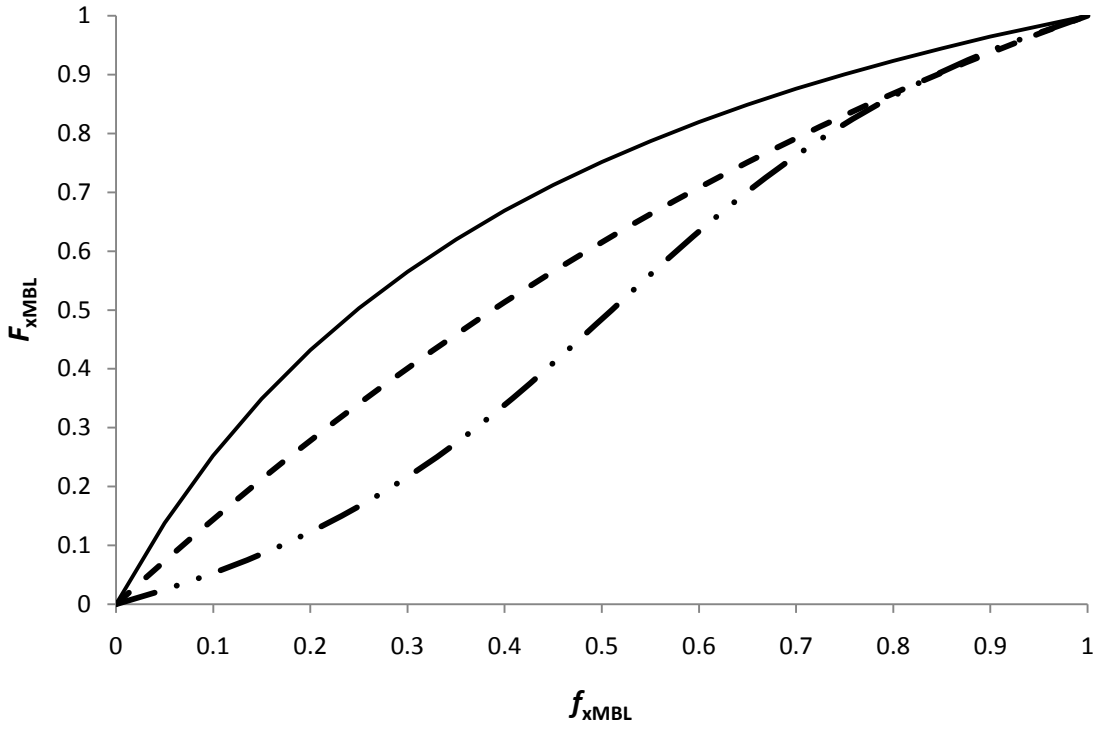

Figure 2-5 - Mole fraction of gamma lactone in copolymer (F_{xMBL}) vs. mole fraction in monomer mixture (f_{xMBL}) for MeMBL/MMA **(—)**, and α-MBL/MMA **(– – –)** with ST/MMA (– • • –**)** as a reference as calculated using the monomer reactivity ratios in Table 2-2.

The implication of these findings is that significant compositional drift will occur if MeMBL is copolymerized in a batch system, and that a fed-batch system must be used to produce copolymers with constant composition. The knowledge of the monomer reactivity ratios will allow for the production of MeMBL copolymers of well-controlled composition. As these low conversion PLP samples have uniform copolymer composition, it is useful to measure the variation of T_g with MeMBL content to provide an indication on how copolymer T_g might be tailored to fit a desired end use. The T_g values from DSC measurements are shown in Figure 2-6 as a function of MeMBL content for MeMBL/ST and MeMBL/MMA copolymers. As both MMA and ST have similar T_g values of 100 to 110 °C, the two curves are similarly shaped. In both cases, the glass transition temperature increases as the MeMBL fraction in the polymer composition increases, and behaves as may be expected based on numerous well known

copolymerization T_g models.[90-92] The MeMBL homopolymer T_g determined is within the 211-220 °C range established by Suenaga et al.[8] The plots show that T_g can be varied over a very wide range to suit a desired application. Chapter 4 will examine how the incorporation of MeMBL affects other physical properties of copolymers of well controlled composition.

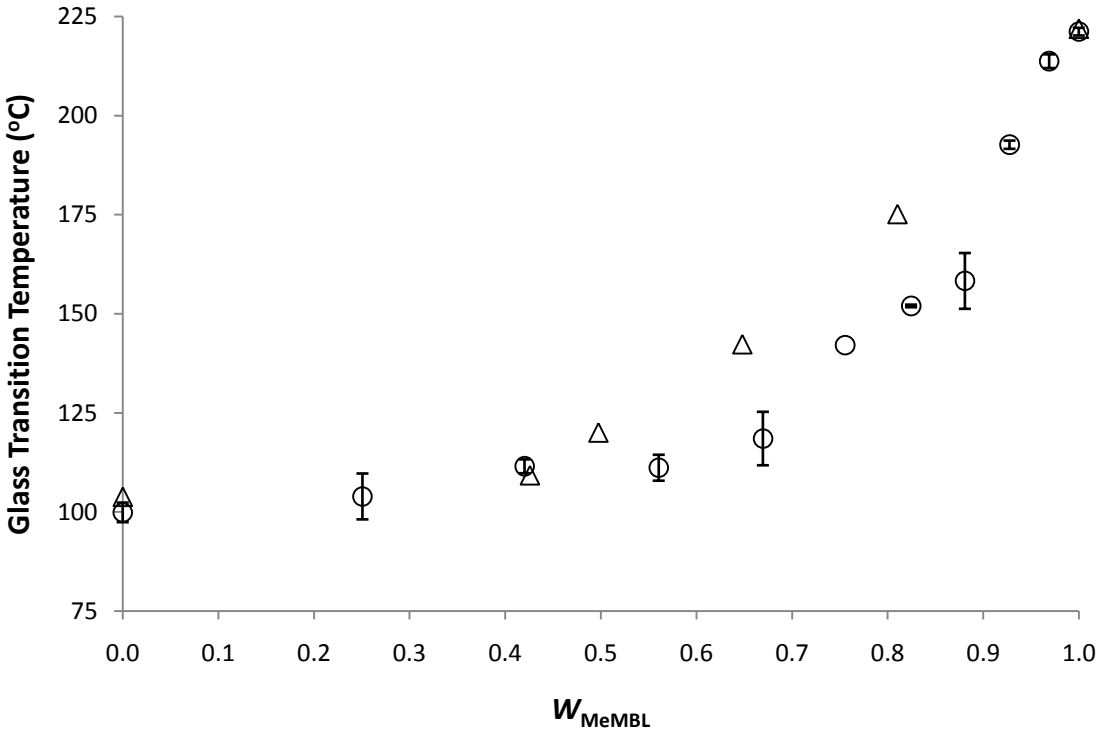

Figure 2-6 - Polymer glass transition temperature (T_g) plotted as a function of MeMBL weight fraction (W_{MeMBL}) in MeMBL/ST (Δ) and MeMBL/MMA (○) copolymers, as determined by DSC.

2.3.2 Homo- and Co- Polymerization Propagation Kinetics

The PLP/SEC technique has been shown to be an effective means of investigating $k_{p,cop}$ when well-structured MWDs (as in Figure 2-7 for MeMBL/ST) are analyzed, with values based on the first inflection point of the MWD according to:

$$k_{p,cop}\ (\mathrm{L \cdot mol^{-1} \cdot s^{-1}}) = \frac{\mathrm{MW_o}}{1000 \rho t_o} \qquad (5)$$

MW_o is the polymer molecular weight at the first inflection point and ρ ($g \cdot mL^{-1}$) is the density of monomer mixture calculated assuming volume additivity. Additionally, the PLP/SEC technique provides a self consistency check, as the MW value at the second inflection point should occur at a value double that of MW_o.

A complete list of the experimental conditions and results of the PLP/SEC studies carried out from 22 to 90 °C is summarized in Appendix A. For MMA and ST copolymerized with MeMBL the majority of experiments were conducted at 33Hz, with some experiments run with pulse repetition rates of 50Hz and 20Hz. MeMBL/BA experiments were typically run at 50Hz due to the much higher reactivity of BA, with some lower temperature experiments run at 33Hz. The $k_{p,cop}$ values obtained at different repetition rates were in good agreement. Typical polymer MWDs and corresponding first derivative curves obtained from PLP experiments conducted at 33Hz and 70 °C for varying MeMBL/ST compositions are shown in Figure 2-7 as measured by the THF LS and RI detectors. As the mole fraction of MeMBL in the comonomer mixture increases, the MWDs shift to the right and the corresponding MW_o values increase. Similar well-structured MWDs with clear primary and secondary inflection points were obtained under all conditions examined.

In the initial stages of this study, estimates for the homopolymer k_p values of MeMBL were obtained by extrapolating $k_{p,cop}$ results from MeMBL/ST (available to 80 mol% MeMBL).[84] With p(MeMBL) fully soluble in DMAc, it was possible to analyze the polymer produced by PLP over a range of temperatures (22 to 120°C) and determine homopolymer propagation coefficients using the newly obtained Mark Houwink parameters. Figure 2-8 shows the MeMBL homopolymer k_p values measured, along with the IUPAC recommended curves for MMA,[72]

ST[73] and BA.[93] The k_p values for MeMBL are similar in magnitude to MMA, while the k_p for ST is significantly lower with a higher activation energy while that for BA is much higher (by a factor of 40 at 50°C) with a lower activation energy. Based on the best fit to the MeMBL data shown in Figure 5, the activation energy (E_a) and pre-exponential factor (A) are estimated as 21.77 kJ·mol^{-1} and $10^{6.363}$, respectively. These Arrhenius parameters are compared to those of ST, MMA and BA in Table 2-3. Figure 2-8 and Table 2-3 show that the propagation kinetics of MeMBL and MMA monomers are very similar, with the activation energies comparable to many other methacrylates.[71, 75] The homopolymer MeMBL k_p values determined are used in subsequent analysis of the MeMBL/ST, MeMBL/MMA and MeMBL/BA copolymer data sets and are available in Appendix A.

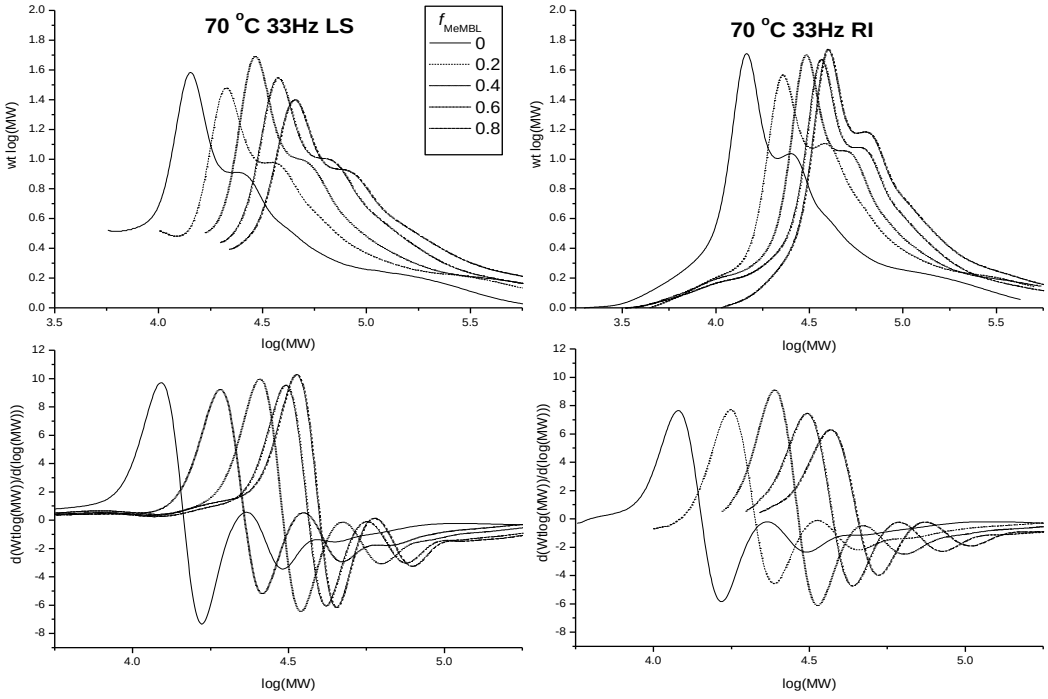

Figure 2-7 - MWDs (top) and corresponding first derivative (bottom) plots obtained for MeMBL/ST copolymers produced by PLP at 70 °C and 33 Hz, as measured by LS (left) and RI (right) detectors. Monomer compositions are given as mole fraction MeMBL (f_{MeMBL}), with increasing f_{MeMBL} values accompanied by a shift of the MWDs and first derivative curves to the right.

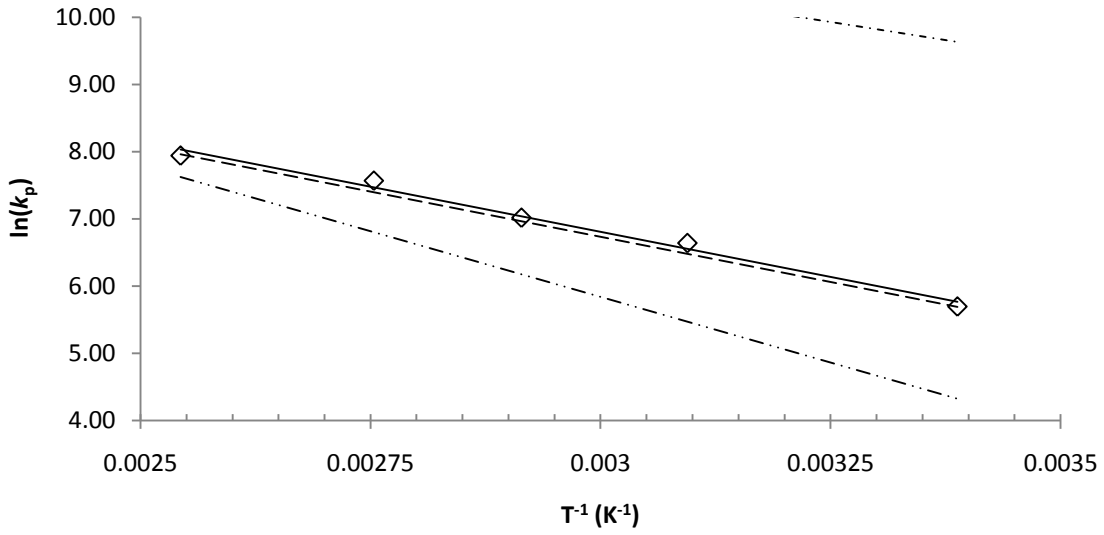

Figure 2-8 - Arrhenius plot of ln(k_p) vs inverse temperature for MeMBL compared to IUPAC-recommended Arrhenius equations for MMA[72] (– –), ST[73] (– • • –) and BA[93] (– • –). The line for MeMBL (◊, —) is best fit for the data points shown.

Table 2-3 - Arrhenius parameters for MeMBL, MMA, BA and ST homopropagation kinetics

Monomer	**E_a** ($kJ \cdot mol^{-1}$)	**$Log_{10}A$** ($L \cdot mol^{-1} \cdot s^{-1}$)	**$k_p(50^oC)$** ($L \cdot mol^{-1} \cdot s^{-1}$)
MeMBL[This Work]	22.32	6.45	687
MMA[72]	22.36	6.43	650
BA[93]	17.90	7.35	28,650
ST[73]	32.50	7.63	237

The terminal model significantly overpredicts the $k_{p,cop}$ data as can be seen in Figure 2-9. Given the failure of the terminal model, the IPUE representation (Equation 3 and 4) has also been fit to the complete set of experimental data in Figure 2-9. All data points were weighted equally, and the fit was performed using the monomer reactivity ratios identified previously and $k_{p,iii}$ values as determined for MeMBL and the other monomers from their Arrhenius parameters presented in Table 2-3. The nonlinear parameter estimation was done in the Predici® package,[94, 95] which uses

a Gauss-Newton technique and calculates 95% confidence intervals from the variance-covariance matrix. Temperature-independent radical reactivity ratios were estimated by fitting Equation 3 and 4 to the experimental $k_{p,cop}$ data over the entire 22-90 °C temperature range as a function of f_{MeMBL}. The radical reactivity ratios of the MeMBL/ST system presented here have been revised from the first estimates presented in Cockburn et al. [84] to provide better estimates and the improved IPUE model fit is shown in Figure 2-9, along with the $k_{p,cop}$ data measured in THF using the two detectors. The primary improvement to the data set comes from adding the newly determined MeMBL homopolymer k_p value to the data sets. The non-linear parameter estimates of the radical reactivity ratios are s_{MeMBL} = 1.01±0.21 and s_{ST} = 0.63±0.06, within the confidence intervals of the values published previously using the ±15% homopolymers k_p value estimates.[84]

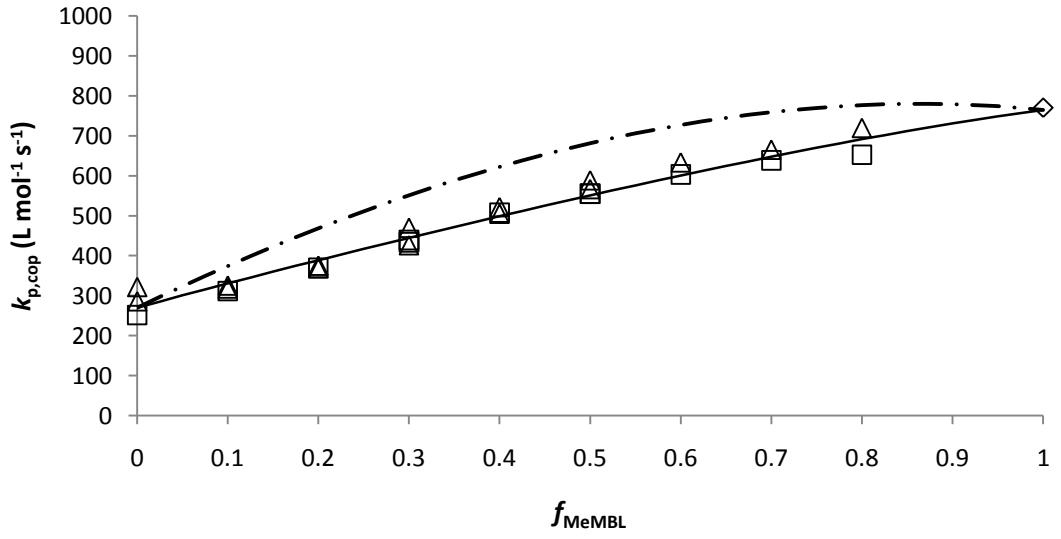

Figure 2-9 - Copolymer propagation rate coefficients ($k_{p,cop}$) data for the MeMBL/ST system vs MeMBL monomer mole fraction, f_{MeMBL}, as measured by PLP/SEC at 50 °C and 33Hz. Predictions calculated from the terminal model (– • –) and IPUE model (—) are shown.. $k_{p,cop}$ data are estimated from THF SEC analysis with RI (□) and LS (Δ) detectors, while The MeMBL homopolymer k_p value measured in DMAc (◊) is also shown.

At 50 °C, the homopolymerization $k_{p,cop}$ values of MeMBL, MMA and ST are 764, 650 and 237 L·mol^{-1}·s^{-1}, respectively, compared to a value of over 28600 L·mol^{-1}·s^{-1} for BA at the same

temperature (Table 2-3).[93] Figure 2-10, which plots the $k_{p,cop}$ values for the MeMBL/BA system at 50 °C and the IPUE and terminal model fits to the data, shows that the $k_{p,cop}$ values of the copolymerization system are much closer to the homopolymerization of MeMBL than of BA. The higher reactivity of BA as well as the side reaction of intermolecular chain transfer[93] presents difficulties in obtaining good PLP structure for $f_{MeMBL} < 0.1$. It is clear, however, that the terminal model underrepresents the experimental data by greater than 50% at high concentrations of BA and does not adequately fit the data. Using the non-linear parameter estimation capabilities of Predici®[94, 95] , it was determined that the shape of the IPUE curve is insensitive to the value of s_{BA} over a large range that encompasses unity, as also was found for MMA/BA copolymerization. [85] The radical reactivity ratios used to generate the IPUE curve in Figure 2-10 were $s_{MeMBL} = 6$ and $s_{BA} = 1$; the improved fit of the model to the data suggests that the presence of BA in the penultimate position increases the addition rate of MeMBL to a MeMBL radical ($s_{MemBL}>1$), as also found for MMA/BA copolymerization. [85]

Figure 2-11 presents the $k_{p,cop}$ values for the MeMBL/MMA system at 50 °C and shows both IPUE and terminal model fits to the data. The plot combines results measured in THF for monomer mixtures with less than 50 mol% MeMBL with results over the complete composition estimated from SEC analysis in DMAc, with good agreement between the two analyses. The $k_{p,cop}$ data shows a slight decrease as MeMBL is added to MMA, then climb to the higher k_p values measured for MeMBL. The overall variation is small as the two monomers differ in k_p values by only approximately 15%. The terminal model provides a reasonable prediction of the slope of the $k_{p,cop}$ curve as a function of f_{MeMBL} but under-predicts slightly the experimental data by about 10%. The data can be better fit using the penultimate model with $s_{MeMBL} = 2.5$ and $s_{MMA} = 0.6$. However, given the scatter in the data, these estimates have large uncertainty and the confidence intervals encompass unity (equivalent to terminal model values). While the actual difference

between the IPUE and terminal model predicitions is of the order of the scatter of the data, the addition of the radical reactivity parameters does improve the data fit.

Figure 2-12 plots the copolymer $k_{p,cop}$ data and IPUE model fits for all three systems measured at 90 ^{o}C. The trends are as found at 50 ^{o}C, with $k_{p,cop}$ relatively constant for the MeMBL/MMA system (between 1550 and 1950 L·mol^{-1}·s^{-1}) and decreasing smoothly for the MeMBL/ST system with decreasing f_{MeMBL} (from 1950 to 800 L·mol^{-1}·s^{-1}). For MeMBL/BA $k_{p,cop}$ also decreases with decreasing f_{MeMBL}, then starts to rise steeply towards the much higher BA value for f_{MeMBL}<0.2. Despite the uncertainty in the s parameters estimated at 50 ^{o}C, the results are well represented by the IPUE model for all cases. In Figure 2-12, the data appear to converge nicely towards the measured MeMBL k_p values and data at both temperatures appears to be well fit by the radical reactivity ratios indicated in this work. MeMBL/ST data and IPUE model fits are shown in Figure 2-13 over the entire range of temperatures studied (22^{o}C to 90^{o}C). Again the IPUE model provides a good fit to the data over a range of temperatures, indicating that the radical reactivity parameters determined for this system are temperature independent. Additional temperature data for MeMBL/MMA copolymers can be found in the supplemental data tables in this work and figures and data tables in Cockburn et al.[84]

2.4 Conclusions

The PLP/SEC technique has been employed to systematically investigate free radical bulk copolymerization of the bio-renewable monomer MeMBL with three monomers commonly used in industry; Styrene, Methyl Methacrylate and Butyl Acrylate. Analysis was conducted using both THF and DMAc eluents for SEC as p(MeMBL) is fully soluble in the latter and copolymer solubility of the systems studied in THF varies with the mol fraction of MeMBL. Investigation of the complete copolymer composition range for each system and of the MeMBL homopolymer provides insight into the reactivity of lactone monomers relative to other common monomers.

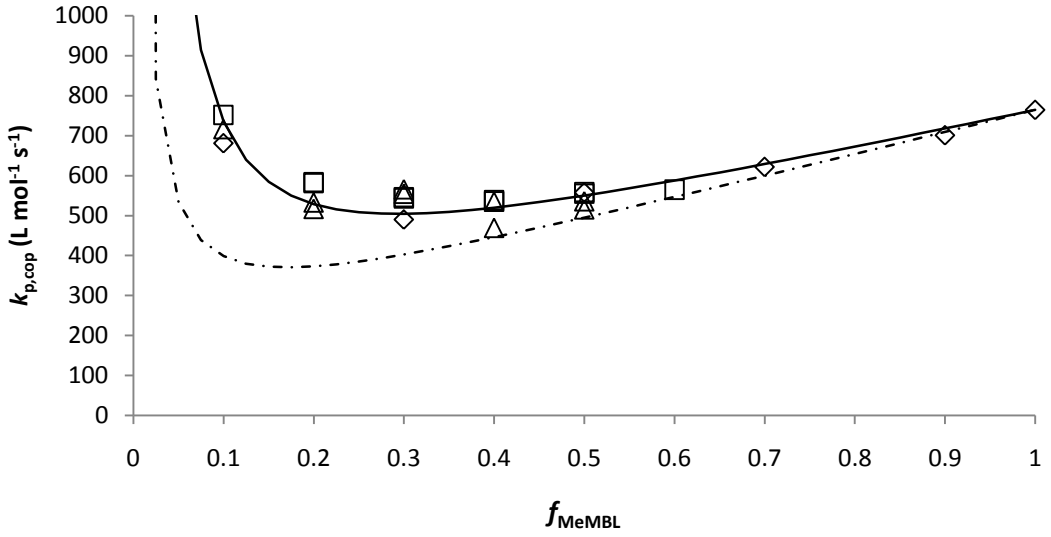

Figure 2-10 - Copolymer propagation rate coefficients ($k_{p,cop}$) data for the MeMBL/BA system vs MeMBL monomer mole fraction, f_{MeMBL}, as measured by PLP/SEC at 50 °C and 33Hz. Predictions calculated from the terminal model (– • –) and IPUE model (—) are shown. $k_{p,cop}$ data are estimated from THF SEC analysis with RI (□) and LS (Δ) detectors, as well as by DMAc SEC analysis (◊).

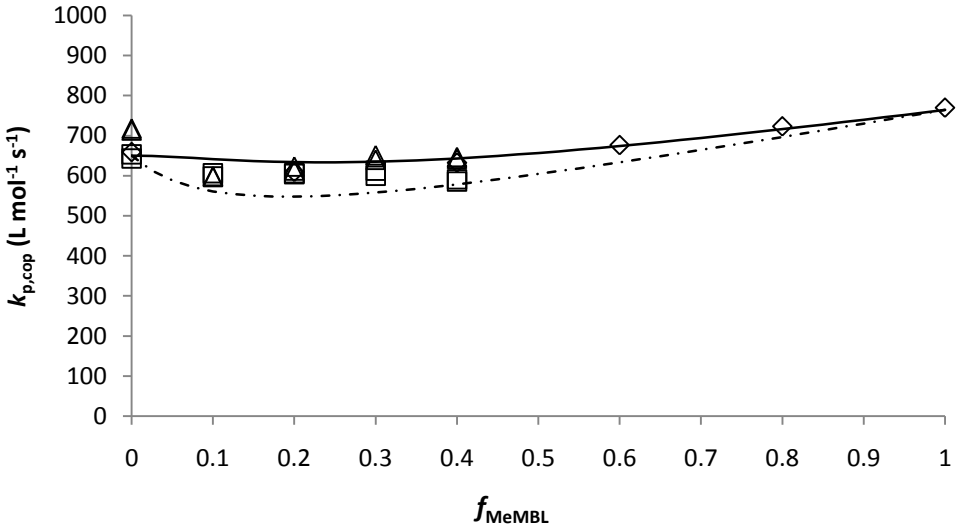

Figure 2-11 - Copolymer propagation rate coefficients ($k_{p,cop}$) data for the MeMBL/MMA system vs MeMBL monomer mole fraction, f_{MeMBL}, as measured by PLP/SEC at 50 °C and 33Hz. Predictions calculated from the terminal model (– • –) and IPUE model (—) are shown. $k_{p,cop}$ data are estimated from THF SEC analysis with RI (□) and LS (Δ) detectors, as well as by DMAc SEC analysis (◊).

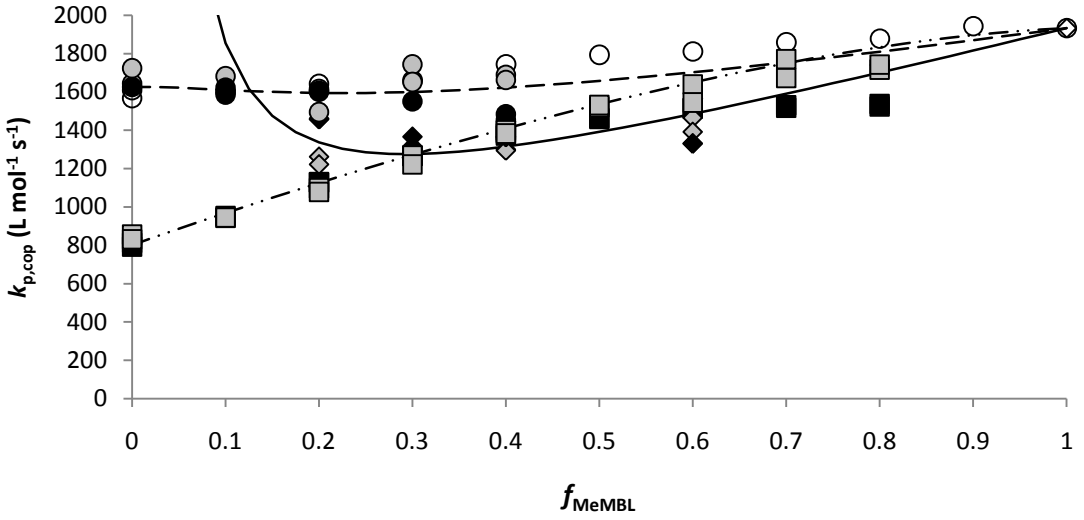

Figure 2-12 - Copolymer propagation rate coefficients ($k_{p,cop}$) data and IPUE model predictions for the MeMBL/ST (□, – •• –), MeMBL/MMA (○, — —) and MeMBL/BA (◊, ——) systems vs MeMBL monomer mole fraction, f_{MeMBL}, as measured by PLP/SEC at 90°C . $k_{p,cop}$ data are estimated from THF SEC analysis with RI (grey symbols) and LS (black symbols) detectors, as well as by DMAc SEC analysis (unfilled symbols).

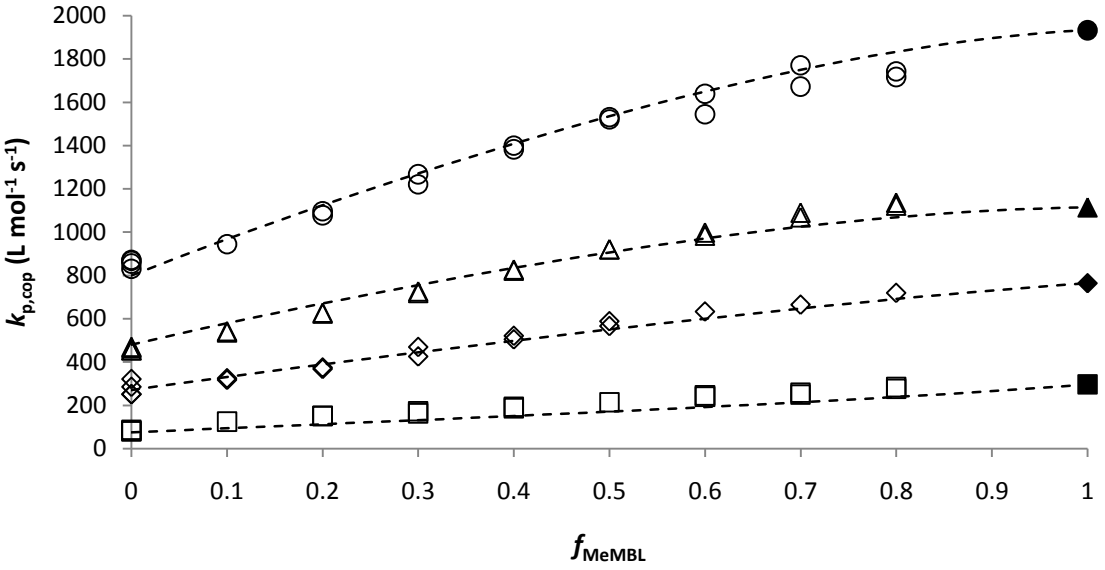

Figure 2-13 - Experimental MeMBL/ST copolymer propagation rate coefficients, $k_{p,cop}$ (L·mol^{-1}·s^{-1}), plotted against MeMBL monomer mole fraction, f_{MeMBL}, over a range of temperatures (□ 22 °C, ◊ 50 °C, Δ 70 °C, ○ 90 °C) from SEC analysis (THF open symbols, DMAc shaded symbols) of PLP experiments at 33Hz.

The homopolymer reactivity of MeMBL has been found to be quite similar to that of MMA, as reflected in the small difference between their homopolymer k_p values (approximately 15%), and an Arrhenius expression for MeMBL has been presented for the first time. Copolymer composition data, as measured using proton NMR, is well-represented by the terminal model in all cases.

MeMBL preferentially is incorporated into copolymer systems with ST, BA and MMA, even more so than MMA copolymerized with the same monomers. This compositional drift will need to be considered when conducting copolymerizations in batch. Fitting of the terminal model to experimental $k_{p,cop}$ data suggests that it does not adequately represent the copolymerization kinetics of any of the systems studied, which were well-described by the implicit penultimate unit effect (IPUE) model.. The kinetic values determined by PLP will be used to design a polymerization system to produce MeMBL copolymers with controlled composition, in order to systematically investigate physical properties of the polymers created, and to evaluate the potential use of this bio-renewable monomer.

2.5 Acknowledgements

I wish to thank Mr.. Kevin Payne, another graduate student in the lab for his assistance in conducting the MeMBL/BA PLP experiments. I am also grateful for the help of Ms.. Rebekka Siegmann, a doctoral candidate in the lab of Dr. Sabine Beuermann in Germany, without whom I could not have analyzed the MeMBL rich polymers.

Chapter 3

Investigations into the Dispersed Phase Polymerization of the MMA homopolymer and copolymers of MeMBL

3.1 Introduction

Having originally been produced via bulk polymerization and solution polymerization in benzene,[8] one of the aims of this research project was to understand the polymerization behaviours of MeMBL and develop a method to successfully produce a variety of homopolymers and copolymers in more easily controllable and comparable systems. To this end, research was first conducted as part of the CHEM 417 undergraduate thesis[96] requirements of the Engineering Chemistry degree program. The first polymerization method studied for the MeMBL/MMA system was emulsion polymerization. Reactions with MMA were highly successful over a range of temperatures (50-75^{o}C) and resulted in conversion of no less than 96% in two hours. Polymerizations with MeMBL were less successful, and resulted in unstable latexes that coagulated to form highly viscous, water containing gels.[96] The water solubility of MeMBL is about 9 percent by weight at room temperature (more than 6x that of MMA), a significant amount that likely causes stability issues in aqueous polymerization systems, as discussed in Qi et al. in their recent study of MeMBL miniemulsion and emulsion homopolymerization behaviour and kinetics.[24] They noted that their latexes had only moderate stability and a shelf life of not more than two hours at low conversion (less than 15 percent) after optimization of their recipe with both a surfactant (SDS) and a co-stabilizer, hexadecane.[24] Because of these difficulties, the polymerization of MMA and MeMBL by a different method, suspension polymerization, was explored. Again, reactions with MMA were successful and produced the desired homopolymer beads. However, aggregation was observed during the polymerization of MeMBL and in all cases a stable system was not obtained. Multiple attempts to control the polymerization process by

systematically varying the concentration of surfactant in the system were ineffective.[96] Again, the high water solubility of MeMBL appeared to be the major contributing factor that prevented the formation of a stable MeMBL suspension in an aqueous system.

Problems with aqueous phase polymerizations led to investigations into organic solvents capable of polymerizing both MMA and MeMBL. This effort concentrated on first finding a method capable of polymerizing MeMBL, then later applying it to produce MMA.[96] The next technique examined was precipitation polymerization. By trial and error, the MeMBL monomer was found to be soluble in a number of solvents, including xylenes, ethyl acetate and *n*-butanol; The MeMBL polymer produced via emulsion polymerization was dried and tested in these solvents and was found to be insoluble.[96] By varying the solvent used in the reaction, it was found that the precipitated polymer was most stable (not observed to coagulate) in *n*-butanol.[96] Given the success with *n*-butanol and MeMBL, polymerizations with MMA in the same solvent were explored.[96] Like MeMBL, the MMA monomer is soluble in *n*-butanol, however, unlike MeMBL, MMA polymer is also soluble in the solvent and so solution rather than precipitation polymerization occurred.[96] Copolymers of MeMBL and MMA were produced in *n*-butanol in addition to MeMBL and MMA homopolymers.[96] The presence of solvent in the sample even after drying and the poor thermal degradation profiles as shown by TGA, along with the inability of MMA to precipitate in *n*-butanol indicated that this polymerization method was not ideal. However, since MeMBL was successfully polymerized via precipitation polymerization in an organic solvent, further research was conducted to find a system that would support precipitation of both MeMBL and MMA.

A literature search on precipitation polymerizations of MMA led to the discovery of a number of investigations carried out via dispersion polymerization (precipitation polymerization with a surfactant). Formulations for dispersions of MMA as published originally in a series of papers by Cao et al.[53, 97] and furthered by Jiang et al.[43-45] provide a basis to develop recipes for stable

dispersions of MeMBL/MMA copolymers with little modification. These studies were extremely limited due to the scope of the undergraduate thesis and timeframe and as such, a major undertaking as part of this thesis has been to thoroughly investigate the dispersion technique.

As part of the process of formulating dispersion recipes for MeMBL and investigating its polymerization behaviours, a good understanding of the mechanisms of dispersion polymerization is essential. A number of researchers, notably the groups of El-Aasser/ Vanderhoff[43-45, 49, 52, 55, 98, 99] and Paine,[51, 54, 100, 101] have studied the dispersion polymerization technique extensively since Almog et al. first published their work on dispersions in alcoholic media in 1982.[46] The effects of initiator, stabilizer, reaction media and temperature on the polymerization have been well characterized for common monomers such as MMA and ST and even for some copolymers, but there remain opportunities to improve our knowledge and understanding of the mechanisms of the dispersion process, especially with new monomers. In particular, the mechanisms that relate to the nucleation of the particle phase are of great interest.

A number of authors have recognized the importance of nucleation on particle size and development in dispersion polymerization.[46, 52, 54, 99, 102-105] It is well accepted that the polymerization process has two reaction loci, beginning as an initially homogenous system where solution polymerization dominates until the polymer produced reaches a critical chain length and ceases to be soluble in the media with polymerization thereafter continuing in both solution and in a pseudo-bulk manner within the polymer particles.[52, 54, 98] Nucleation, by various mechanisms including homogenous nucleation, heterogenous nucleation and coagulative nucleation, occurs after the critical chain length of the polymer is reached and the small nuclei rapidly grow into larger particles by aggregation until such point in time as they become mature particles, effectively stabilized by steric stabilizers such as poly(vinyl pyrrolidone), PVP, which function by both grafting and adsorbing onto the growing polymer particles.[49, 54, 55] A steady flux of nuclei which form larger aggregates that are swept up by the mature particles is supplied over the course

of the reaction until either the monomer or radical source is depleted.[49, 55] The aggregates of nuclei that are generated in the reaction are typically about one tenth as large as the mature particles and are largely considered to be unstable and quickly captured by the mature particles.[45, 49, 54]

In the process of creating MeMBL copolymer dispersions and verifying the previous work of Cao et al. and Jiang et al. with MMA for our own comparisons, we found a distinct population of small particles present and detectable throughout the polymerization of both monomers, as well as afterwards. Although the dispersion polymerization technique has been the subject of some attention over the past 20 years and more recently,[57, 58] there is still room to improve our understanding of the mechanisms involved in nucleation and particle growth/stability. This section details further study of the small particle populations that have been observed and offers additional insight into the nature of nucleation and particle growth in dispersed systems. Additionally, as will also be described in this chapter, copolymerizations with MeMBL and MMA and controlled radical polymerizations of MMA using catalytic chain transfer agents (CCT)[106-108] have been used to further study the dispersion polymerization technique.

3.2 Experimental

3.2.1 Materials

MMA inhibited with 10-100 ppm of MEHQ (99% purity) was purchased from Sigma Aldrich and used as received. MeMBL inhibited with 50 ppm of hydroquinone (97.5% purity, major impurity gamma valerolactone) was obtained from DuPont Central Research Laboratories and used as received. All other materials including methanol (99.9% purity, Fischer Scientific), the initiator Vazo 67 (2,2'-Azobis(2-methylbutyronitrile), DuPont) and PVP-40 (Poly Vinyl Pyrrolidone, Avg MW 40 kDa, K value 29-32, Sigma Aldrich) were used without further purification. Materials were not purified as previous research has indicated that doing so has no effect on the molecular

weight or particle size of the polymer produced.[105] Distilled, deionized water was used in all experiments.

3.2.2 Polymerization and Characterization

All dispersion polymerizations were carried out in a 250 mL jacketed glass reactor. The standard polymerization recipe is shown in Table 3-1. Polymerizations were conducted at 60^{o}C and stirred at 180 rpm under Nitrogen atmosphere for 3 to 9 hours. The 60^{o}C temperature was chosen since it was used in the work by Cao et al.[53, 97] and because the boiling point of the 70% methanol, 30% water solution is approximately 72^{o}C and may present control issues at reaction temperatures (70^{o}C) used by Jiang et al.[43-45] Preliminary tests with different stirring speeds (150, 240, 360 rpm) revealed minimal effect on the particle sizes formed, but higher speeds did tend to cause aggregation of the particles in some trials, thus a lower setting (180rpm) between the rates used by Cao et al. [53, 97] (120rpm) and Jiang et al. [43-45] (400rpm) was used. However, it should be noted that a comparison of rpm settings may not be reliable due to geometric differences in the tanks and agitators used in each study. The total solid contents of the polymer particles formed in the dispersion polymerization at final conversion is about 10%, as in previous studies.[43-45, 53, 97] For each polymerization, all ingredients were initially charged into the reactor and brought up to temperature except for the initiator (0.4g) dissolved in monomer (20.0g) which was added to start the reaction as in previous studies. [43-45] The addition of the initiator and monomer solution to start the reaction typically would cause a drop in the temperature of the vessel to about 57^{o}C. The reaction temperature quickly returned to the 60^{o}C setpoint within a few minutes (3-5 minutes) and control of the temperature during the reaction was within ±1^{o}C. The composition of the methanol water continuous phase was varied in some experiments keeping the total proportions of the recipe seen in Table 3-1 the same. Conversion for all experiments conducted was measured by gravimetric analysis. All polymer samples were immersed in an ice bath to stop the polymerization and were isolated from solution by drying at room temperatures for 18 hours and

further drying in a vacuum oven at -25inHg at 60°C for 24 hours. Gravimetry results were corrected to account for the presence of PVP in the sample.

Table 3-1– Recipe for Dispersion Polymerization (60°C, 180 rpm)[a] in Glass Reactor

Ingredient	Weight (g)	Amount[a] (%)
Total Monomer	20.0	100
Vazo 67[b]	0.4000	2.0
PVP 40[c]	3.0	15
Methanol/Water (70/30 wt/wt)	200.0	-

[a] Based on monomer
[b] 2-Amino-2-methylbutyronitrile
[c] Poly(vinyl pyrrolidone), PVP 40 MW = 40,000 g/mol K value 29-32

3.2.3 Particle Size Characterization

The particles produced by dispersion polymerization were analyzed by SEM and light scattering techniques. The average particle size (PS) and particle size distribution (PSD) of each sample without any washing were obtained from measurements using a Beckmann LS 13 320 Laser Diffraction particle size analyzer. Scanning electron microscopy (SEM, Jeol JSM 840) and Transmission Electron Microscopy (TEM, Phillips CM20) were also used to investigate the morphology of the particles. For SEM, a drop of diluted latex was placed on an aluminum stub and dried in a hood at room temperature and a 15Å gold coating was applied prior to testing at 10keV acceleration voltage. TEM studies were carried out at 80kV acceleration voltage with an ultrathin window EDS system.

3.2.4 Molecular Weight Analysis

Size exclusion chromatography (SEC) was performed using a Viscotek 270max separation module and a refractive index (RI), viscosity (IV) and light scattering (low angle LALS and right angle RALS) triple detector setup. A set of two porous PolyAnalytik columns with an exclusion limit molecular weight of $20 \cdot 10^6$ g·mol^{-1} were

used in series at 40°C. Distilled THF was used as the eluent at a flow rate of 1 $mL \cdot min^{-1}$. The number-average (M_n), weight-average molecular weight (M_W) and the polydispersity index (PDI = M_W / M_n) of the molecular weight distribution (MWD) are calculated using a calibration curve based on the RI detector which was constructed using narrow molecular weight polystyrene standards ranging from 6910 to 3,300,000 $g \cdot mol^{-1}$. The SEC setup described in Chapter 2 was also used for analysis, but the most polymers in this chapter required columns capable of analyzing higher MW samples and a device with a greater calibration range.

3.3 Results and Discussion

In a typical dispersion polymerization, such as those described by Cao et al.[53, 97] and Jiang et al.[43-45] and reproduced here, the reaction begins homogenously on the addition of monomer and dissolved initiator to the preheated continuous phase. After a short period of time, typically less than 10 minutes (less than 5% conversion), the reaction mixture begins to turn translucent as polymer particles begin to precipitate from solution, stabilized by the grafted PVP surfactant. Eventually, by about 30 minutes (about 10% conversion) the polymerization appears to be opaque and "milky" in colour, owing to the scattering of light by many dispersed particles in the continuous phase.[49] The number of large particles formed in the reaction is set at low conversion, and the cube of the volume of these particles has a linear relationship with conversion. [97] The reaction proceeds with particle size increasing with conversion and plateauing within a few hours.

Before starting the discussion of the dispersion polymerizations in earnest, it should be noted that for all polymerizations presented, there appears to be a limit to the degree of conversion that can be achieved. This is a well known occurrence seen in bulk and multi phase polymerizations when the T_g of the polymer being formed is above the reaction temperature.[109] Polymerizations carried

out at 60°C are well below the T_g of MMA (105°C) and greatly below that of MeMBL (215°C). Akkapeddi noted the limiting conversion of α-MBL bulk polymerizations to be about 72% at 60°C[6] and the works by Cao and others never present conversion vs. time data, but lack any data above 90% conversion in other plotted figures.[43-45, 53, 97] Among other factors, the limit to the final conversion depends on the temperature of the reaction and also how long the reaction is allowed to proceed, as the ultimate value is approached slowly on nearing the limit.[109] In his review of the dispersion technique, Barrett states that dispersions of MMA in petrol at reflux temperatures can achieve conversion of 99% in as little as one hour.[41] Thus, the limiting conversion is not unexpected in this case given the low temperatures of operation and is in line with that seen for similar monomers in literature.[6, 109]

Our experiments confirm the general trends reported about dispersion polymerizations in the literature.[43-45, 53, 97] However, we note an additional observation not previously reported, the presence of a distinct and separate population of small particles present over the entire course of the dispersion polymerizations. Our results show that the small particle population is stable (i.e. detected over a range of reaction conditions with variations in number but always constant in size) – a point not addressed previously.[43-45, 49, 53, 54, 97] While dispersion polymerization literature proposes the existence of a population of small particles, the focus has been limited to the initial phases of the polymerization during which the stable large particles are formed, with their number then remaining constant over the course of the polymerization.[45, 49, 54] To our knowledge, only Mandal and Mandal have noted the presence of the smaller population of particles in their work with polypyrrole dispersions.[103] These small nuclei were similar to those detected here, making up 1-2% of the mass of particles detected and being about a tenth the size of the larger particles which were formed and whose size increased linearly with conversion.[103] An example of the typical output from the LS 13 320 software is shown in Figure 3-1 with the volume distribution (top) consisting mostly of large particles and the number distribution (bottom) of the

same sample dominated by a much smaller particle population. Figure 3-1 shows a sample taken at the end (210 minutes, 85% conversion) of a reaction conducted in a 70|30 MeOH|water dispersion. It should be noted that the data shown in the figures in this chapter is from a single experiment of each condition that is representative of multiple repeated experiments. Figure 3-2 shows the averaged results for conversion vs. time, large particle diameter and small particle diameter of all experimental replicates conducted for the MMA dispersion described in Table 3-1 where error bars are based of ±1 standard deviation from the average of all measurements. Similar plots (not shown) were created for all other conditions presented in this chapter, provided in Appendix B.

Using the LS 13 320 to measure the particle size growth at regular intervals over the course of the polymerization, it is possible to plot the growth of the polymer particles vs. time or conversion. By separately keeping track of the distributions of the distinct large (>0.8μm) and small (<0.4μm) particle populations, the change in the number of particles is followed. Typical particle size evolutions of the large particle population for a number of MMA experiments produced in a 70|30 MeOH|Water dispersion are shown in Figure 3-3 with a linear relationship between the average particle volume and conversion seen on the secondary axis (note that the linear relationship for only one of the data sets is shown). The linear relationship seen with large particle growth shows that the number of these particles in the system is fixed, as has been stated previously in the literature.[97] While there may be some scatter between experimental replicates in terms of the final particle size measurements, reflected in Figure 3-2, all reactions show the linear profile with respect to the cube of particle size.

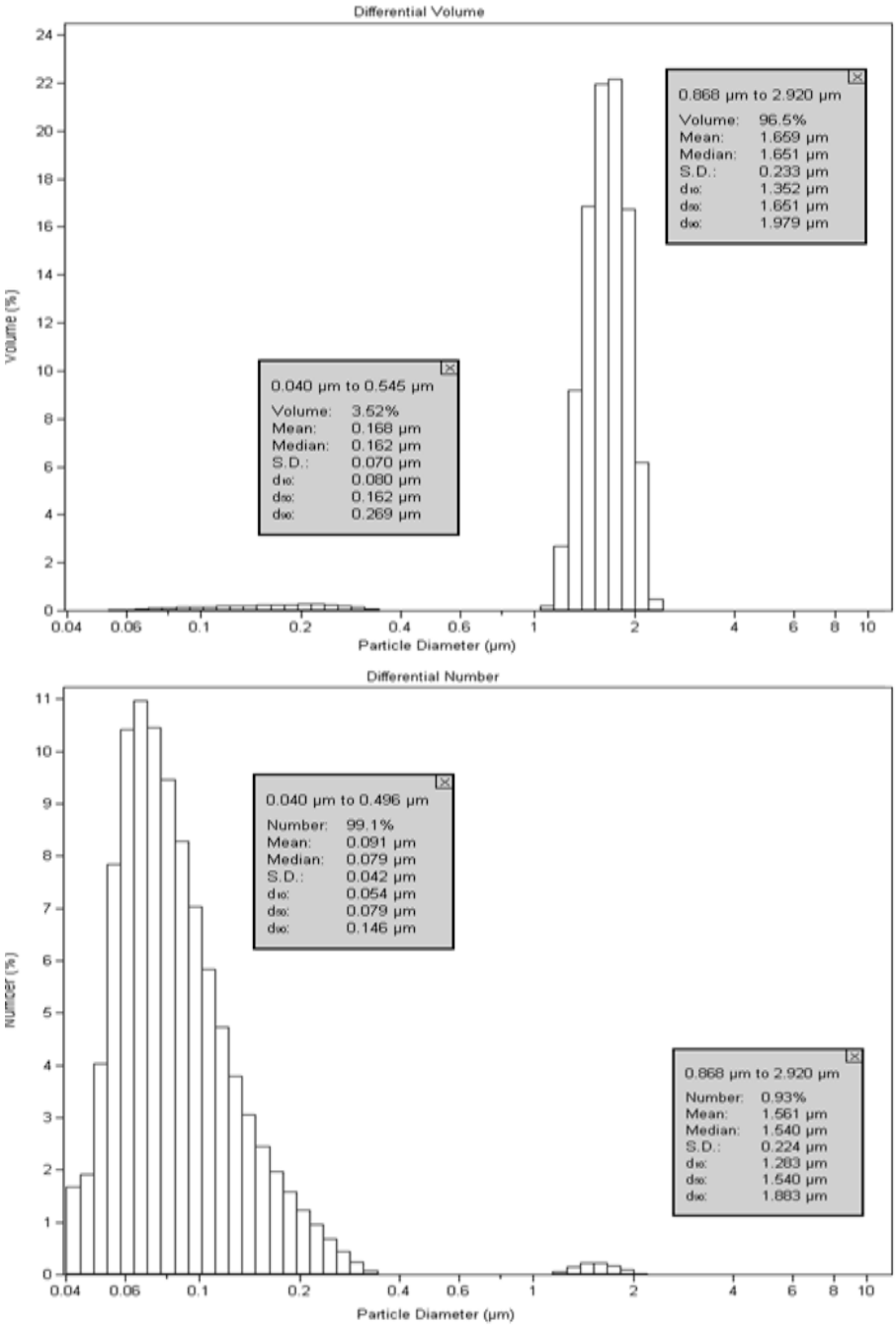

Figure 3-1 – Beckman LS310 Laser Particle Size analyzer output for a typical MMA dispersion polymerization showing volume (top) and number (bottom) particle size distributions at the end of the reaction.

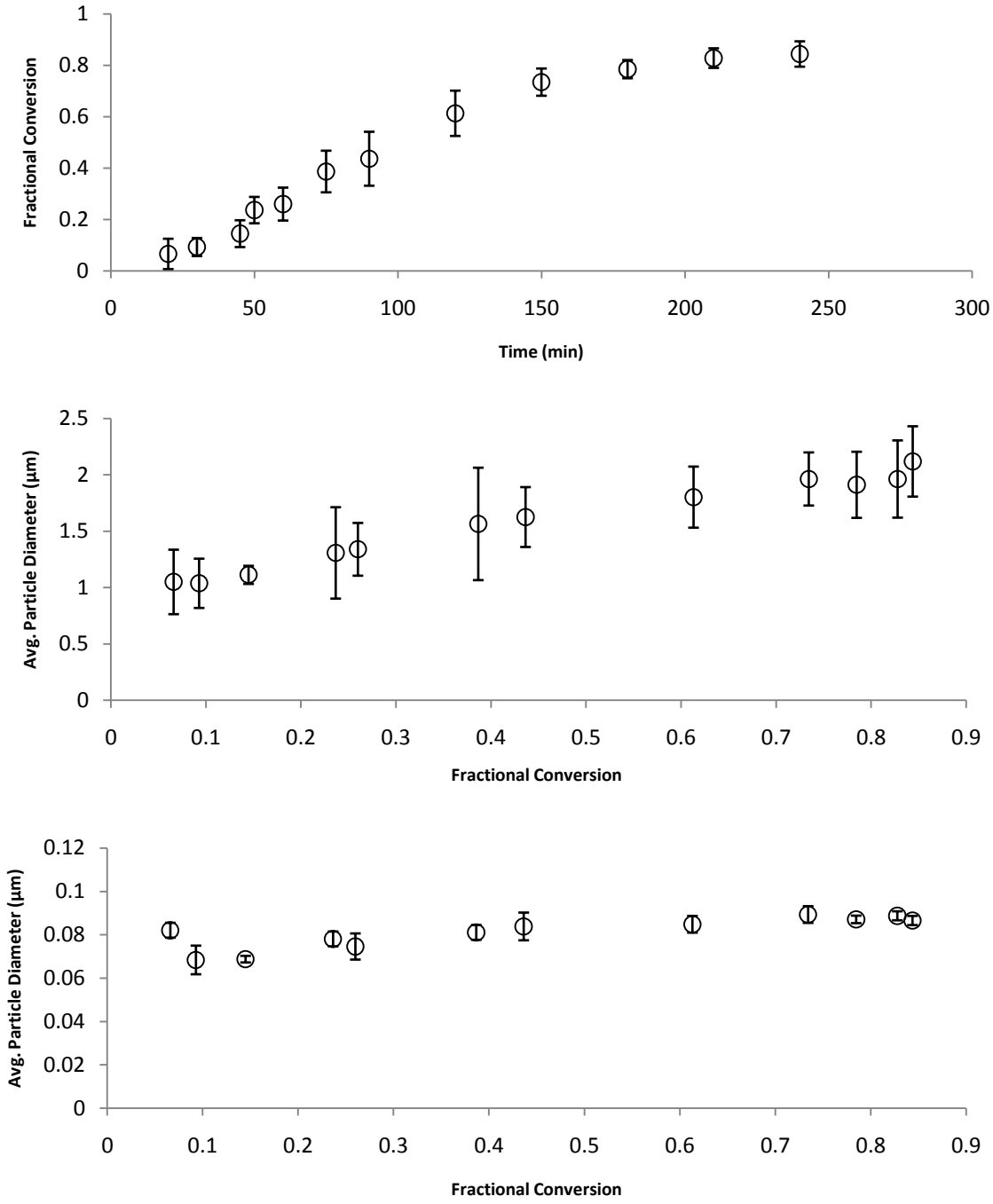

Figure 3-2 - Fractional conversion vs. time (top), volume average particle diameter of large particles as a function of fractional conversion (middle) and number average particle diameter (bottom) for MMA dispersion polymerizations carried out at 60°C in a continuous phase of 70|30 MeOH|Water composition, as in Table 3-1.

.

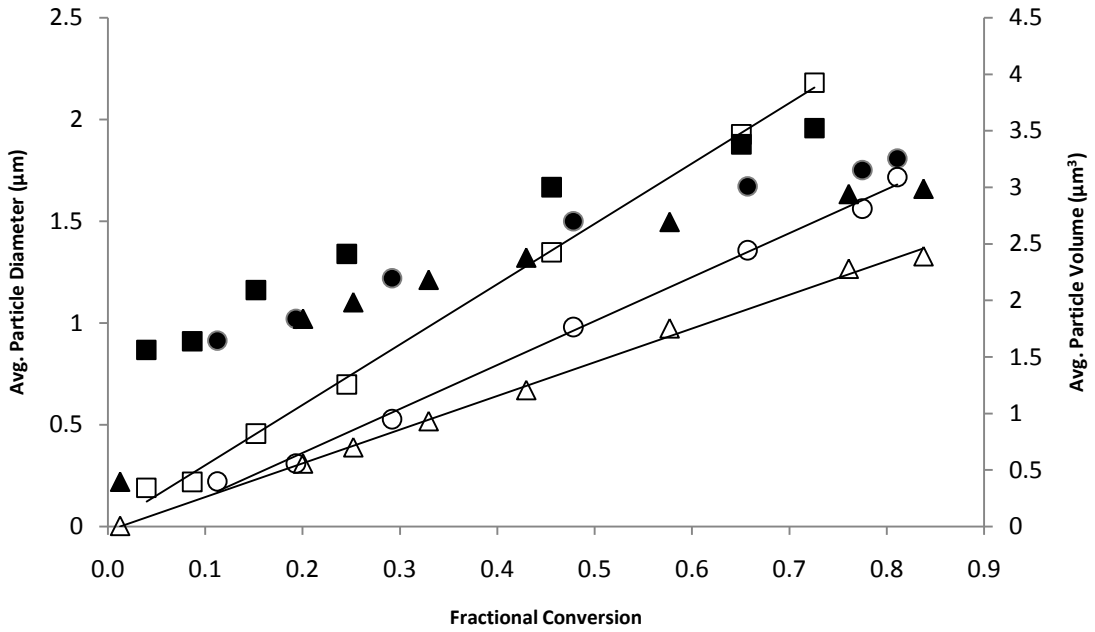

Figure 3-3 – Volume average particle size (left axis) vs. fractional conversion for MMA dispersions carried out at 60°C in a 70|30 MeOH|Water continuous phase (shaded) and relationship between the average particle volume^3 vs. fractional conversion (right axis, un-shaded)) for the observed large particle population. Different shapes correspond to different experimental replicates.

Over the course of the reaction, the average size of the small particle population is consistently between 60 and 80 nm, as shown in Figure 3-2. To examine whether the number of particles in the system changes, the following formula[110] is applied:

$$N_p = \frac{\frac{\chi \cdot m \cdot \Phi_v}{\frac{\pi}{6} \cdot \rho \cdot {D_{p,v}}^3}}{V_r} \quad [1]$$

where φ_v is the volume fraction of the average particle size measurement, χ is conversion, m is the total mass of monomer added initially to the system, $D_{p,v}$ is the volume average size of the particle, ρ is the density of dry polymer and V_r is the total volume of the polymerization. Figure

3-4 shows the number of particles per litre for three typical reactions. The number of large particles in the reaction is more or less fixed at 10^{13}/L from an early point in the reaction. The number of small particles present is also more or less constant around 10^{15}/L but with much greater fluctuation. As the average size of the small particles does not significantly change, it can be concluded that they are continually generated and consumed during the course of the reaction.

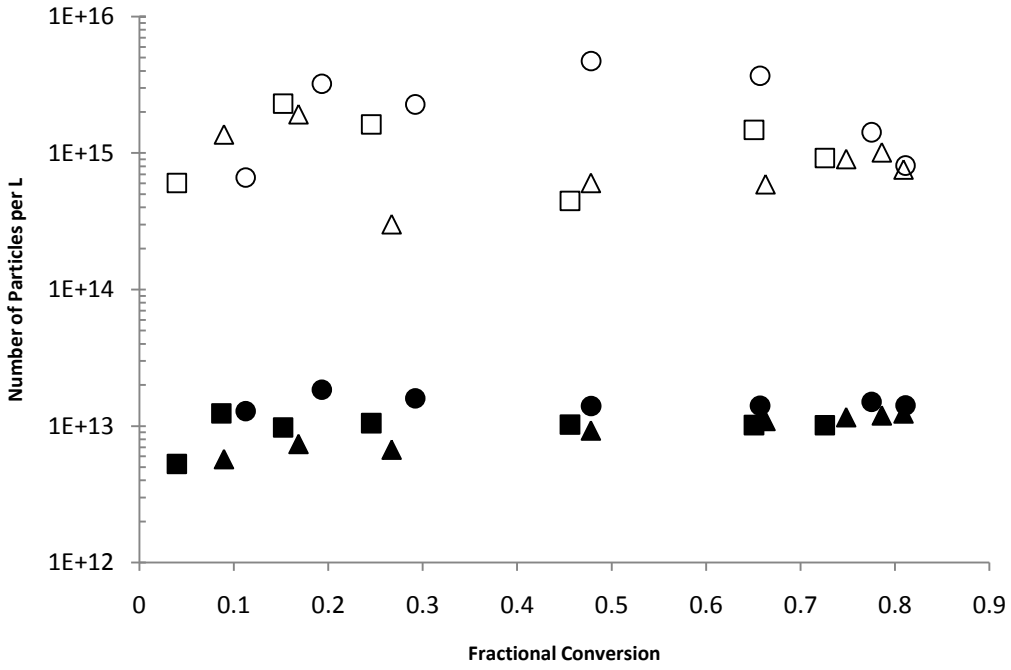

Figure 3-4 – Number of particles per L vs. fractional conversion for three typical MMA reactions carried out at 60°C in a 70|30 MeOH|water dispersion polymerization, where the symbols for the number of large particles (shaded) and small particles (open) are matched for the same experiment.

In order to confirm that the particles observed in the LS 13 320 exist, SEM was employed to optically view the respective distributions, with particular attention being paid to finding small particles. Our results thus far do agree with the mechanisms of particle nucleation discussed in the literature, with small particles generated and swept up by growing larger particles. [46, 52, 54, 99, 102-105] Where our results differ is in the detection of the small particle population throughout and after the reaction. Part of this discrepancy may be that Jiang et al.[43-45] and other works by El-

Aasser[49, 55, 99] use SEM exclusively to characterize the particle size of their dispersions and had not noted the presence of the small population of particles we observed in their final latexes. Cao et al. use SEM and a laser particle size detector to characterize their dispersions but do not detect the small particles with either device.[53, 97] Our SEM images obtained also show polymer particles in the expected 1-2μm range that are quite monodisperse, with only occasional evidence of particles somewhat smaller than average, as seen in Figure 3-5. Populations of small particles are not apparent with SEM until one purposefully looks for them. The SEM samples examined in this study were prepared by diluting the polymer latex in a 1:50 ratio with a mixture of the same makeup as the continuous phase used for polymerization. A single drop of diluted latex was placed onto a cleaned and polished aluminum stub and air dried. The large particle population dominated what was seen on the stub, especially in the center of the sample; the population of small particles are likely masked by the much larger particles. However, some small particles were found at the edges of the dried latex droplet, caught in the microscopic striations in the faces of the metal as the methanol-water continuous phase had evaporated and pulled the polymer particles towards the center, as was seen recently by Moraes et al.[111] with their multimodal latexes of styrene. To verify that these particles were not just surface imperfections on the aluminum stub, TEM was also used to observe the small particle population. SEM and TEM images for pMMA particles are shown in Figure 3-5 and Figure 3-6, respectively.

TEM proved to be a much better method than SEM for observing the small particle populations observed by the laser light scattering detector. Undiluted MMA latexes were examined by TEM and clearly showed both the large particles observable by SEM and small particles in the size range expected based on light scattering results. The smallest particles (less than 100nm) were often observed in clusters as shown in Figure 3-6**.** It is possible that these clusters have been formed during sedimentation of the latex; however, they could also be the same primary nuclei seen by dynamic light scattering by Shen et al. which were thought to clump together on reaching

sizes of approximately 15-20nm.[49] The TEM images corroborate the light scattering results, especially when one considers the number of small particles contained in the clusters observed compared to the few particles of much larger size and volume. Having proven that the light scattering results are valid, the Beckman LS 310 particle size analyzer was predominantly used to describe the particle size distributions in this work.

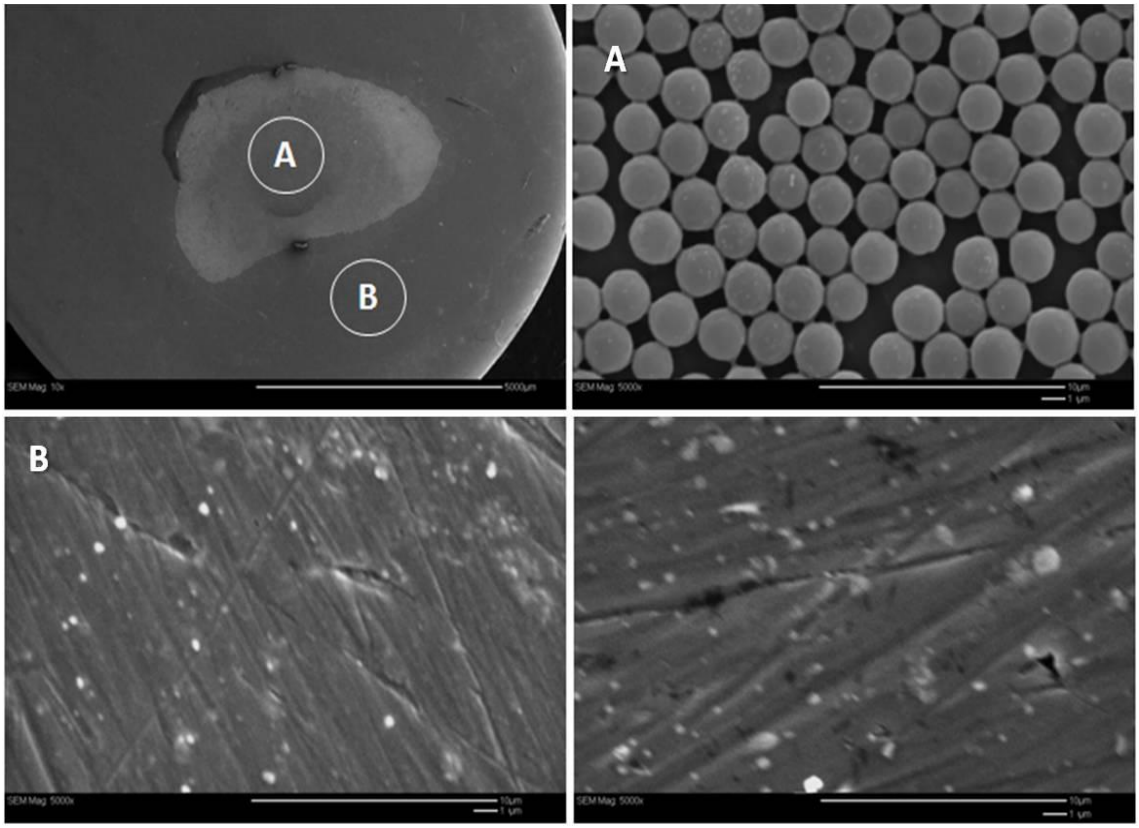

Figure 3-5 – SEM image of pMMA particles shown at 10x and 5000x magnification. Top left shows the sample on the aluminum stub. Top right shows polymer sampled from the center (A) of the stub, bottom left shows polymer sampled from outside of the main concentration of polymer (B). The image on the bottom right shows a blank aluminum sample stub.

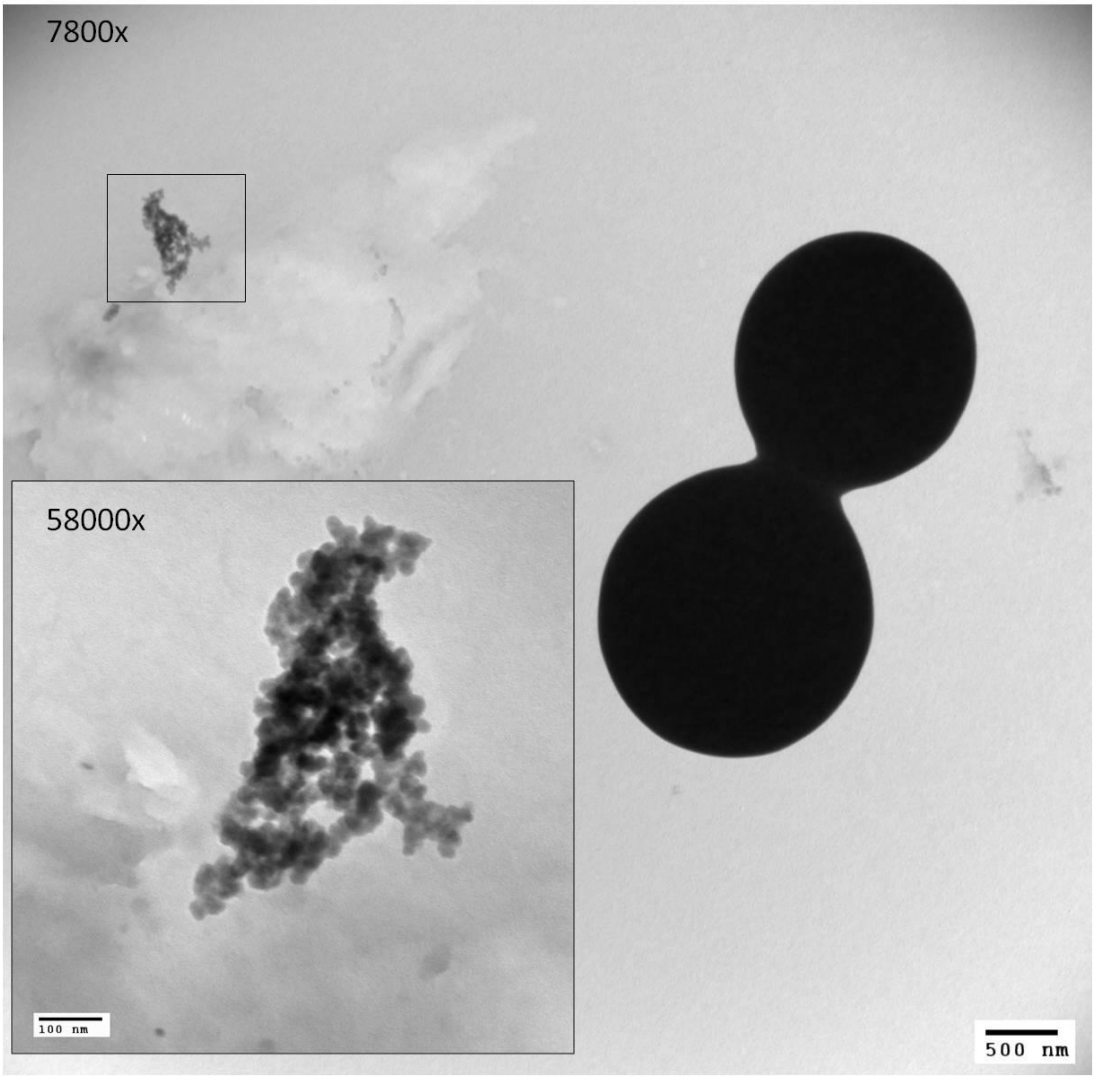

Figure 3-6 – TEM images of pMMA particles shown at 7800x and 58000x magnification for polymer produced at 60°C in a 70|30 MeOH|Water continuous phase at 180rpm.

3.3.1 Particle Nucleation – MMA homopolymer

Having shown that there is a significant population of small polymer particles throughout dispersion polymerizations, an improved understanding of the variables that affect the relative amounts of small and large particles may provide insight into the nature of nucleation and particle growth. Based on previous research, the amount of initiator, surfactant concentration and the makeup of the continuous phase are known to affect particle size and the rate of reaction, among other properties.[43-45, 53, 97] MMA dispersion polymerizations based on the standard recipe in Table

3-1 were examined, with the amount of initiator varied from the base case of 2% to 4% and 0.5%. A separate set of experiments were also conducted where the composition of the continuous phase was varied from the base case of 70|30 MeOH|Water to cases with more (80|20) and less (60|40) methanol respectively, holding all other parameters in Table 3-1 constant. Additionally, the PVP content in the reaction was varied over a set of experiments from 10% to 15% to 20%, holding all other parameters in Table 3-1 constant. The final volume average particle sizes observed increased from 1.76μm to 1.95μm to 2.20μm as the fraction of initiator was increased from 0.5% to 2% to 4%, respectively, a trend also found by Cao and others. [43-45, 53, 97] In addition, rates of reaction increased with initiator content, as expected and seen in plots of conversion vs. time along with the average particle diameter (for large particles) vs. conversion in Figure 3-7. The number of large particles (not shown) is more or less fixed over the course of the reaction. Our results with small particles show that their fraction, number and size do not differ significantly with the amount of initiator, shown in Figure 3-8.

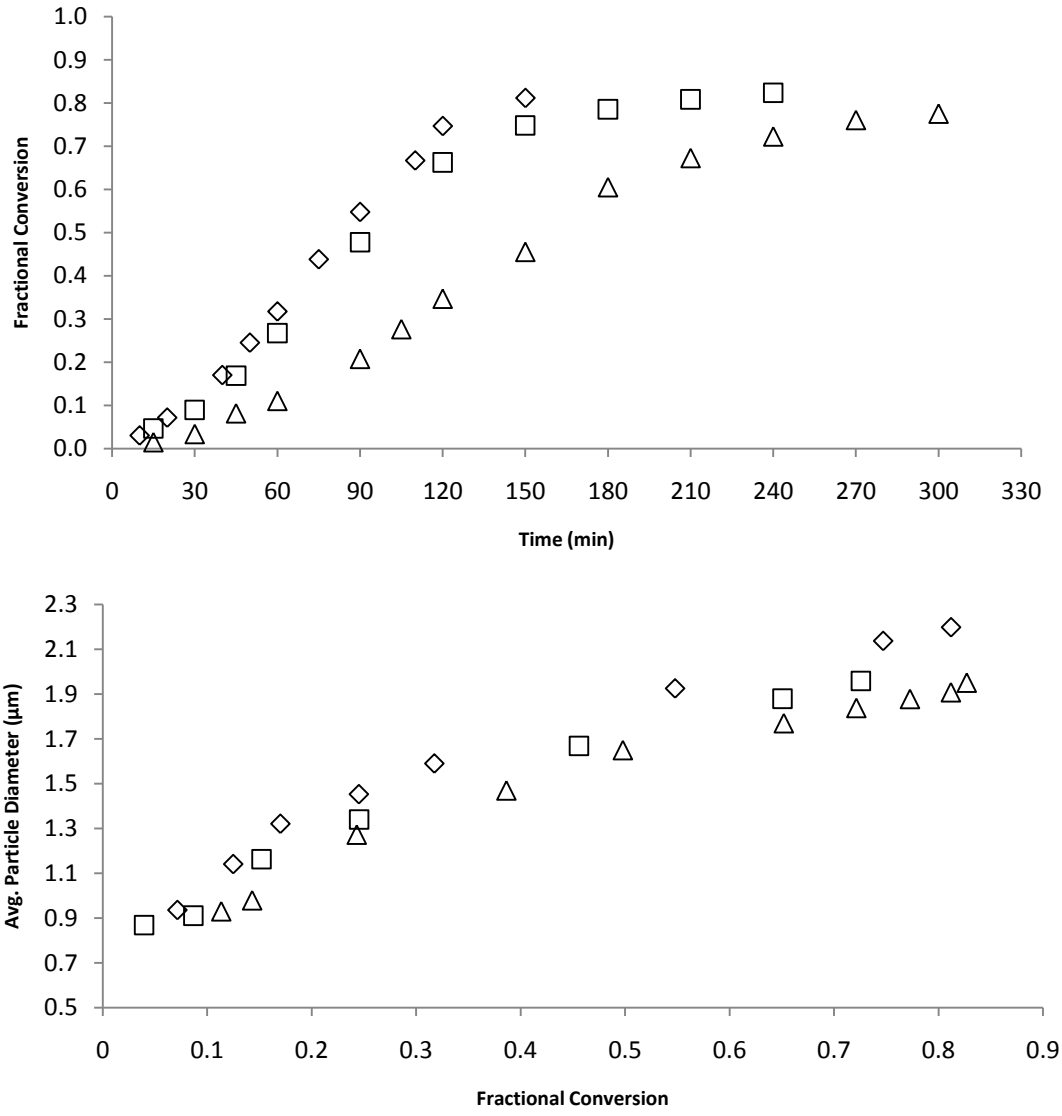

Figure 3-7 – Fractional conversion vs. time (top) and volume average particle diameter of large particles as a function of fractional conversion (bottom) for MMA dispersion polymerizations carried out at 60°C in a continuous phase of 70|30 MeOH|Water composition for reactions with varying concentrations of initiator (0.5%(Δ), 2%(□), and 4%(◊)).

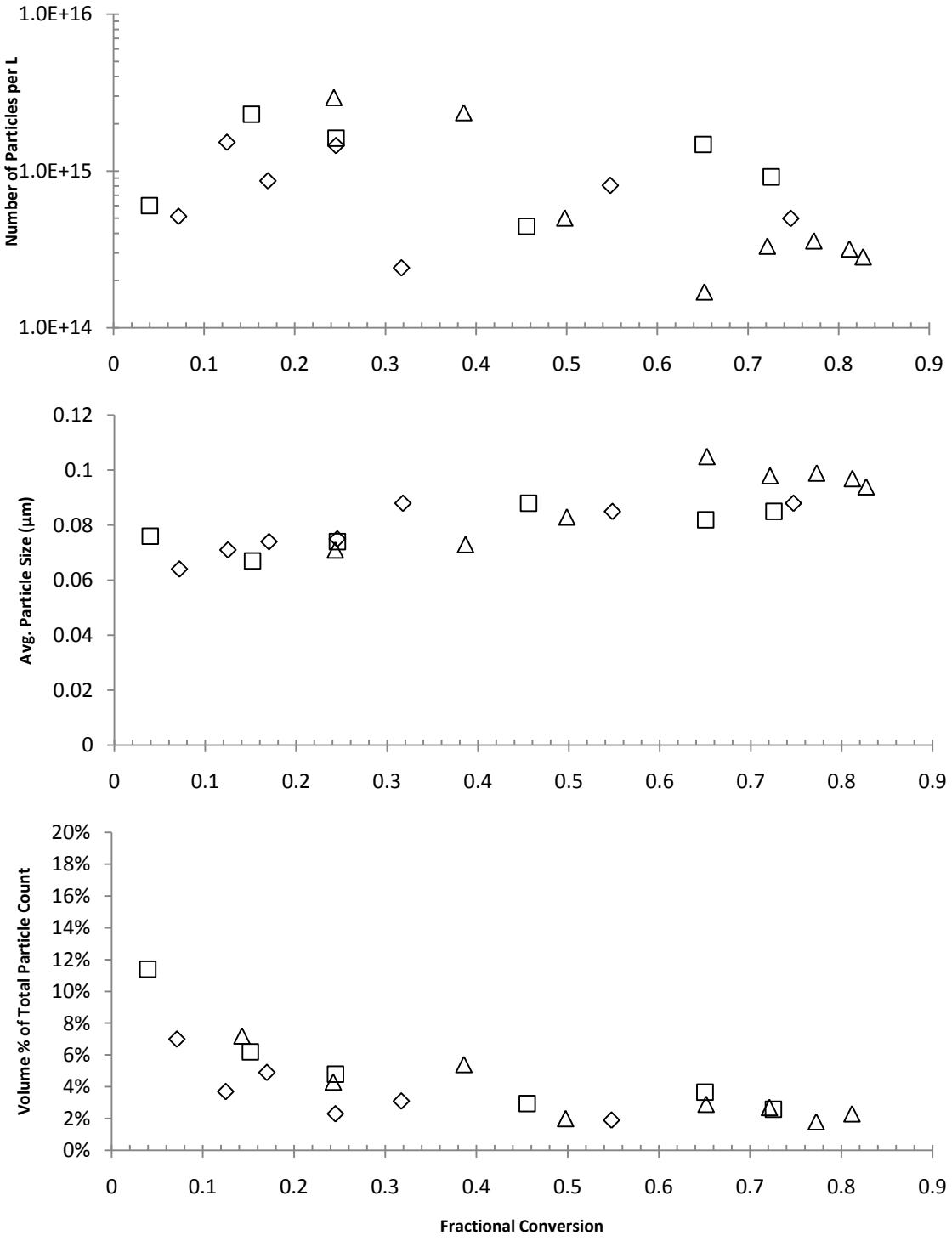

Figure 3-8 - Number of particles per L vs. fractional conversion (top), number average particle size vs. fractional conversion (middle) and volume fraction of total particle count for small pMMA particles noted in dispersions carried out at 60°C in a 70|30 MeOH|Water continuous phase with 0.5%(Δ), 2%(□), and 4%(◊) initiator.

The flux of radicals in the system is most certainly affected by the amount of initiator used, as is evidenced by decreased time for the first signs of opacity to occur with more initiator. Cao et al[97] and Shen et al.[49] proposed that the increased rate of radical generation leads to a higher concentration of precipitated oligomer chains which agglomerate into larger primary particles due to the relatively slow rate of adsorption of the stabilizer. They also proposed that the fewer large particles in the system will be less likely to capture nuclei and oligo-radicals due to their lower number density and overall surface area.[97] In contradiction to this second hypothesis, Figure 3-8 shows that radical flux does not affect the steady state concentration, volume fraction and size of the small particles. Given that the rate of radical generation is greater with more initiator, but that there is no real difference seen in the number and fraction of small particles in the system throughout the polymerization, it may be concluded that the small particles are incorporated by the primary particles as fast as they are generated. Thus, the final size of the large particles is controlled by the number that is nucleated early in the reaction. As stated above, Shen et al.[99] propose that more initiator is used because more initiator generates a greater number of small chains initially which are understabilized, leading to faster coalescence and larger particle sizes prior to initial stabilization by the PVP surfactant, which acts as a protective colloid. However, Paine saw the same effects in his work with styrene dispersions and postulated that larger particles are obtained with more initiator because overall, lower MW polymer is created which is less well stabilized by grafted PVP-pMMA since polymers of relatively lower MW are more soluble in the continuous phase.[51] This is also a reasonable explanation for what is observed. In either case, once formed, the large particles are able to sweep up the smaller particles at whatever rate they are generated (most likely faster with higher concentrations of initiator). This means that at steady state, the number and size of the small particle population is unaffected.

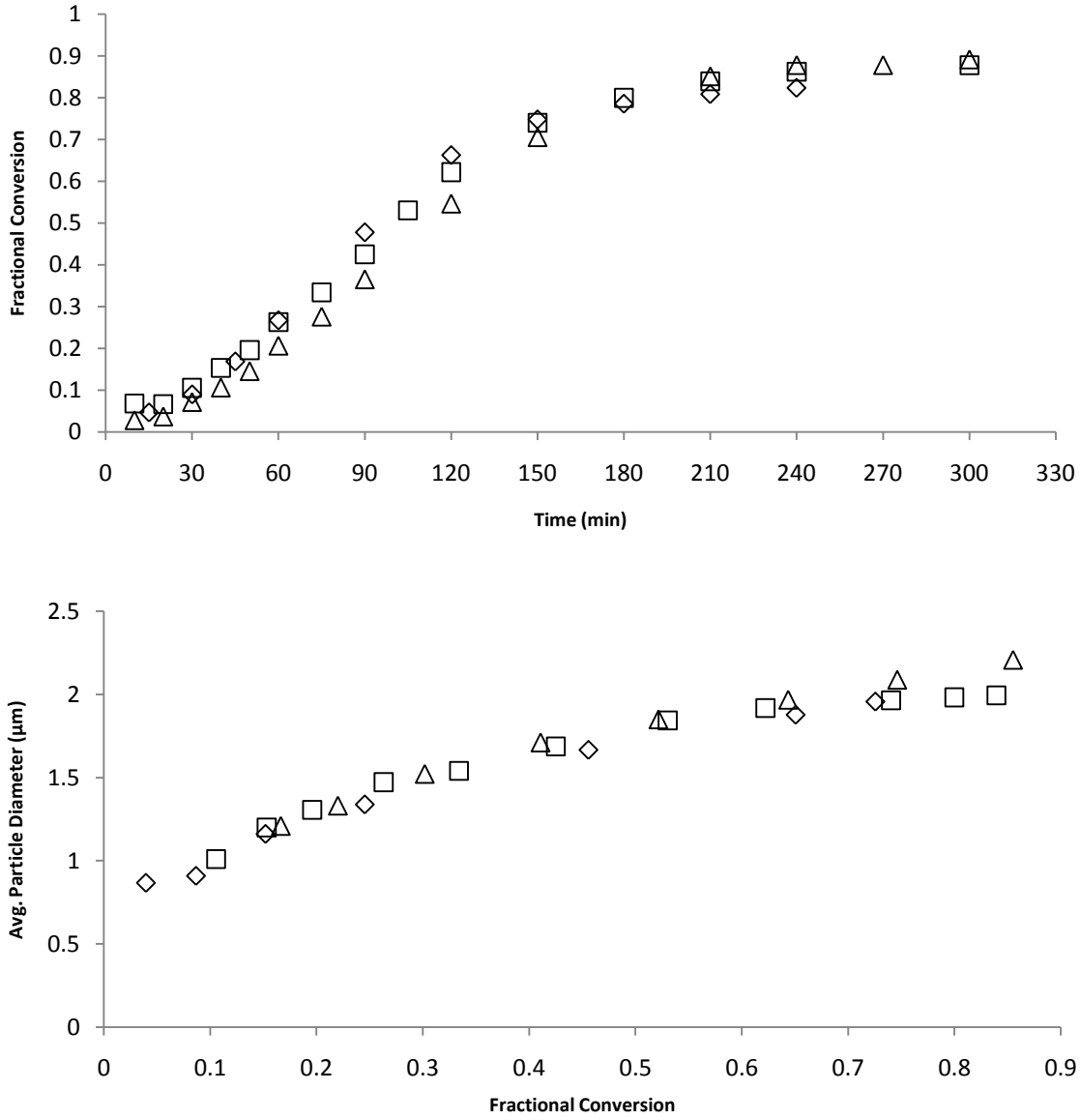

Figure 3-9 – Fractional conversion vs. time (top) and volume average particle diameter of large particles as a function of fractional conversion (bottom) for MMA dispersion polymerizations carried out at 60°C in a continuous phase of 70|30 MeOH|Water composition for reactions with varying concentrations of surfactant (20 % (□), 15% (◊), 10%(Δ)).

The amount of surfactant used in a dispersion polymerization has been reported to affect the particle size and the stability of the polymerization by some authors, [43-45, 53, 97] while other authors have noted no effect of increases in surfactant beyond certain concentrations.[46] The surfactant content in the reaction mixture for this study was varied by ±5% (relative to monomer)

from the recipe in Table 3-1holding all else equal. Multiple experiments were conducted at 10, 15 and 20 percent PVP content with respect to monomer. Changing the amount of surfactant in the polymerization had little effect on the rate of reaction as evidenced by the fractional conversion vs. time plot in Figure 3-9. The volume average particle size of the large particle population also does not vary. Work by both Cao and Jiang show a slight change in the average particle size with an increase in surfactant concentration.[43, 97] At the same time, experiments conducted by the El-Aasser group saw that a majority of the surfactant remained free in solution after polymerization and could be recycled many times, with only 1.1 wt% (of 4wt% supplied) being physically adsorbed or grafted to the polymer.[99] The largest effects of surfactant on particle size were reported when moving from low (1%) to larger (10%) concentrations of surfactant.[99] Additionally Almog et al.[46] did not observe an effect when surfactant concentration exceeded $15g \cdot L^{-1}$ (15% surfactant used in this study corresponds to approximately $15g \cdot L^{-1}$). Thus, it is possible that in the range of surfactant concentrations examined, the amount of free surfactant already greatly exceeded the minimum required, and resulted in a negligible difference in large particle size. Looking at Figure 3-9, it is seen that dropping surfactant concentration to 10% may form slightly larger particles (2.2 μm vs. 2.0μm) as one would expect, but no real distinction can be made between 15% and 20% surfactant loadings. This lack of sensitivity to surfactant does not necessarily refute the supposition that the time taken to initially stabilize the first particles in solution is important. Cao et al. estimated that only 1 in every 340 reactions involving the MMA monomer is of the chain transfer to surfactant type.[53] The effects of changing the surfactant concentration on the fraction of small particles, shown in Figure 3-10, are no greater than those observed when changing the amount of initiator; as more surfactant is added, there is no change in the size of the small particles. It is difficult to observe any definitive trends in the volume fraction of the small particle population due to the scatter in the data, but there may be an increase in the number of particles with increased surfactant level.

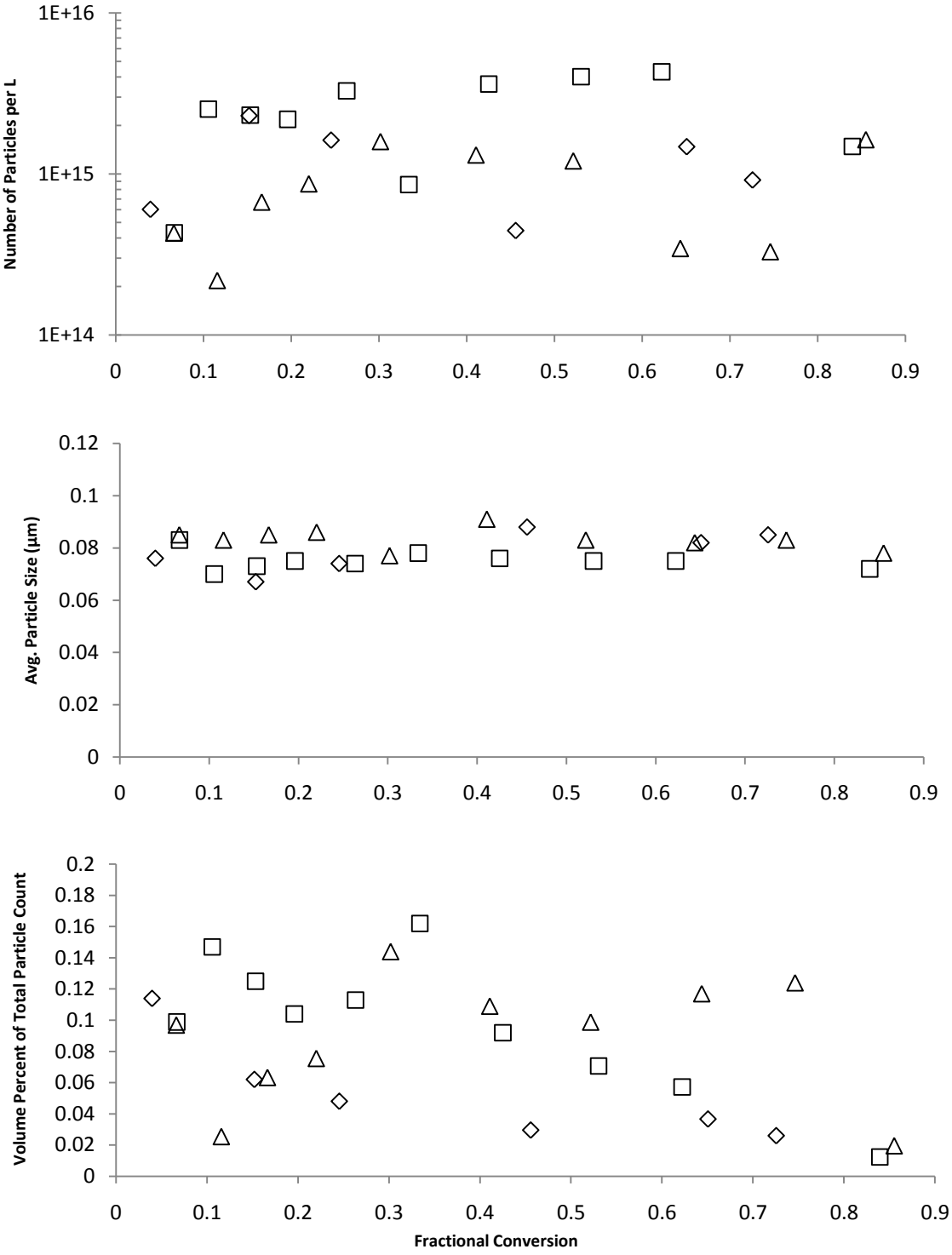

Figure 3-10 - Number of particles per L vs. fractional conversion (top), number average particle size vs. fractional conversion (middle) and volume fraction of total particle count for small pMMA particles noted in dispersions carried out at 60°C in a 70|30 MeOH|Water continuous phase with 10%(Δ), 15% (◊) 20%(□) surfactant.

The previous work by Cao et al.[53, 97] and by Jiang et al.[43-45] with MMA showed that the composition of the continuous phase had a great impact on polymerization rate as well as particle size. We also found that as the proportion of methanol in the continuous phase is increased, the overall rate of reaction decreases. This is believed to be due to the increased polymer solubility and thus longer critical chain length of the polymer in the continuous phase. The increased MeOH fraction may also change the monomer partition behaviour between the two phases. Figure 3-11 shows profiles of fractional conversion vs. time for the dispersion polymerizations carried out in continuous phases of 60|40, 65|35, 70|30 and 80|20 MeOH|Water composition. The 70|30 MeOH|Water mixture was chosen as the base case for this study since it had been shown to produce the most stable and well characterized distributions in the literature.[43-45, 53, 97] Since growing polymer chains are more soluble in greater fractions of methanol, solution polymerization is expected to be more important. This leads to a lower observed polymerization rate in the 80|20 continuous phase compared to the 60|40 case where a greater fraction of a polymerization occurs in the particles at a higher rate (due to the decrease in k_t caused by high polymer content within the particles). Like Jiang et al.[43-45] we observed that the stability of MMA polymerizations with greater than 30% water was poor, with coagulation and aggregation being observed early in the reaction, limiting the ability to measure particle size distributions in the laser particle size analyzer for the 60|40 experiments. Polymerizations carried out in the 65|35 continuous phase were more stable for a longer period and so were used for particle size measurements. The trends in particle size distribution observed for the dispersions in the different continuous phase compositions were similar to those found in literature,[43-45, 53, 97] with the average particle size increasing with increasing methanol content as seen in Figure 3-11. The size of the particles in the 80|20 continuous phase are much larger, as most polymerization occurs in solution and thus fewer particles are nucleated (the number of large particles remains constant as found for all other cases). The particle size distributions, shown in Figure 3-12 were narrow and monodisperse for the 70|30 continuous phase whereas particles produced in the 60|40 and 80|20

continuous phases were more polydisperse in nature, the former being much broader than the 70|30 case and the latter having multiple peaks. As shown in Table 3-2, we observed the same inverse correlation seen between particle size and MW noted by Paine, with molecular weight increasing as particle size decreases.[51] The distributions referenced in the table are shown in Appendix B. As stated by Paine, the reason for this is the locus of polymerization. In the 60|40 or 65|35 continuous phases where we expect the critical chain length of MMA is shortened, the rate of reaction is increased and MW is higher which corresponds to a more bulk like polymerization, as noted in the conversion vs. time plot in Figure 3-11. The opposite is true when looking at the 80|20 continuous phase case, where more polymerization is expected to occur via solution mechanisms and MW is lower. Polymerization in the particle phase would still take place in the 80|20 case, however the rate of capture of oligomeric radicals that precipitate from solution will be lower as the surface area of the particles that capture them is much smaller than in the 60|40 and 65|35 cases.[51]

Table 3-2 – Molecular Weights of MMA polymer as a function of continuous phase composition

Sample	Time (min)	Conversion	Mn ($g \cdot mol^{-1}$)	Mw ($g \cdot mol^{-1}$)	PDI
60|40	35	33%	247000	83300	3.37
70|30	180	79%	147000	474000	3.23
80|20	240	60%	94000	21000	2.22

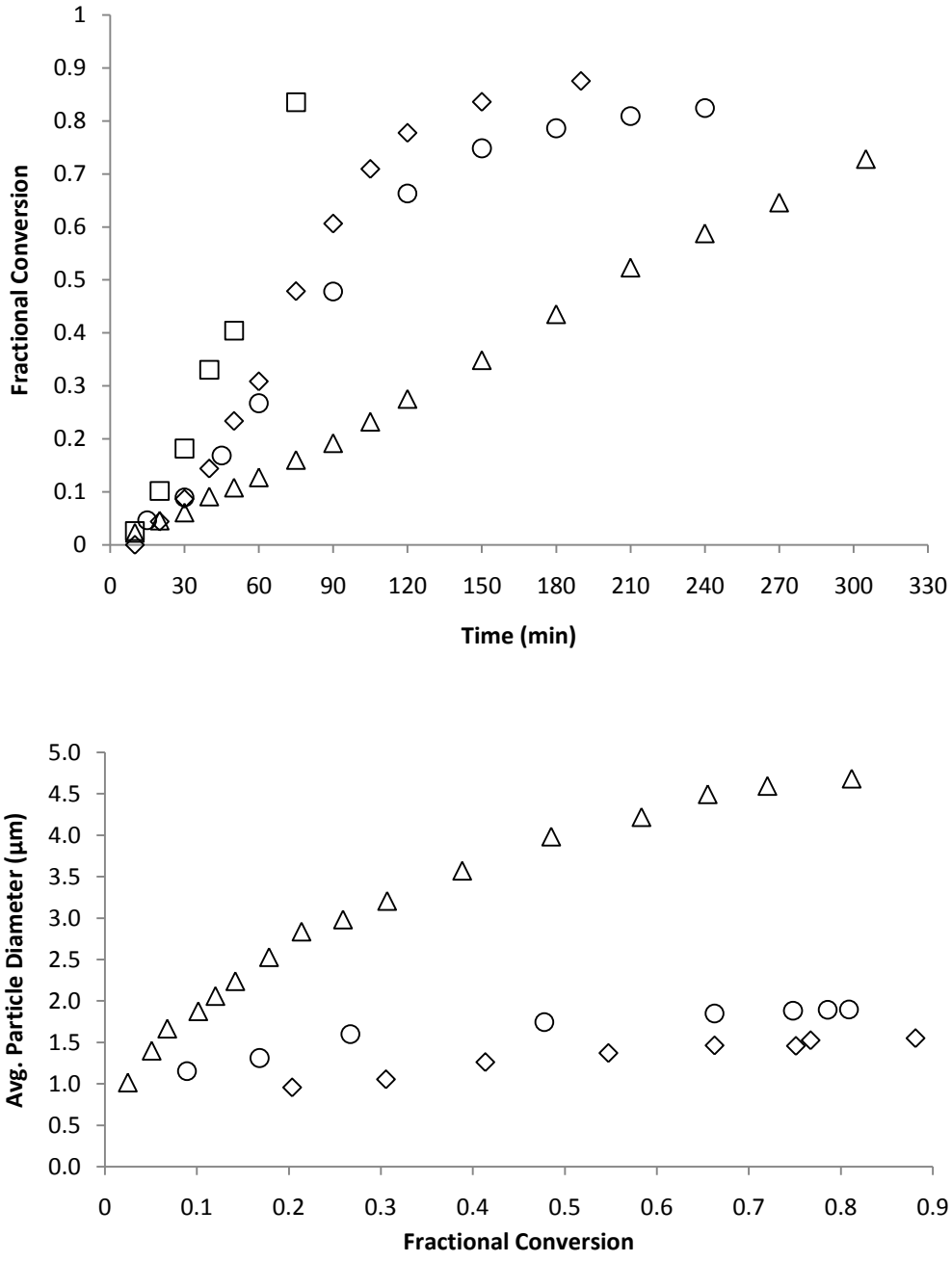

Figure 3-11 – Fractional conversion vs. time (top) and volume average particle diameter of large particles as a function of fractional conversion (bottom) for MMA dispersion polymerizations carried out at 60°C in continuous phases of 60|40 (□), 65|35 (◊), 70|30 (○) and 80|20 (Δ) MeOH|Water composition.

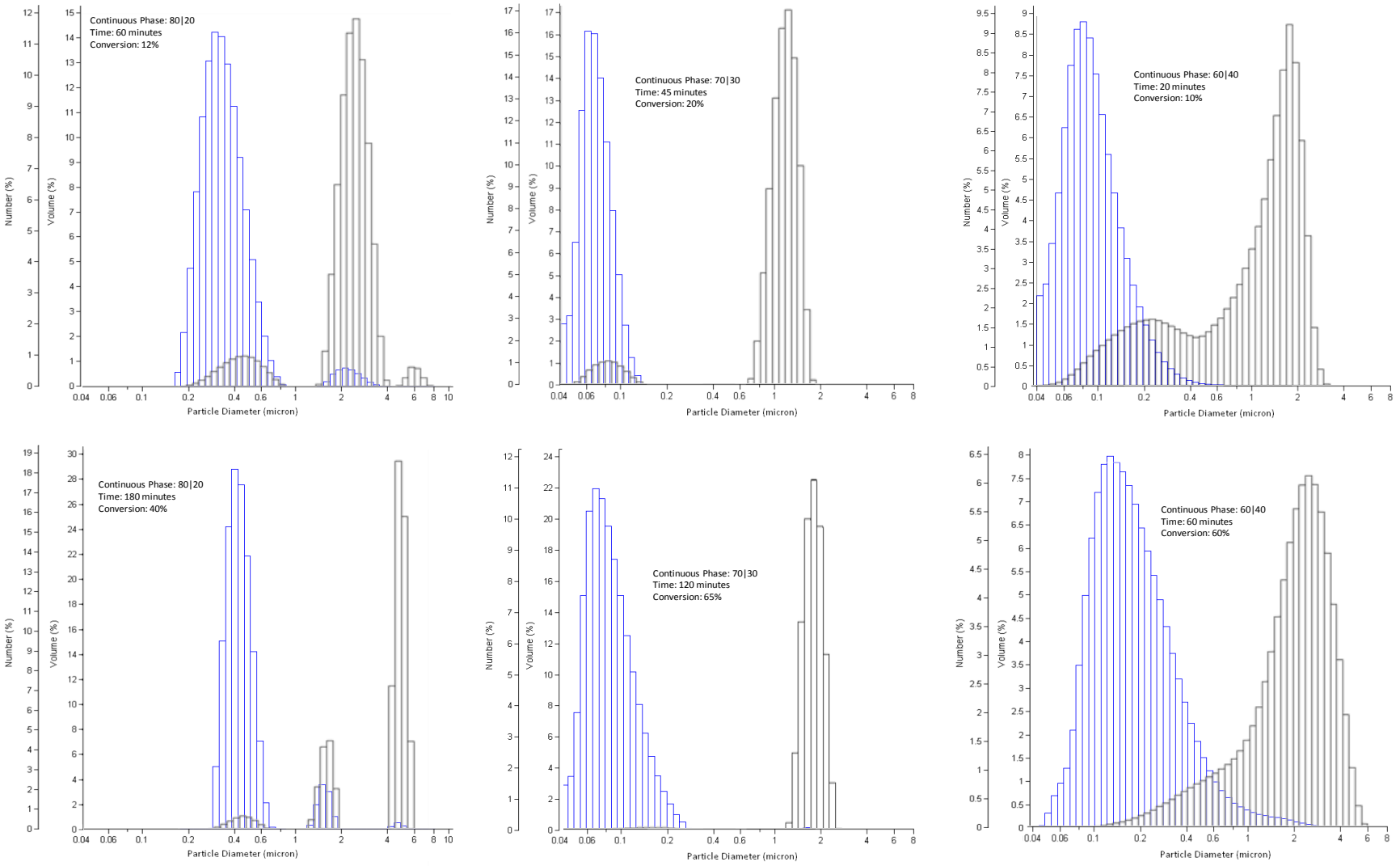

Figure 3-12 - Beckman LS310 Laser Particle Size analyzer output for a typical MMA dispersion polymerization showing volume (black) and number (blue) particle size distributions for reactions carried out in continuous phase compositions of 80|20 (left), 70|30 (middle) and 60|40 (right) MeOH|Water content.The top plot refers to earlier and the bottom plot to later timepoints/conversions.

There is a notable difference in the number of small particles seen in the reaction with changes in the continuous phase in Figure 3-13. As the fraction of water added to the system increases from 30% to 35%, the size of the small particles does not change but their number increases, in keeping with what would be expected on lowering the critical chain length due to lower polymer solubility. The lower critical chain length leads to an increased rate of reaction by producing more small particles which quickly aggregate into primary particles, causing a more bulk-like polymerization. The increased reaction rate may also result from a higher partitioning of monomer and perhaps initiator to the particle phase as the water content increases. Only the data for the 65|35 and 70|30 MeOH|Water continuous phase polymerizations is shown in Figure 3-13 as results from polymerizations beyond this range of methanol content (60|40, 80|20) proved difficult to analyze owing to some overlapping of multiple or broad peaks, as seen in Figure 3-12. In the 80|20 case, more than 2 populations were seen, and some of the populations were not detectable in terms of both number and volume fraction, making comparison difficult. For the 60|40 experiments, very broad distributions prevented estimation of small and large populations because there was no discernable transition between them. Looking at the 80|20 distributions in Figure 3-12, the size of what might be considered small particles does appear to be significantly larger than that seen under any other condition, which is a curious observation that cannot be fully explained, although the size of these small particles is still approximately 1/10 the size of the largest particles and so still conforms to Paine's observations. [54] Since the solubility of the initiator in the continuous phase is increased with less water (vazo 67 is insoluble in water and soluble in MeOH), it is plausible that this is a contributing factor to the larger particle sizes seen for the 80|20 experiment, especially considering that a large portion of the polymerization appears to take place in the solution phase. The sizes of the nuclei that precipitate from solution should differ according to the critical chain length of the polymer under the polymerization conditions, and this may also partially explain the larger small particle size in the 80|20 case; however, this cannot be quantified and changes are not observed in measurements of the number average size

of the small particles for the other cases. As the TEM image in Figure 3-6 showed, the light scattering readings most likely are of aggregates of small particles, much smaller than 80nm, made up of multiple chains that precipitated at their critical chain length.[49]

3.4 Particle Nucleation - Copolymers

The next aspect of this investigation into the nature of particle formation in dispersions, and the original aim of this work, studies the impact of the addition of MeMBL monomer to the recipe presented in Table 3-3. The total monomer content was varied by increments of 25 mol% MeMBL (25%, 50% and 75% MeMBL with the remainder consisting of MMA) and the other parameters (initiator, surfactant, methanol and water) were adjusted to keep the same proportions as originally presented in Table 3-1, ensuring a constant solids content throughout all experiments. All experiments were conducted in a continuous phase of 70% MeOH, 30% water at 60°C.

Table 3-3 – Recipes for MeMBL|MMA Copolymer Dispersion Polymerizations (60°C, 180 rpm)[a] in Glass Reactor

	Weight (g)		
Copolymer (MeMBL|MMA)	25|75	50|50	75|25
MeMBL	5.6	11.2	16.8
MMA	15.0	10.0	5.0
Vazo 67[b]		2%[a]	
PVP 40[c]		15%[a]	
Methanol/Water (70/30 wt/wt)		1000%[a]	

[a] Based on total monomer weight
[b] 2-Amino-2-methylbutyronitrile
[c] Poly(vinyl pyrrolidone), PVP 40 MW = 40,000 g/mol K value 29-32

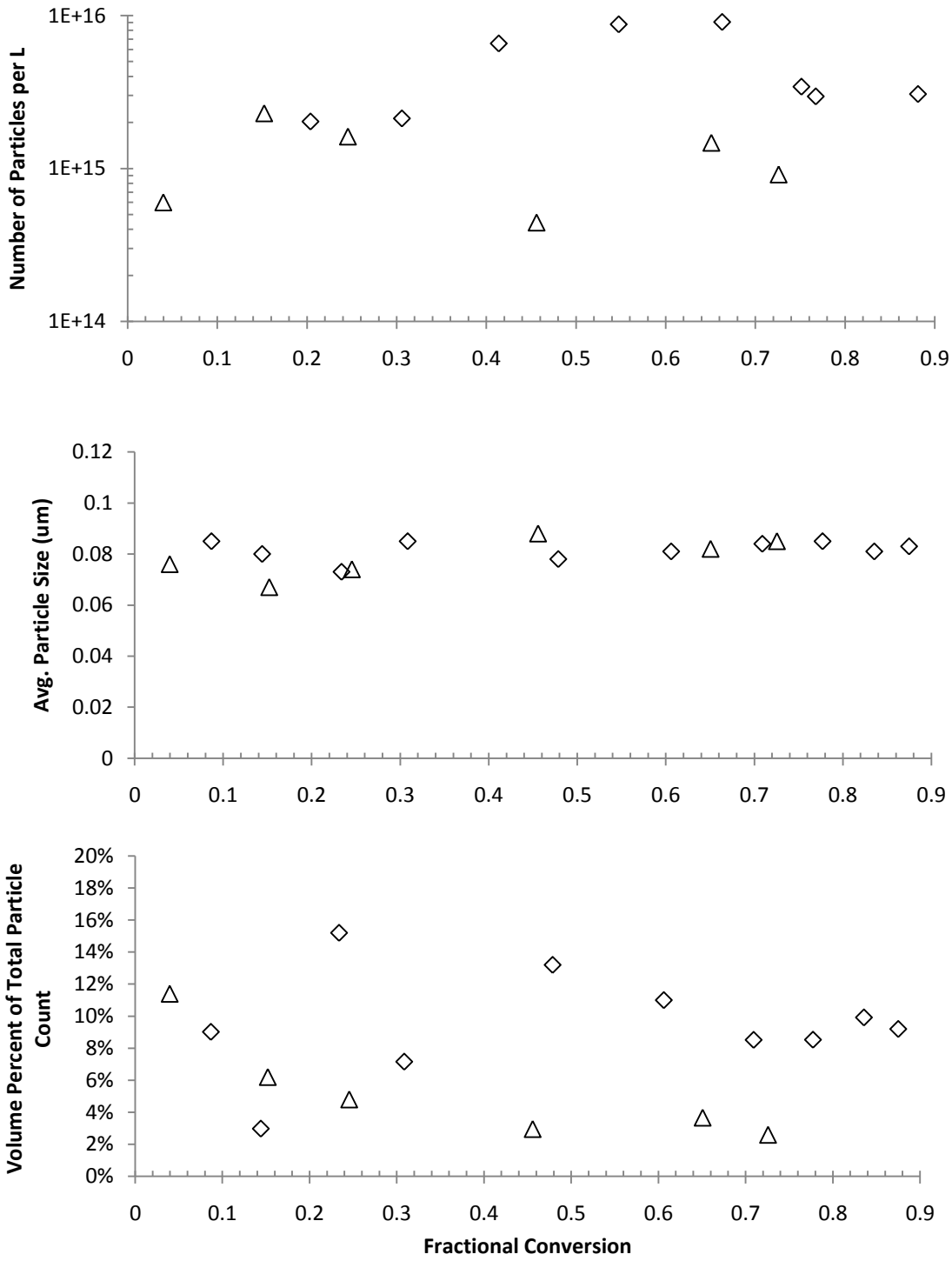

Figure 3-13 - Number of particles per L vs. fractional conversion (top), number average particle size vs. fractional conversion (middle) and volume fraction of total particle count for small pMMA particles noted in dispersions carried out at 60°C in 70|30 (Δ) and 65|35 (◊) MeOH|Water continuous phase compositions.

The results from the addition of MeMBL to the recipe are interesting, as they display characteristics seen in other experiments with MMA accomplished by changing other reaction parameters. For example, Figure 3-14 shows the profiles of fractional conversion vs. time for the copolymer dispersion polymerizations and particle size as a function of conversion. The slower rate of polymerization observed with MeMBL in the reaction is similar to that of the reactions conducted in an 80|20 MeOH|Water continuous phase. The slower rate cannot be attributed to kinetic rate coefficients, as k_p for a MeMBL/MMA mixture is similar to that of MMA (See Chapter 2), and the termination rate coefficients should also be similar. Thus, we suspect that the critical chain length for the copolymer is changed relative to the MMA homopolymerizations.

While adding MeMBL monomer to dispersion polymerizations was seen to have a notable effect on the large particle population (seen also with SEM measurements as in Figure 3-15), there appears to be a minimal impact on small particle properties, shown in Figure 3-16 for copolymerizations. The average size of the small particles formed in copolymer dispersions does not change appreciably with the addition of more MeMBL. All copolymer dispersions produce particles that are, for the most part, slightly smaller than those formed in MMA dispersions (Figure 3-15). Likewise, it is hard to see any definitive trends in changes to the number or volume fraction of the small particles on the addition of more MeMBL for batch polymerizations and there is no structural difference between the PSDs of MMA and copolymer dispersions except that the size of the large population in copolymer experiments decreases with increasing MeMBL content, as expected. That being said, the number of small particles seen is typically greater than that produced in MMA dispersions. This trend is what was observed when the water fraction in the continuous phase was increased for MMA polymerizations.

Examining the plot of particle size vs fractional conversion (Figure 3-14) shows that as more MeMBL is added to the system, the particle size observed decreases, which was also observed

when the continuous phase was changed to 65|35 MeOH|Water. It is most likely that the critical chain length of pMeMBL is shorter than that of pMMA. In the case of MMA homopolymerization, an increase in the MeOH content creates a longer j_{crit}, resulting in slower rates of reaction and slower nucleation, with fewer, larger particles formed. If we suppose that the critical chain length of pMeMBL is shorter than that of pMMA, we see consistent trends with changes in the continuous phase with respect to the effects on the diameter of large particles (increases towards longer j_{crit}), the number of large particles (increases towards shorter j_{crit}) and the number of small particles (increases towards shorter j_{crit}). Experimental evidence from prior work[96] supports the notion that the j_{crit} of pMeMBL is shorter than that of MMA; experiments conducted in BuOH resulted in the precipitation polymerization of MeMBL and solution polymerization of MMA. It is likely that the ring structure of MeMBL contributes to a more rigid polymer chain that is less well solvated compared to MMA in the same solvents. The only parameter that does not follow the same trend, comparing changes to the continuous phase with the addition of MeMBL to polymerizations, is that of rate. With changes to the continuous phase, more water equates to a shorter MMA chain length and faster rate. With MeMBL addition, more MeMBL does not cause the reaction to proceed more quickly and in fact any MeMBL addition appears to retard the rate of reaction, which runs counter to what was seen with MMA if the j_{crit} is a contributing factor. The difference with MeMBL may be due to two factors; monomer solubility and T_g. The MeMBL monomer is known to be much more water soluble than that of MMA[24] and so it is probable that it prefers to reside in the continuous phase, resulting in a lower monomer concentration in the particles and a more solution like polymerization.[42] Cao also showed that as the temperature of reaction increased, the fraction of MMA monomer in the continuous phase decreased, independent of concentrations of initiator and surfactant.[53] They reported that the rate of MMA monomer transfer from the continuous phase to the polymer phase may be lower than the polymerization rate in the particles. [53] The fact that the T_g of MeMBL is over 100^{o}C higher than that of MMA and more than 150^{o}C higher than the reactor temperature

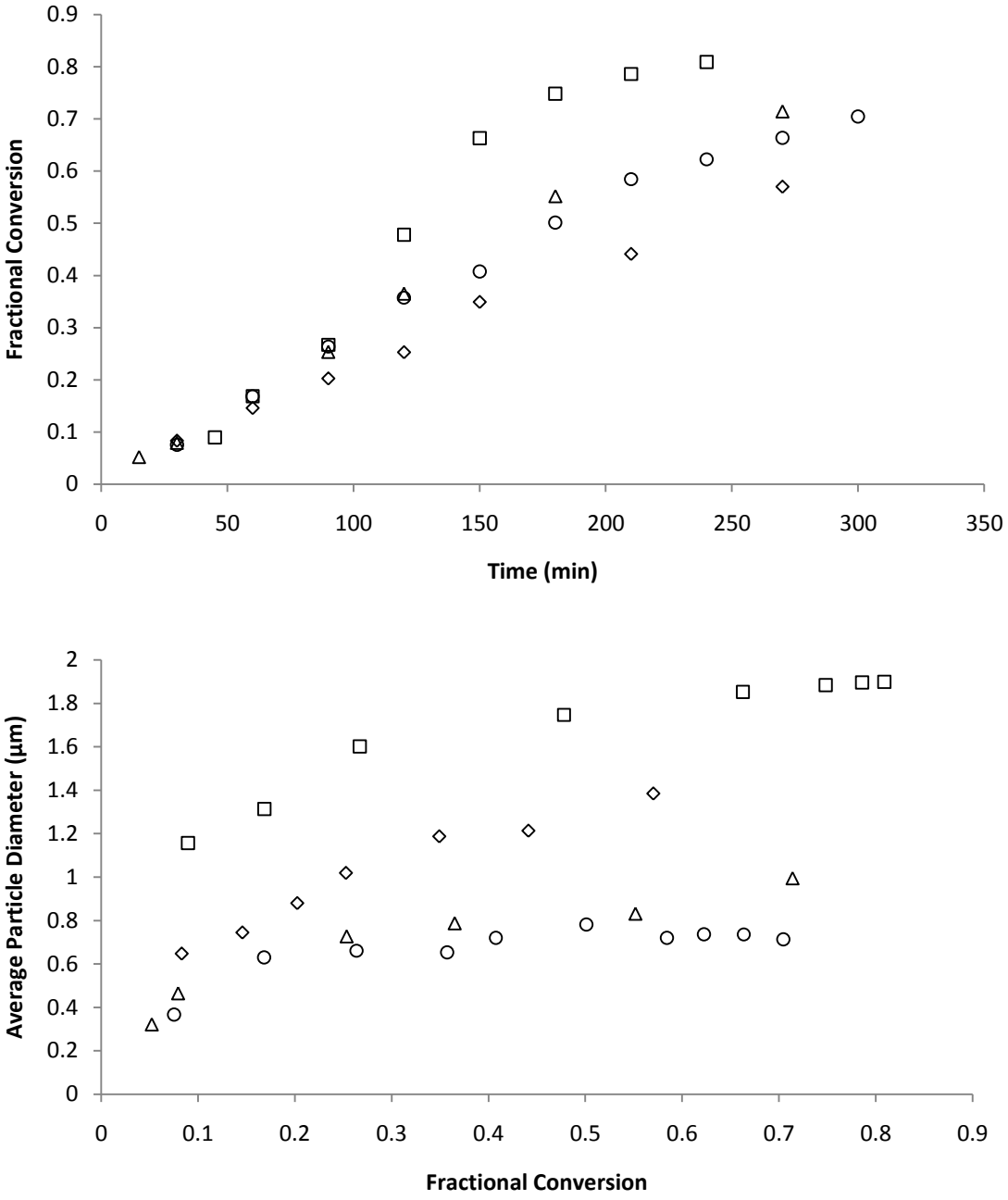

Figure 3-14 – Fractional conversion vs. time (top) and volume average particle diameter of large particles as a function of fractional conversion (bottom) for MeMBL/MMA copolymer dispersion polymerizations carried out at 60°C in a 70|30 MeOH|Water continuous phase. MMA (□), 25/75(◊), 50/50 (Δ) and 75/25 (○) MeMBL/MMA ratios are presented.

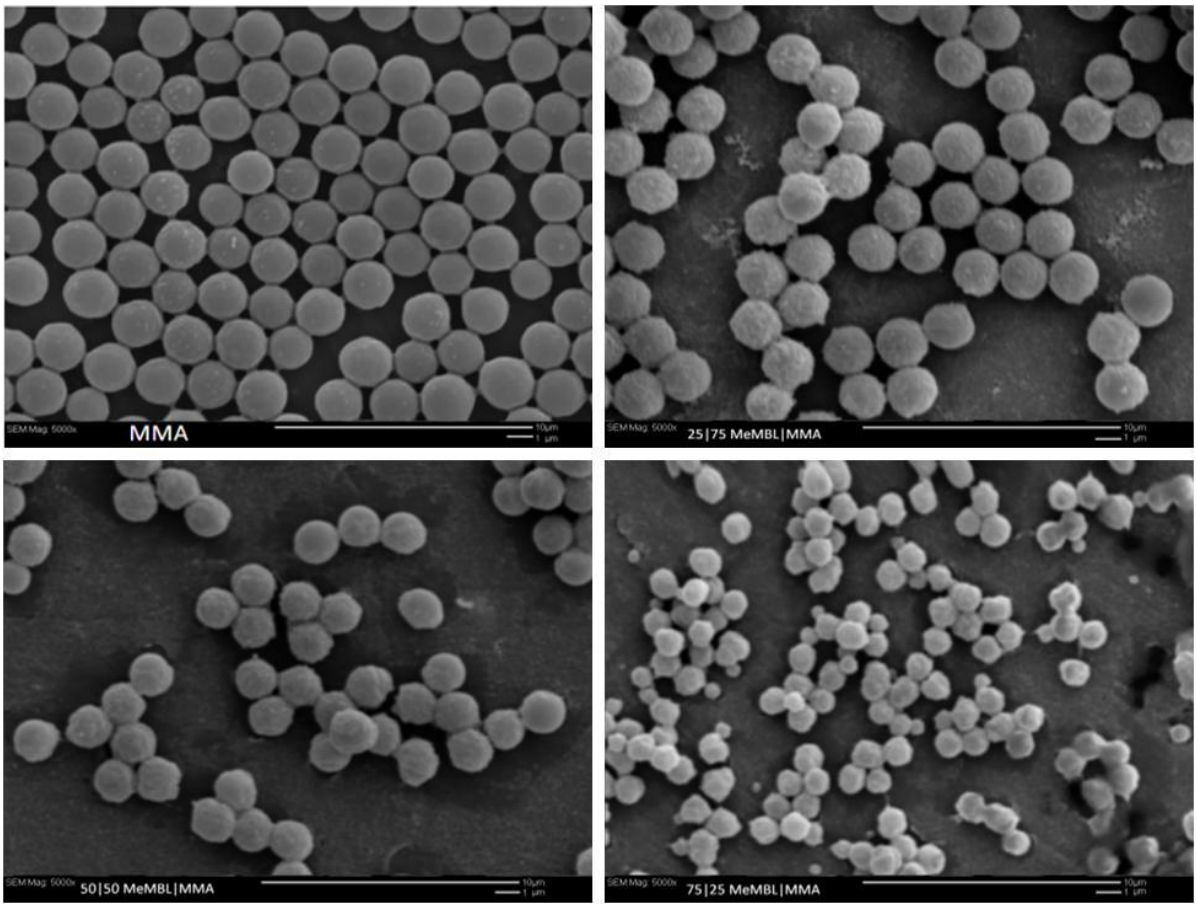

Figure 3-15 – SEM image of pMeMBL/MMA copolymer particles. pMMA (top left, approx. 1.9µm) is shown compared to copolymers with 25 (top right, approx. 1.6µm), 50 (bottom left, approx. 1.3µm) and 75 (bottom right, approx. 1µm) percent MeMBL.

would also affect monomer partitioning and result in a more solution like polymerization. So, if the differences seen in rate can be attributed to other properties of MeMBL, the experimental evidence does support a lower critical chain length for MeMBL compared to MMA. The impact of T_g and monomer partitioning could be explored through dispersion polymerization in a different solvent or solvent mixture that has much higher boiling points than the current methanol-water continuous phase. Xylenes, with a boiling point of more than 138^oC are an option for testing the impact of T_g and monomer partitioning given their miscibility with the MeMBL monomer and insolubility with the polymer. [96] Quantifying how much MeMBL monomer resides in the various phases of polymerization by methods such as gas chromatography would also be a useful endeavor.

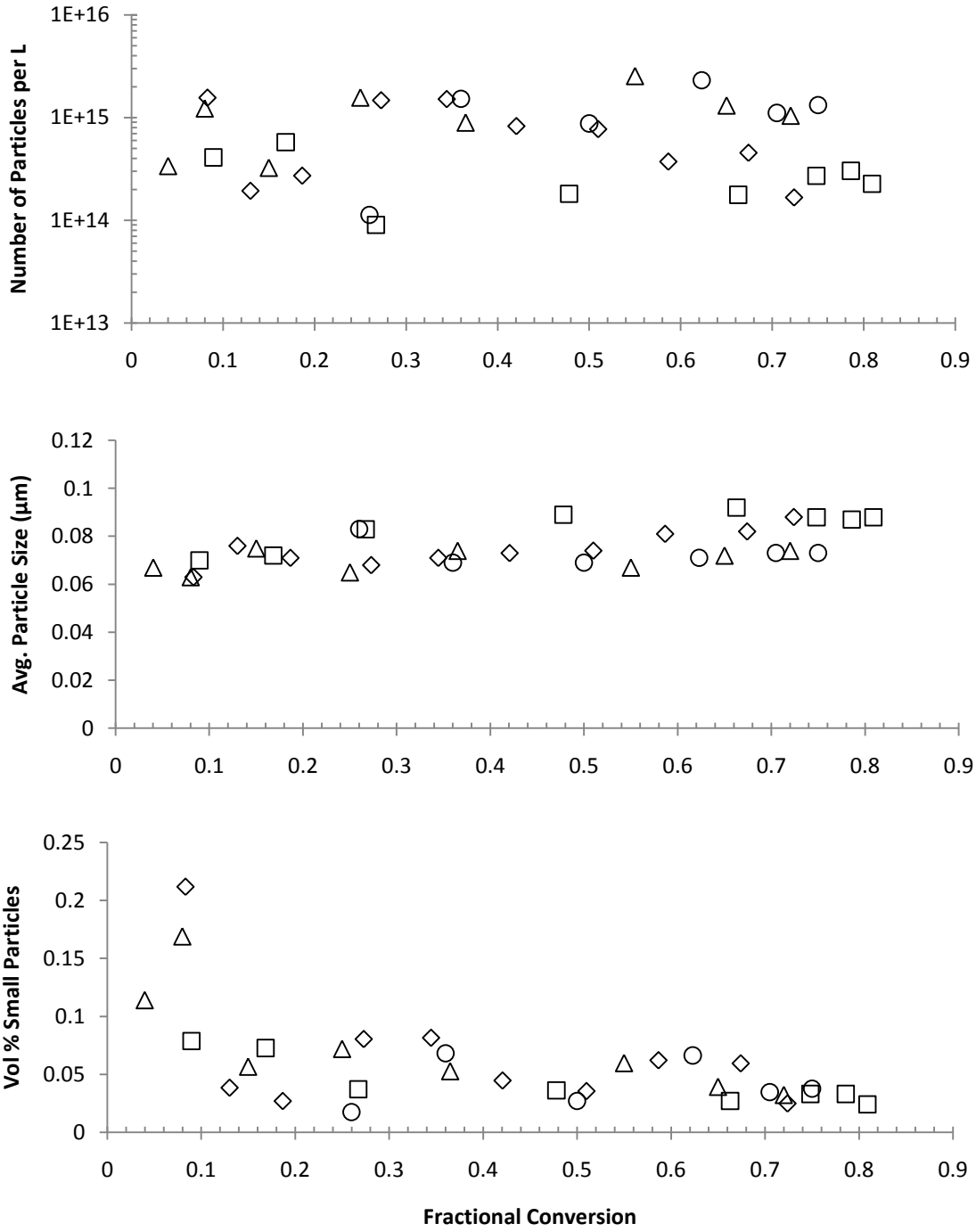

Figure 3-16 - Number of particles per L vs. fractional conversion (top), number average particle size vs. fractional conversion (middle) and volume fraction of total particle count for small MeMBL/MMA copolymer particles noted in dispersions carried out at 60°C in 70|30 MeOH|Water continuous phase. MMA (□), 25/75(◊), 50/50 (Δ) and 75/25 (○) MeMBL/MMA ratios are presented.

3.5 Investigation of Critical Chain Length (j_{crit})

Many of the observations made thus far in this study of dispersion polymerization suggest that the critical chain length of the polymers formed is an important factor in determining the size, characteristics and distribution of both small and large particle populations. The critical chain length for polymers is difficult to estimate as it changes depending on the system in question and a number of factors including temperature (affects solvency), monomer and solvent concentration (partitioning) and solvent type (affects solvency of polymer).[49, 99] None of the works by the El-Aasser group and others [43-45, 49, 51-55, 97, 99, 100, 105] have sought to quantify the actual critical chain length of the polymers studied owing to the inherent difficulties in doing so, especially since by the time the polymer particles form visibly (typically within minutes of the start of the reaction) the critical chain length has long been exceeded. Additionally, even the earliest particles detected will represent multiple, entangled polymer chains of the critical chain length, preventing reliable estimation in that way.[49] To further express the difficulties in measuring the j_{crit}, Bunyakan et al. were able to stop their acrylic acid precipitation polymerization in toluene at the first signs of polymerization at about 1% conversion. Testing this polymer revealed a MW that corresponds to chains of approximately 2081 units when the critical chain length is expected to be much lower, typically on a molecular scale of 5-20 monomer units for precipitation systems.[60, 61] We have postulated that the critical chain length of MeMBL is smaller than that of MMA based on experimental results. Because the critical chain lengths of MMA and MeMBL are not known at this point, we need to test the assumption that MMA polymerizes less by the solution polymerization mechanism due not to its critical chain length being longer than that of MeMBL, but because its monomer favours the polymer phase, once formed. Thus, we want to eliminate the formation of the particle phase, which can be accomplished by polymerizing MMA with a catalytic chain transfer (CCT) agent by the same dispersion recipe already studied.

CCT polymerizations are a type of controlled radical polymerization where the ultimate chain length (thus MW) of the polymer is regulated by a catalyst, known as a cobalt chain transfer agent (CCTA).[106-108] The reaction of MMA via CCT mechanisms with Cobalt(II) catalysts (the CCTA used in this study) is well described by Smeets et al.[112] In theory, with enough catalyst, the chain length of MMA polymer produced can be kept below the critical chain length, and the polymerization characteristics in solution can be studied and compared to the solution-like polymerization of MeMBL. CCT polymerizations do not alter the critical chain length of the polymer, but act in a similar manner by ensuring that the critical chain length is not reached during polymerization, therefore an increase in CCT catalyst content should have a similar effect to shortening the critical chain length.

MMA polymerizations were carried out according to the recipe in Table 3-4, which differs from that of Table 3-1, only by the addition of a CCT catalyst. The amount of CCT catalyst was varied in order to study its effect on the polymerization of MMA with the goal of eliminating particle formation. The cobalt chain transfer agent, [(difluoroboryl) dimethylglyoximato]cobalt(II), COBF, was prepared according to Bakac et al.[113] For the structure of the CCTA, refer to Smeets et al.[114] Due to the sensitivity of the catalyst to oxygen, the procedure for setting up CCT dispersion polymerizations is not the same as for normal dispersion polymerizations. A volume of MMA monomer (depending on the amount of catalyst used) was used to dissolve the CCT catalyst and was degassed under Nitrogen for a half hour. About 1mL of MMA was used to dissolve all of the initiator and kept aside. The remaining amount of MMA monomer was added to the continuous phase and purged by nitrogen for at least a half hour while being brought up to temperature. Once the reaction temperature was achieved and degassing was complete, the MMA monomer solutions containing the CCT catalyst and dissolved initiator were injected simultaneously.

Table 3-4 – Recipe for CCT Dispersion Polymerization (60°C, 180 rpm)[a] in Glass Reactor

Ingredient	Weight (g)	Amount[a] (%)
Total Monomer	20.0	100
COBF Catalyst	varied	ppm
Vazo 67[b]	0.4000	2.0
PVP 40[c]	3.0	15
Methanol/Water (70/30 wt/wt)	200.0	-

[a] Based on monomer
[b] 2-Amino-2-methylbutyronitrile
[c] Poly(vinyl pyrrolidone), PVP 40 MW = 40,000 g/mol K value 29-32

For the dispersion polymerizations carried out using CCT catalysts, Figure 3-17 shows the volume-average particle size evolution for large particles and conversion vs. time profiles for varying catalyst concentrations. In this figure, we see that as the amount of catalyst is increased, the particle size decreases significantly, even with only modest catalyst content. The volume-average particle size for normal dispersion polymerizations is almost 2μm and falls to less than 0.8μm on the addition of 5ppm of CCTA and further to less than 0.6μm with 10ppm CCTA; Correspondingly, there is an increase in the number of particles observed (not shown).The same effect was noted by Paine on the addition of a chain transfer agent to the polystyrene dispersions he studied.[51] Particles were not observed to form when more than 50ppm of CCTA was added to the reaction mixture. The conversion vs. time profiles for the different amounts of CCTA show interesting characteristics. When the CCTA is introduced to the polymerization recipe, it extends the period of time where solution polymerization dominates the reaction. In dispersion polymerizations without CCTA, the onset of particle formation is first observed within 10 minutes of the start of reaction by a change in colour as the initially clear transparent solution becomes turbid and translucent and with increasing conversion milky white and opaque. The addition of CCTA causes a delay in the onset of turbidity, with the addition of more catalyst resulting in further delay. 5ppm of CCTA was observed to remain transparent until about 30

minutes into the reaction, 10ppm until over 1 hour and 50 and 100ppm never polymerized to an extent that polymer precipitated from solution. The 50 and 100ppm polymerizations display the very linear conversion vs. time profile expected of solution polymerization, similar to the copolymerization conversion profiles and MMA polymerizations in an 80|20 MeOH|Water continuous phase, albeit with a much lower slope.

An even more interesting and unexpected result is that the polymer created with 50ppm of CCTA at 60^{o}C appears to be at its solubility limit, as the reaction mixture is clear and translucent in the reactor but immediately forms a milky dispersion on sampling from the reactor and cooling down of the reaction mixture. This means that for this system, the polymer that crashed out at the end of the reaction is very close to the critical chain length for MMA. SEC analysis of the polymer (isolated by drying under a stream of forced air and using the apparatus described in Chapter 2 because of its lower calibration and detection range) was used to determine the MW. The number-average MW of this polymer was found to be 2330 g·mol^{-1}, a chain length of 23 MMA monomer units. This fits well with the expected size range reported by Bunyakan et al.[60, 61] The polymer produced with 100ppm of CCTA (which remained in solution) was similarly analyzed and its MW was determined to be about 1900 g·mol^{-1}. While lower concentrations of catalyst were not successful in sustaining solution polymerization over the entirety of the reaction, they do provide additional information about the nature of MMA dispersion polymerization. Despite having different inhibition periods caused by the CCTA and reaching a slightly lower ultimate conversion with more CCTA, the rate of conversion after the particle phase is formed is virtually identical. Molecular weight analysis of the CCT and regular dispersion MMA polymers showed that the CCTA was somewhat effective in narrowing the PDI of the polymer, which was expected; final distributions from samples near full conversion are summarized in Table 3-5 and shown in Appendix B.

Assuming that the j_{crit} of MMA is on the order of 20-30 monomer units, less than 2% of the polymerization of an average MMA chain takes place in solution. Furthermore, the high average MW suggests that the CCTA plays a minor role in the dispersed phase (due either to mass transfer or solubility issues governing partitioning) and that polymerization in the dispersed phase for this monomer is the major loci of reaction, as has been suggested in the literature. [52, 54, 98] Comparing the effect on large particles of adding a CCTA to the dispersion polymerization corresponds fairly closely to changes seen with the addition of MeMBL. Taking these results together, it is reasonable to conclude that MMA does polymerize less than MeMBL via the solution mechanisms in a normal dispersion polymerization. That being said, it is also reasonable to conclude that MeMBL/MMA mixture polymerizes much more via solution than MMA due to its higher affinity for the continuous phase and higher polymer T_g, despite its lower j_{crit}. Future tests have been envisioned to create MeMBL and MMA polymers of very low MW and narrow PDI by methods such as ATRP to test their solubility in the continuous phase or use online turbidity monitoring of the reaction to detect the first signs of particle formation and confirm the critical chain lengths of the polymers.

Table 3-5 – Molecular Weight distribution data for Dispersion and CCT Dispersion Polymers near final conversion

Sample	Time (min)	Conversion	Mn ($g \cdot mol^{-1}$)	Mw ($g \cdot mol^{-1}$)	PDI
CCT – 100ppm	480	13%	1,750	1,910	1.09
CCT – 50 ppm	465	19%	2,330	2,860	1.22
CCT - 10ppm	240	69%	115,000	225,000	1.96
CCT - 5ppm	240	73%	168,000	427,000	2.54
Dispersion	180	79%	147,000	474,000	3.23

Figure 3-18 shows that there is little difference in the characteristics of the small particles in reactions using a CCTA, but that there are many more of them compared to a typical dispersion polymerization. The number of small particles is approximately the same for both 5 and 10ppm of

CCTA but the addition of the CCTA has resulted in an orders of magnitude increase in the number of small particles compared to a dispersion polymerization with no CCTA. Thus, there is a significantly higher volume fraction of small particles in CCT dispersions (more than 30% compared to less than 10% for dispersion polymerizations without CCT. Like many of the other cases presented, the typical size of the small particles formed does not differ between the base (dispersion) and test (CCT) cases. This combination of effects is very similar to the effects of changing MeMBL content in copolymerizations. The production of more small particles and their greatly increased volume fraction seen with the addition of the CCTA shows that it is effective in simulating the reduction of the chain length of the polymer and allowing relatively more to be produced in solution; these points further support the belief that the population of small particles is inherent to the dispersion polymerization process and that the initial period of solution polymerization is important to their formation.

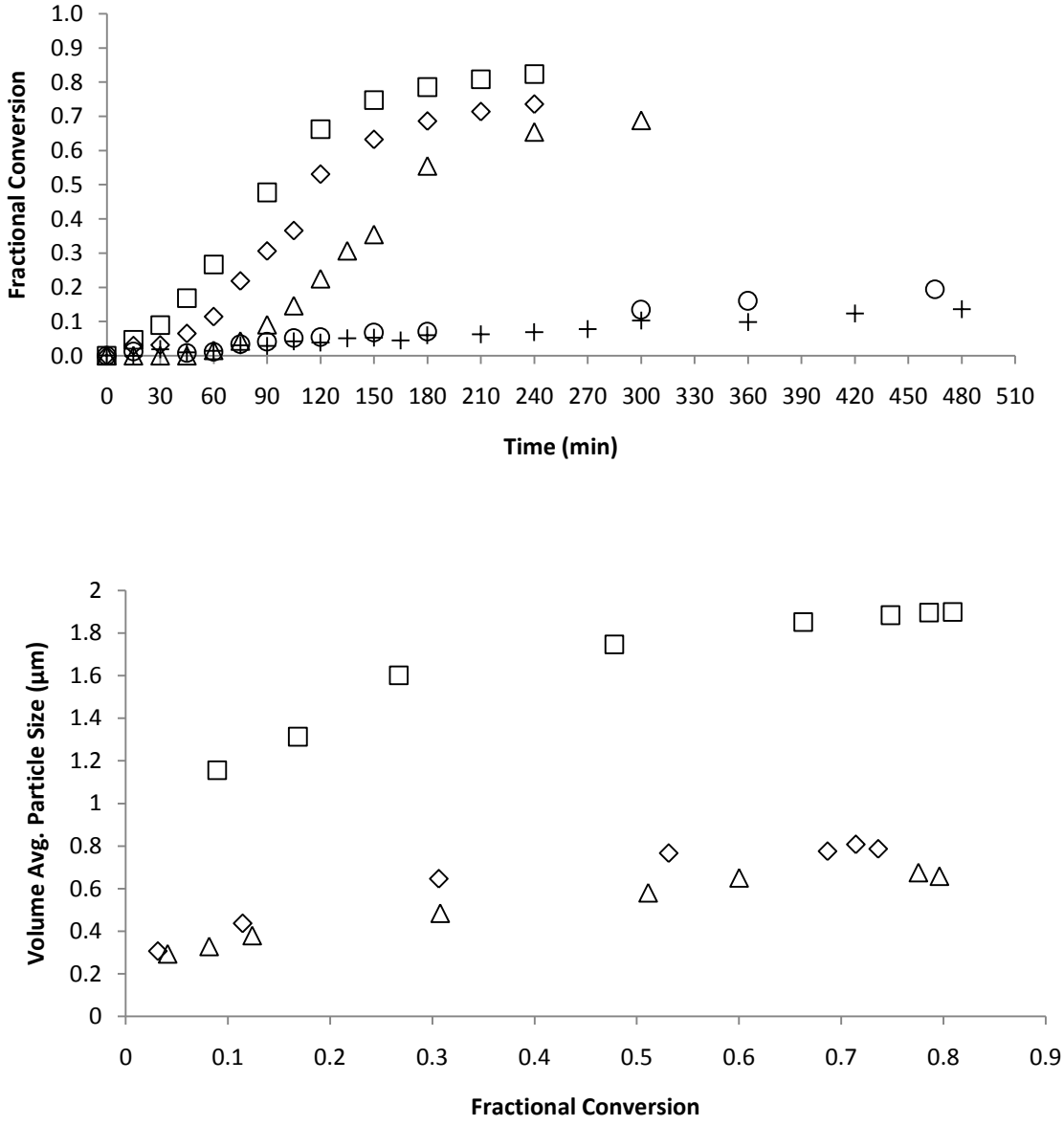

Figure 3-17 – Fractional conversion vs. time (top) and volume average particle diameter (bottom) of large particles as a function of fractional conversion for batch MMA CCT dispersion polymerizations carried out at 60°C in a 70|30 MeOH|Water continuous phase. Experimental results for dispersion (0ppm, □), 5ppm(◊), 10ppm (Δ), 50ppm (○) and 100 ppm (+) catalyst concentrations are presented.

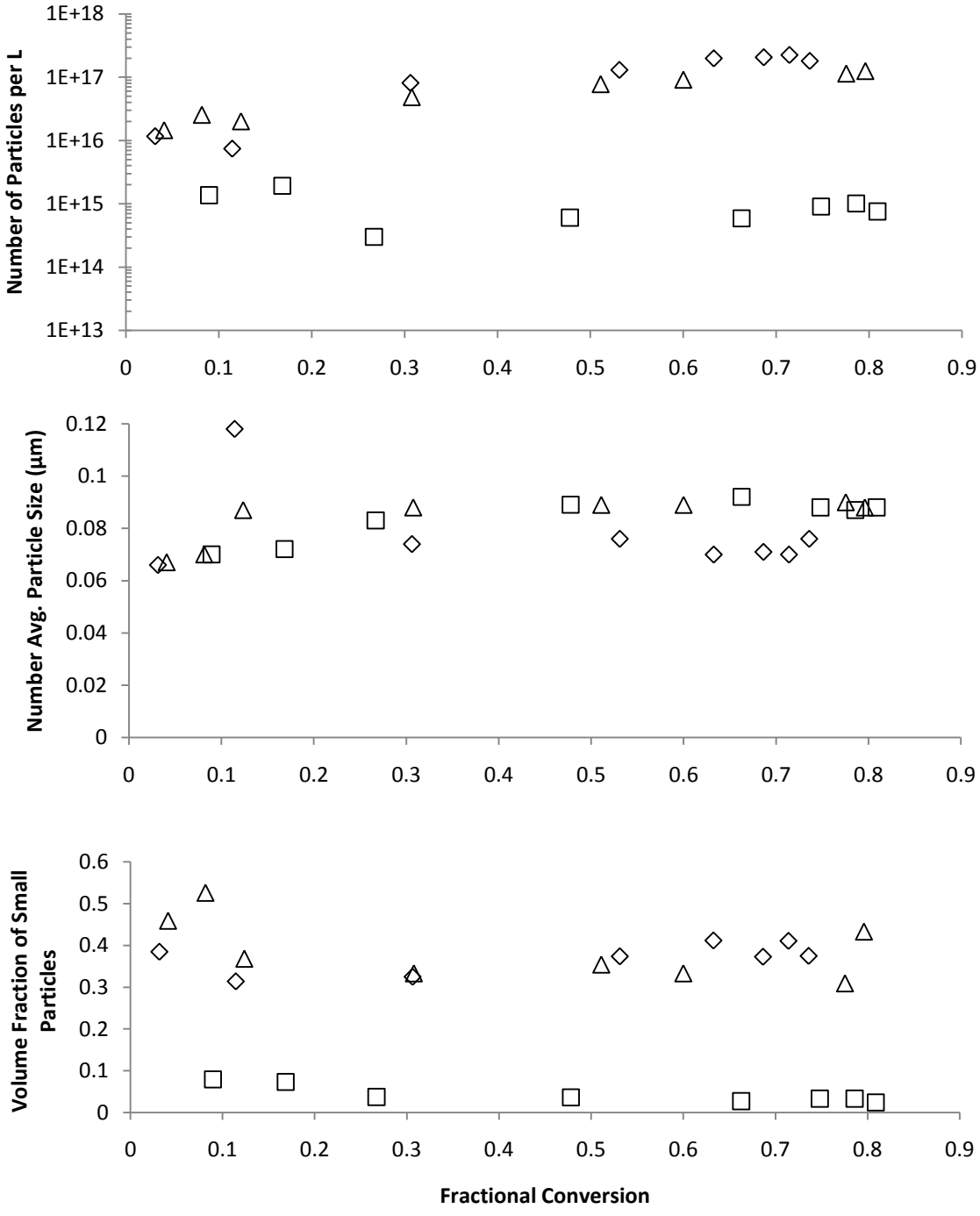

Figure 3-18 - Number of particles per L vs. fractional conversion (top), number average particle size vs. fractional conversion (middle) and volume fraction of total particle count for small particles as a function of fractional conversion for batch MMA CCT dispersion polymerizations carried out at 60°C in a 70|30 MeOH|Water continuous phase. Experimental results for dispersion (0ppm, □), 5ppm(◊) and 10ppm (Δ) catalyst concentrations are presented.

3.6 Conclusion

The results of this study support Paine's assertations[54] that there are aggregates of nuclei generated in a reaction that are typically one tenth as large as mature particles and it is these smaller aggregates that are captured by the mature particles in order to grow. The principle difference between what is reported in this work and previous literature is the recognition that the small particles are stable and observable by laser light scattering detectors long after polymerization has been stopped and under a variety of conditions including different surfactant concentrations and reaction media compositions. The small particle populations appear to be most affected by changes that alter the critical chain length of the precipitating polymer, such as changes to the composition of the continuous phase and the addition of other monomers with different critical chain lengths. The effects of the various parameters tested are summarized in Table 3-6. When considering the results as measured by the light scattering detector, initiator concentration does not appear to affect the properties of the small particles. The effects of altering the critical chain length of the precipitating polymer are the most prevalent and are consistent when comparing changes in continuous phase composition, changes in MeMBL content and changes in CCTA concentration. Interestingly, the small particle population appears to have a consistent particle size that is unaffected by changes to any other reaction parameters, indicating that none of the parameters tested in this work is able to greatly influence nucleation/the initial formation of small particle agglomerates from the particles that precipitate from solution at their critical chain length. Rather, it appears that the amount of time that it takes for a sufficient concentration of stabilizing moieties to develop from the onset of the reaction and stabilize the first polymer chains that precipitate is likely the principle aspect that determines the number of large particles that are observed. When the continuous phase is changed to lower the critical chain length, an increased number of small and large particles are seen as nucleation is enhanced and more particles are stabilized by relatively less surfactant. Further investigation into the effects of stabilizer type on the time taken to form the initial large particles and changes in the

characteristics of the small and large particle populations may yield further information on this subject.

Table 3-6 - Effects of changes in continuous phase composition, initiator and surfactant concentration on the recipe presented in this chapter with respect to the rate of polymerization, volume fraction of small particles and average diameter and number of particles per litre of small and large populations. Note that the direction of the arrow represents an increase across changes to that parameter.

Parameter		R_p	D_p Large	NP/L Large	D_p Small	NP/L Small	Volume Fraction Small
Continuous Phase	60|40	⇧	⇩	⇧	N/C	⇧	⇧
	70|30						
	80|20						
Initiator	0.50%	⇩	⇩	⇧	N/C	N/C	N/C
	2%						
	4%						
Surfactant	10%	N/C	⇧	⇩	N/C	⇩	N/C
	15%						
	20%						
MeMBL Content	MMA	⇧	⇧	⇩	N/C	⇩	N/C
	25%						
	50%						
	75%						
CCT Content	MMA	⇧	⇧	⇩	N/C	⇩	⇩
	5ppm						
	10ppm						
	50ppm						
	100ppm						

3.7 Acknowledgements

I wish to thank Mr. Iain Lounsbury for his assistance in conducting the experimental work on the effects of initiator, surfactant and continuous phase over the course of summer 2010. I would also like to thank Dr. Niels Smeets, a postdoctoral fellow in our lab who prepared the CCTA for use in those experiments.

Chapter 4

Synthesis and Physical Property testing of MeMBL dispersion copolymers

4.1 Introduction

A thorough understanding of the characteristics and properties of polymers is necessary to ensure the quality, service performance and design of the products made from and sold to customers downstream.[115, 116] The widely varied nature of polymers, from soft foams to rigid composites, means that a great variety of tests and standardized methods have been developed in order to obtain relevant data for the many types of materials.[115, 116] While some tests are quite specialized for particular polymer classes and even industries (i.e. rubber, adhesives), others are more generalized such as methods for determining molecular weight (MW) and glass transition temperature, (T_g). The term physical testing refers to the physical characteristics of polymers in the very literal sense and does not examine chemical changes.[116] That being said, some common physical tests do encompass chemical changes in the polymers, such as thermal analysis and ageing.[116] The goal of this chapter is to evaluate the relevant physical properties for polymer processing, which include polymer molecular weights, glass transition temperatures, decomposition profiles and melt flow indices, in order to evaluate mechanical properties of MeMBL/MMA copolymers. In addition, testing the tensile, flexural and impact strengths of copolymers will allow the quantification of the effect of MeMBL incorporation on physical properties, in order to evaluate potential applications of these new materials. First however, knowledge gained from pMeMBL/MMA kinetics study (Chapter 2) is used to develop a dispersion polymerization process (Chapter 3) to produce copolymers of constant composition.

4.2 Experimental

4.2.1 TGA – Thermal Gravimetric Analysis

The thermal decomposition profiles of the polymers produced were measured by a TA Instruments TGA Q500 Thermo Gravimetric Analyzer (TGA). TGA helps to characterize the decomposition and thermal stability of materials under a variety of conditions. Changes in the mass of sample are measured as a function of temperature and may indicate, among others, vaporization, oxidation and decomposition of the sample.[117] Samples were analyzed under nitrogen atmosphere with temperature increased at a rate of 10^{o}C/minute to 500^{o}C and then 25^{o}C/minute to 800^{o}C to completely degrade any remaining polymer.

4.2.2 DSC – Differential Scanning Calorimetry

The glass transition temperatures of the copolymers were determined by a TA Instruments DSC Q100 Differential Scanning Calorimeter. The T_g of a polymer defines the point where a polymer becomes brittle on cooling and soft (rubbery) on heating. Below the T_g, polymers have a glassy appearance; above the T_g, polymers become soft and are able to undergo plastic deformation without breaking.[117] DSC determines the T_g of a polymer sample by measuring the amount of heat required to raise the temperature of the sample as a function of temperature. The T_g is marked by a step change in the recorded signal caused by a change in the heat capacity of the sample. Samples of up to 10 mg were placed into aluminum sample pans and sealed for testing in the DSC. The applied heating rate was 10°C/minute over a range of 50 to 230 °C. The first heating and cooling cycle were used to erase any thermal history in the polymer and data was collected from the third scan. T_g's were taken at the inflection point between the onset and end point temperatures. Nitrogen atmosphere was used to minimize thermal degradation of the copolymer.

4.2.3 Preparation of Polymers for Physical Properties Testing

The polymer produced (~16g per reaction) was first dried by letting the majority of methanol and water evaporate at room temperature in a fumehood. When no liquid was observed with the polymer (after a period of a few days), the polymer, it was placed in a circulating air oven at 85^{o}C for 24 hours. The oven-dried polymer was then placed in a vacuum oven at 60^{o}C for a further 24 hours to try to remove any residual monomer and solvents. Dried polymer was placed in air-tight containers and purged with nitrogen for storage until testing. The properties investigated of the MeMBL/MMA copolymers made by batch and semibatch polymerization techniques include polymer glass transition temperature (via DSC) and decomposition profiles (via TGA). Attempts were made to determine the tensile, flexural and impact strengths of the polymers as well, but these trials met with a number of issues. DSC and TGA testing was completed at Queen's University. Polymer physical properties processing was first conducted at the University of Waterloo in the laboratories of Dr. Leonardo Simon in order to make use of the expertise and facilities of that group and later, also at Queen's University. The initial preparation of all polymer samples tested in both locations was the same. Processing equipment used included a co-rotating conical twin screw extruder (Haake Minilab Microcompounder), a lab scale Ray Ran injection moulding device (Ray Ran, RR/TSMP) and a compression moulding setup consisting of two independently controlled heating plates, thermostats and jack. Applicable standards for polymer testing include ASTM D638 (tensile properties), ASTM D790 (flexural properties) and ASTM D256 (izod notched impact test).

4.3 Results and Discussion

4.3.1 Semibatch Copolymerization

The recipes and a general characterization of batch dispersion MeMBL/MMA copolymerizations have been detailed in Chapter 3 (Table 3-3). In that chapter, we developed a method suitable for

the production of MeMBL copolymers and investigated how particle size and polymerization rate varied with copolymer composition. However, due to the extreme differences in monomer reactivities, as determined in Chapter 2, the composition of the batch copolymers such as those created in Chapter 3 will not be uniform, as MeMBL is consumed faster than MMA. The compositional drift for copolymers produced in batch is seen in Figure 4-1, as measured by ^{1}H NMR using the procedures described in Chapter 2. For a majority of applications of polymers, composition must be well controlled and consistent over a reaction and from batch to batch. In order to better control the composition of the copolymers, a semibatch copolymerization technique was employed whereby the more reactive MeMBL was fed into co-monomer mixtures of MeMBL and MMA at a constant rate over a 6 to 7 hour period. The feed time was determined based on inspection of many conversion-time profiles obtained for batch copolymerizations that saw a relatively linear rate of conversion/reaction. The 6-7 hour period allowed polymerization to occur to the point where limiting conversions were observed and polymerization was allowed to proceed for approximately one hour after the final addition of MeMBL monomer in order for it to be incorporated into the polymer. The same materials and apparatus as described in Chapter 3 were employed here. The ratio of MeMBL to MMA monomer in the initial monomer mixture was set based on the copolymer composition curve presented in Chapter 2, Figure 3. As seen in Table 4-1, the initial monomer feed ratios for the copolymers were set to 90/10, 25/75 and 50/50 mol% MeMBL|MMA for the 25, 50 and 75 mol% MeMBL|MMA copolymers, respectively. All of the initiator was charged with the initial monomer dose and no additional initiator was fed in over the subsequent reaction. The composition of the polymer produced via semibatch copolymerizations is also shown in Figure 4-1. While there is still some slight drift in composition over the course of a reaction, it is small compared to the batch polymerizations.

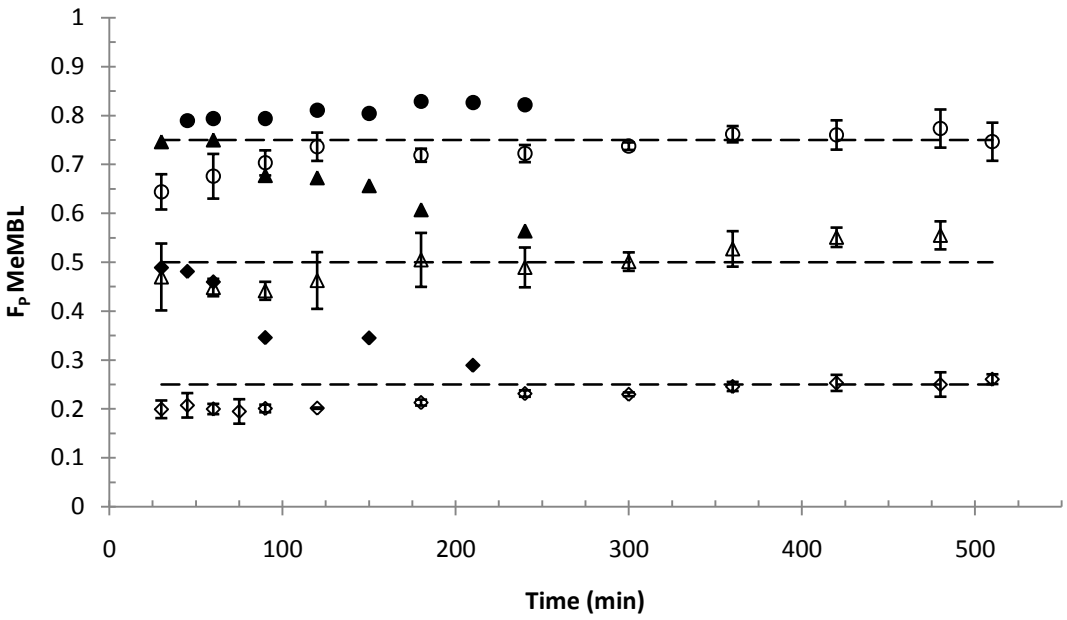

Figure 4-1 – Mole fraction of MeMBL in copolymer (F_pMeMBL) vs. time for batch (filled) and semibatch (open) MeMBL/MMA copolymer dispersion polymerizations carried out at 60°C in a 70|30 MeOH|Water continuous phase. 25|75(◊), 50|50 (Δ) and 75|25 (○) MeMBL/MMA ratios are presented.

Table 4-1– Recipes for MeMBL|MMA Copolymer Dispersion Polymerizations (60°C, 180 rpm)[a]

	Weight (g)		
Copolymer (MeMBL|MMA)	25|75	50|50	75|25
Feed MeMBL	3.73	7.47	11.2
Initial MeMBL	1.87	3.73	5.6
Initial MMA	15.0	10.0	5.0
Vazo 67[b]		2%[a]	
PVP 40[c]		15%[a]	
Methanol/Water (70/30 wt/wt)		1000%[a]	

[a] Based on total monomer weight
[b] 2-Amino-2-methylbutyronitrile
[c] Poly(vinyl pyrrolidone), MW = 40,000 g/mol

4.3.2 Semibatch vs. Batch Copolymerizations

The batch and semibatch rate curves, shown in Figure 4-2 along with volume average particle size measurements for the large particle population, are similar, with the semibatch conversion measurements showing less variation between the copolymer recipes compared to batch. It is interesting to note that the increase in polymer particle size with MMA content is more clearly seen in semibatch than in batch polymerizations. Where MeMBL addition is not controlled (i.e. in the batch polymerizations), the copolymer particle size tends to be smaller, driven by increased early incorporation of MeMBL. The initial particle size measurements for semibatch 50|50 and 75|25 copolymers line up very closely with initial particle size measurements for the batch 25|75 and 50|50 copolymers, respectively. This observation is consistent with the initial comonomer compositions charged (i.e. for the 25|75 copolymer 10% MeMBL in semibatch and 25% MeMBL in batch) in the semibatch recipes compared to batch. This suggests that the nucleation of the particles (and thus the diameter of the resulting large particle population) is determined by the initial comonomer composition in the reaction and the j_{crit} of those mixtures; copolymer particles where MeMBL is added via semibatch are larger, due to reduced MeMBL content during the nucleation phase of the polymerization.

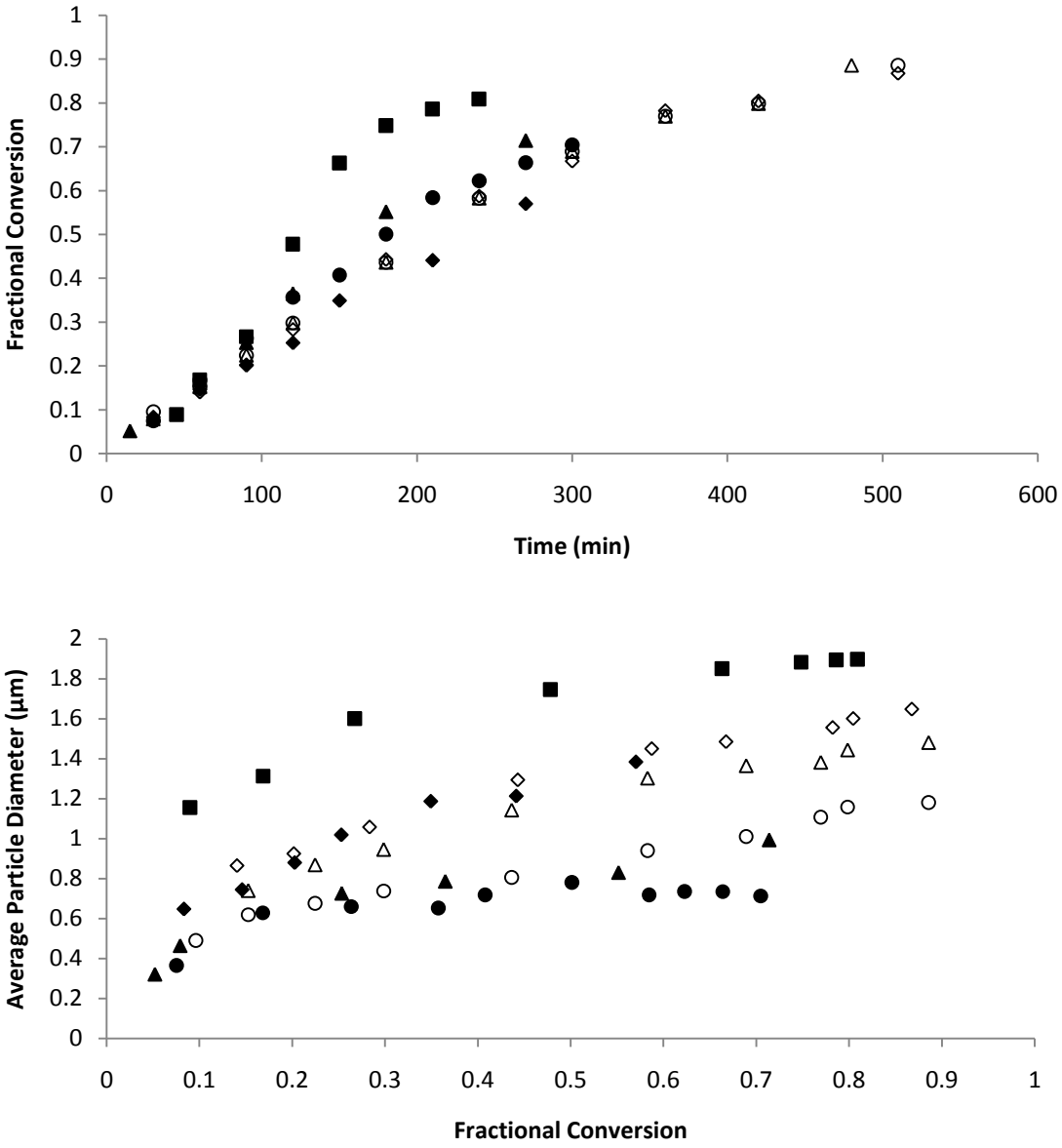

Figure 4-2 – Fractional monomer conversion vs. time (top) and volume average particle diameter of large particles as a function of fractional conversion (bottom) for batch (filled) and semibatch (open) MeMBL/MMA copolymer dispersion polymerizations carried out at 60°C in a 70|30 MeOH|Water continuous phase. MMA (□), 25|75(◊), 50|50 (Δ) and 75|25 (○) MeMBL/MMA ratios are presented.

4.3.3 Semibatch vs. Batch TGA

The thermal decomposition profiles of the copolymers produced via semibatch polymerization can be seen in Figure 4-3. Negligible mass loss occurs before 100^{o}C, indicating good removal of methanol and water from the latex by the drying process. The mass losses (about 5%) seen above 100^{o}C until about 200^{o}C may be the evaporation of residual monomer from the samples; while dried in a vacuum oven prior to testing, it is possible that some monomer remained trapped in the polymer. It would be desirable to see if this mass loss is related to residual monomer by testing polymers that have been "washed"; that is to say dissolved in a solvent such as THF, reprecipitated by methanol and subsequently isolated from the supernatant by decanting, and further dried in a vacuum oven. Unfortunately, after the initial tests were completed, the TGA instrument was damaged and is currently inoperable. The rapid decrease in mass for all polymers noted around 350^{o}C shows where thermal degradation occurs. Increasing MeMBL fraction shifts the onset of thermal degradation to higher temperature, from approximately 250^{o}C for pMMA to about 300^{o}C for 75|25 p(MeMBL-co-MMA). The degradation profile up until the point of thermal degradation should be relatively flat, with almost no mass loss having occurred. The more gradual sloping of the curves to about 300^{o}C seen with certain samples indicates some vinyl (pMMA-CH=CH$_2$) rather than saturated (pMMA-H) chain termination, which promotes degradation at lower temperatures.[118-122] Vinyl termination is seen to occur with disproportion termination of polymeric radicals[123] and appears to be more noticeable in the pMMA homopolymers, and is reduced with increasing MeMBL content. Once vinyl chain unzipping of MMA units begins, depropagation is likely stopped in the copolymer when a MeMBL unit is encountered.

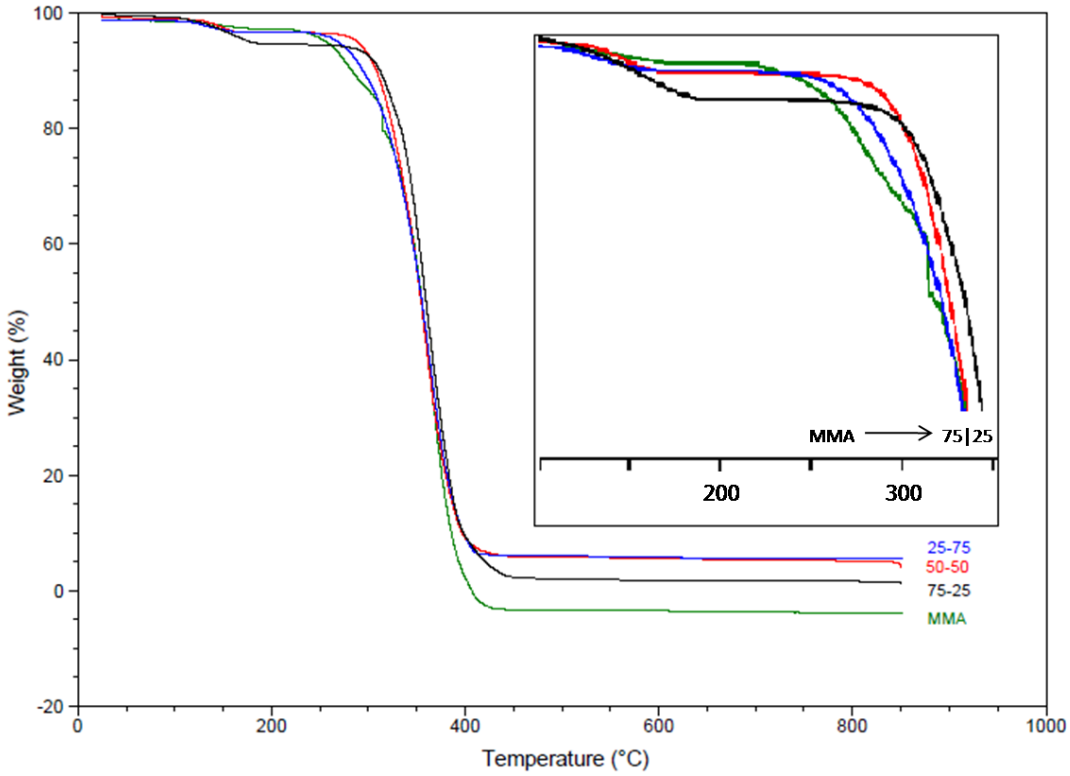

Figure 4-3 – Thermal decomposition profiles of MeMBL/MMA copolymers; from bottom MMA (green), 75|25 (black), 50|50 (red), 25|75 (blue). MeMBL content increases from left of blown up section.

4.3.4 Semibatch vs. Batch DSC

Based on TGA measurements, the maximum temperature that polymer samples were exposed to was kept below 250°C to minimize the likelihood of degradation. The maximum temperature of 230°C was chosen as it was above the expected MeMBL homopolymer T_g[8] yet below the point where degradation becomes more likely. The T_g of the polymer is seen to increase as the fraction of MeMBL increases. The measured T_g of pMMA (Table 4-2) is higher than the typical value of about 105°C but is in line with results from the literature that found that very dry polymer, especially those with a high MW (discussed further later in this chapter), and a more regular, ordered structure have a higher T_g.[124-126]

Semibatch polymer samples that were both "washed" (as described in TGA results and discussion) and unwashed were tested via DSC; in all cases the T_g's determined for the washed

polymers are higher. The process of dissolving the polymers in THF (even though the 75% MeMBL content copolymers are not soluble) should remove both excess PVP surfactant and allow residual monomer to escape the dispersion particles and polymer chain entanglements. Since the polymer T_g increased when washed, it is likely that residual monomer (with a lower T_g) was having a plasticizing effect.[127] Even trace water content in polymers has been shown to have a significant effect on T_g and processing polymers in this way is thus expected to have a significant impact.[126] The differences between washed and unwashed polymer T_g's are shown in Figure 4-4 and quantified in Table 4-2. The increase in T_g with increasing MeMBL fraction is expected (see Chapter 2, Figure 3). All further DSC results are based on analysis of washed polymers. No values are given on the Y axis for heat flow ($W \cdot g^{-1}$) as it is the relative rate of change as a function of temperature and not the absolute value that is important in identifying the T_g.

Table 4-2 – Glass transition temperatures for washed vs. unwashed MeMBL/MMA copolymers

MeMBL|MMA	Unwashed T_g (^oC)	Washed T_g (^oC)
0-100	121	127
25-75	122	135
50-50	143	169
75-25	160	198

Figure 4-5 shows a series of T_g plots measured for MeMBL/MMA copolymers taken over the course of a single polymerization. The batch experiments have measured T_g's that are higher than the ultimate T_g's measured from semibatch polymers at final conversion and all of the observed batch polymer T_g's decrease towards the semibatch value as time (and conversion) increase, similar to the decrease in overall MeMBL fraction in the polymer is with conversion (Figure 4-1). The semibatch copolymer shown in Figure 4-5 has a more constant T_g over time, consistent with its more uniform copolymer composition.

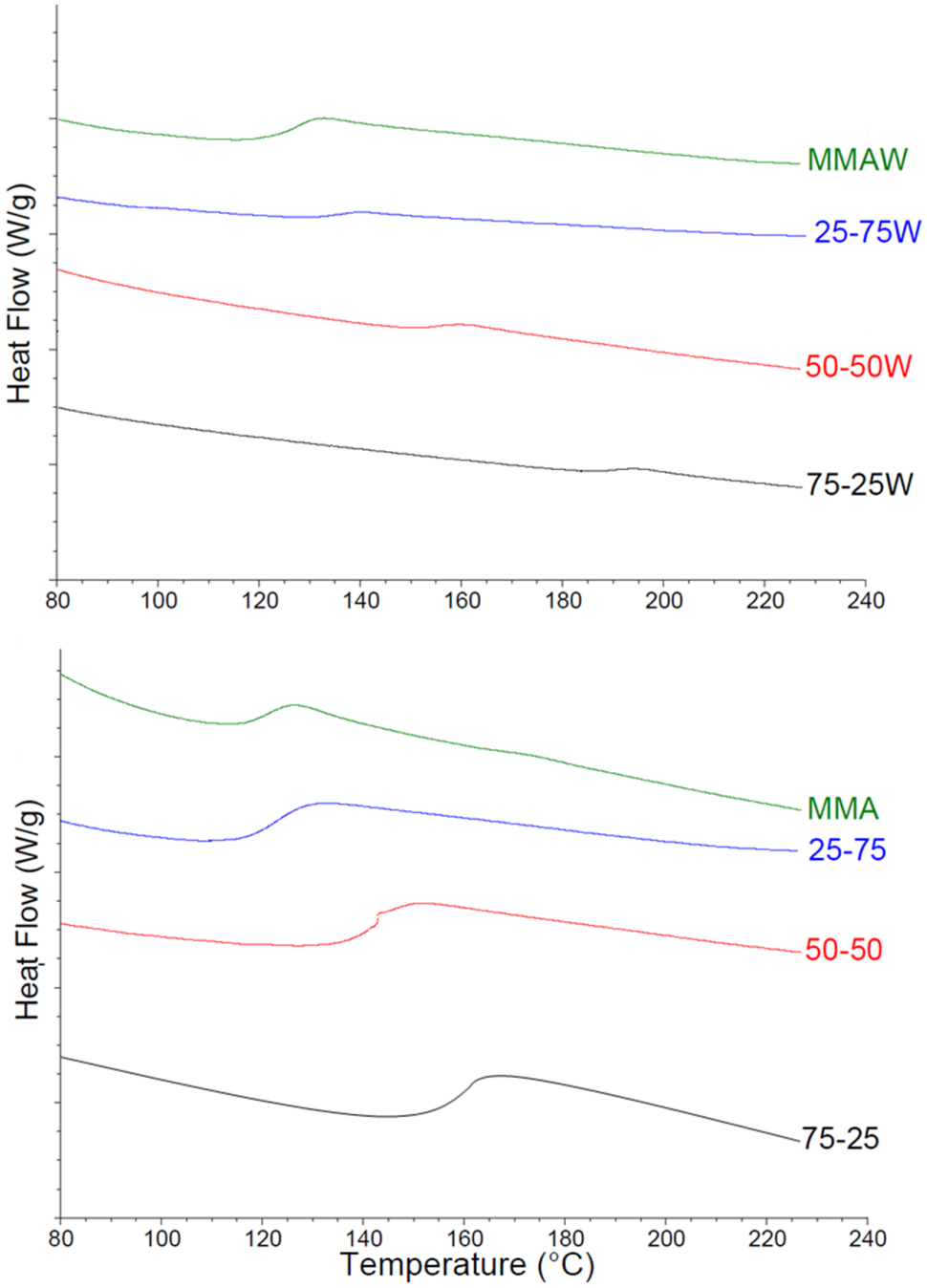

Figure 4-4 – Differential Scanning Calorimetry curves (exotherm down) for washed (W, top) and unwashed (bottom) MeMBL/MMA copolymers. In each plot, from top to bottom pMMA (green), 25|75 (blue), 50|50 (red), 75|25 (black).

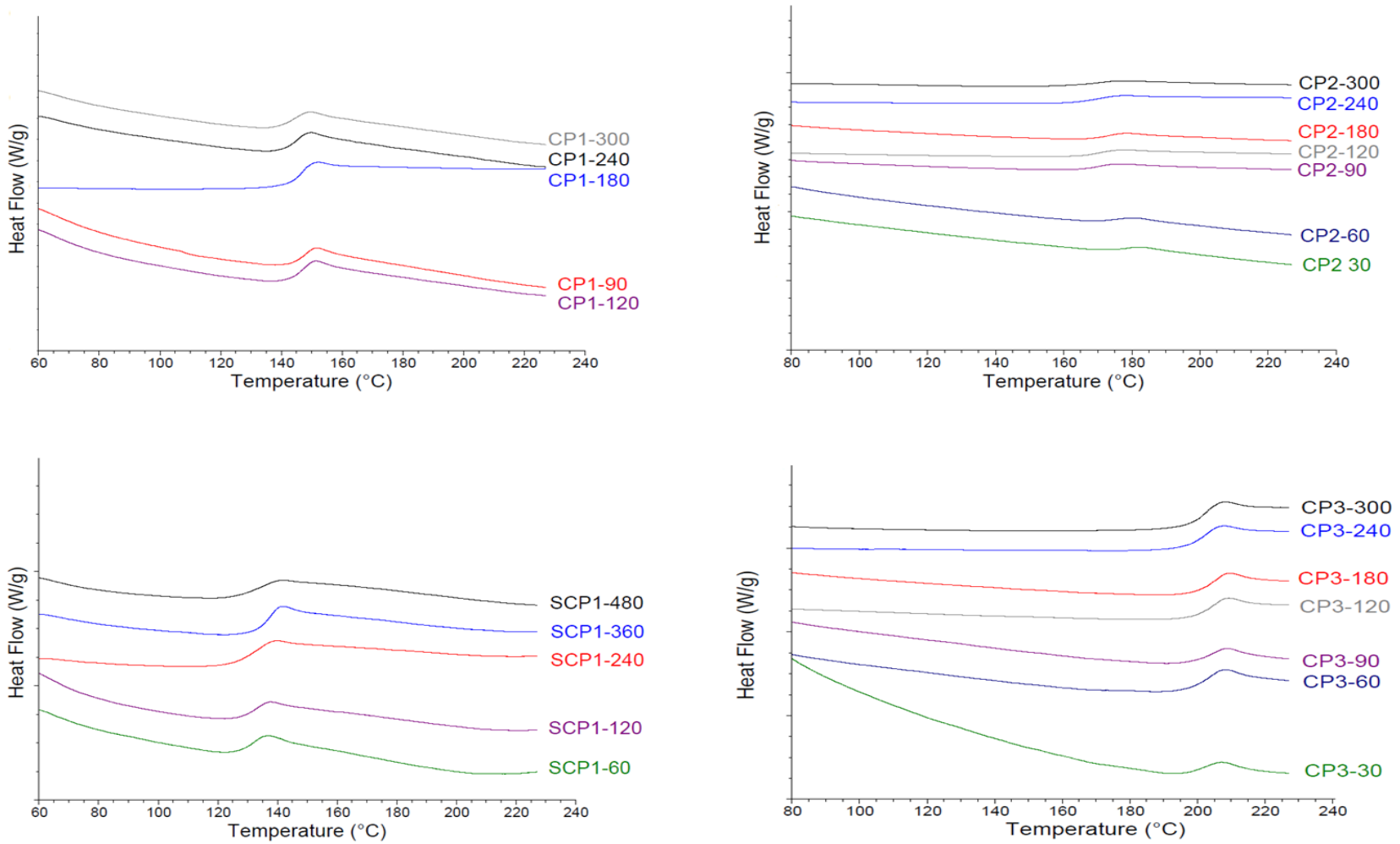

Figure 4-5 – Differential Scanning Calorimetry curves (exotherm down) for washed MeMBL/MMA copolymers. In each plot, the earliest sample is shown at bottom, with samples increasing in time moving to the top of each plot. Top left 25|75 batch copolymer, top right, 50|50 batch copolymer, bottom left, 25|75 semibatch copolymer, bottom right, 75|25 batch copolymer.

When the T_g's measured in Figure 4-5 are compared to the fraction of MeMBL polymer ($F_{p,\ MeMBL}$) measured in the sample (the same samples as in Figure 4-1), the data displays consistent trends, seen in Figure 4-6. The T_g for the 75|25 batch copolymer is high and relatively constant, as the MeMBL content in the polymer was also relatively constant over the course of polymerization. In contrast, a strong decline in T_g is seen with the 50|50 batch copolymer, as its composition changed significantly over the course of the polymerization. The T_g for the semibatch 25|75 copolymer rises slightly as MeMBL content rises and that of the 25|75 batch copolymer falls as MeMBL content falls.

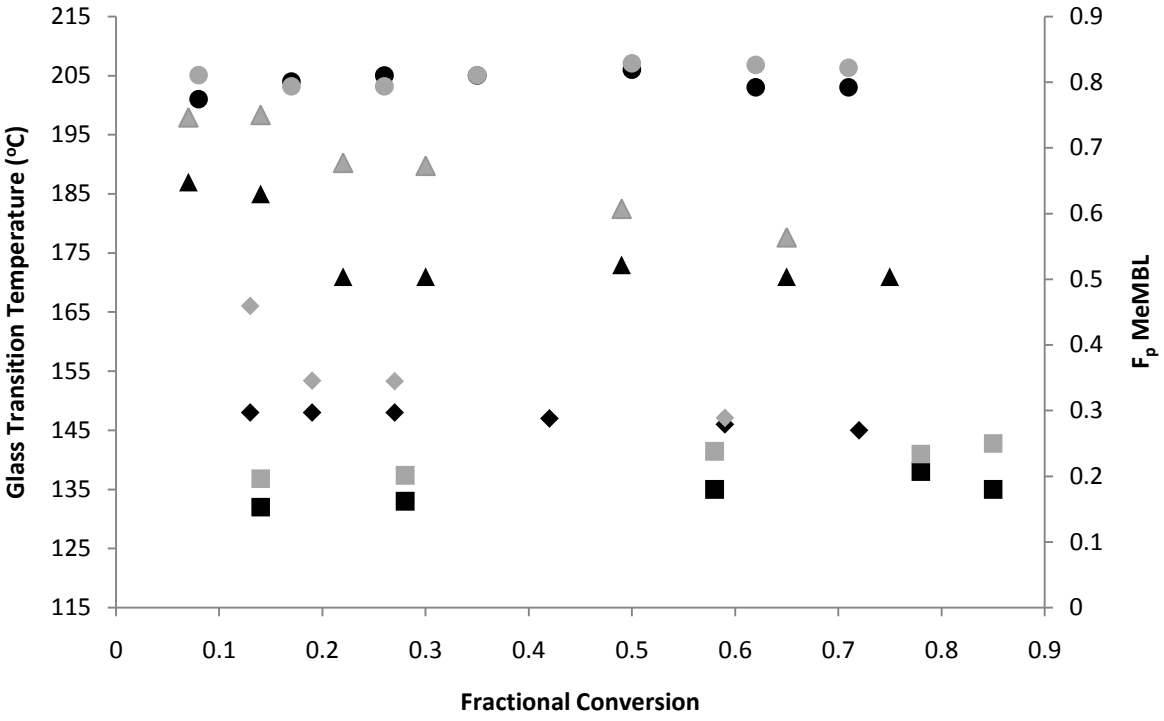

Figure 4-6 – MeMBL/MMA copolymer glass transition temperature (°C, left axis, black shading) and fraction of MeMBL in the copolymer, F_pMeMBL (right axis, grey shading) for 25|75 semibatch (□) and batch (◊), 50|50 batch (Δ) and 75|25 batch (○) copolymers.

These results have shown that it is possible to tailor the T_g of a copolymer by the addition of MeMBL to MMA homopolymer. However, when the glass transitions of these polymers are

compared to those measured from samples of well controlled composition as created by PLP, seen in Chapter 2, Figure 6, the copolymer T_g's (all for "washed" polymer) are notably different, as shown in Figure 4-7.

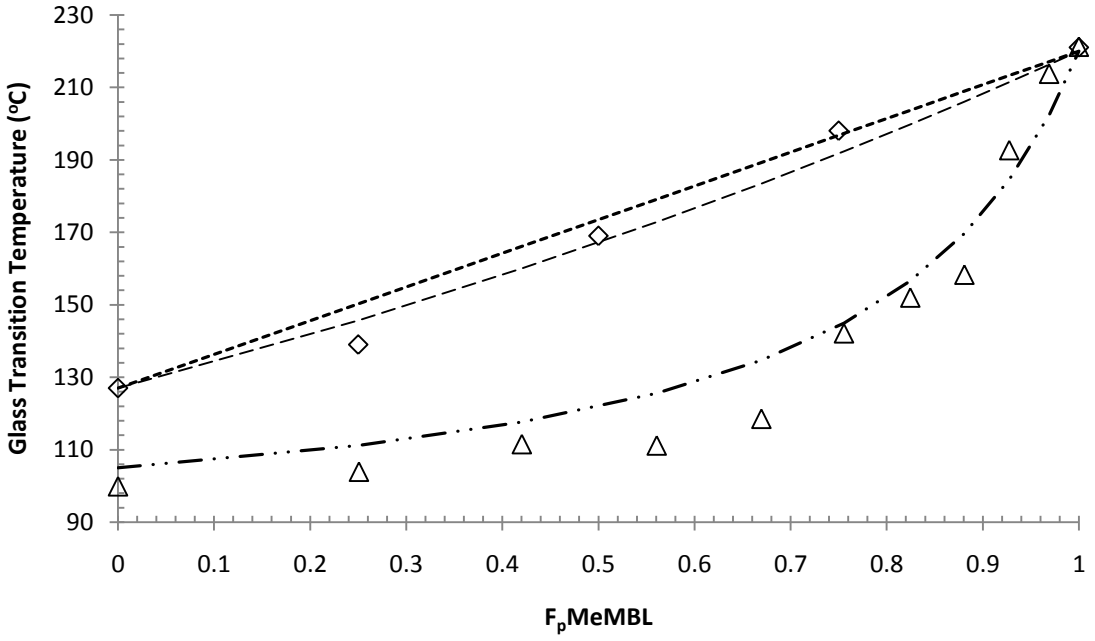

Figure 4-7 - MeMBL/MMA copolymer glass transition temperature (°C) as a function of the fraction of MeMBL in the copolymer, F_pMeMBL for copolymers produced by dispersion (◊) and PLP (Δ) techniques. Approximations based on the Gordon-Taylor equation[92] (k = 1 ····) and Couchman equation[90] (k = 4, —·· —, k = 1, — — —) are shown for the data.

Unlike the PLP copolymers, whose T_g can be roughly approximated by the Couchman equation,[90] the T_g's of dispersion copolymers are not very well approximated by this and other classical, well known relationships, including the Fox[91] and Gordon-Taylor[92] equations using the same parameters and are almost linear in their relationship. The Fox, Couchman, and Gordon Taylor equations are listed below in equations 1 through 3.

$$Fox\ Equation\colon \frac{1}{T_g} = \frac{w_1}{T_{g1}} + \frac{w_2}{T_{g2}} \quad (1)$$

$$Couchman\ Equation: lnT_g = \frac{w_1 lnT_{g1} + kw_2 lnT_{g2}}{w_1 + kw_2} \quad (2)$$

$$Gordon - Taylor\ Equation: T_g = \frac{w_1 T_{g1} + kw_2 T_{g2}}{w_1 + kw_2} \quad (3)$$

The Fox equation is the simplest and estimates the T_g as an inverse of the weight fraction of the copolymers over their homopolymers T_g's. In both the Couchman and Gordon-Taylor equations, the parameter *k* is a ratio of the isobaric heat capacities of both monomers and is used in conjunction with the polymer weight fractions and homopolymers T_g values. Setting *k* to 1 in each case results in a linear approximation of T_g as a function of polymer weight fraction. Curves shown in Figure 4-7 are calculated based on weight fraction and displayed as a function of mol fraction.

To fit the PLP T_g measurements, *k* was set to 4 for the Couchman equation; to approximate the dispersion polymer T_g measurements, *k* was set to 1 for both the Gordon-Taylor and Couchman equations. Since the monomers are the same in both cases, presumably the heat capacities should not change. At this point, this inconsistency is not well understood and it is interesting that PLP homopolymer pMMA has a T_g close to that commonly quoted in literature while the dispersion product is significantly higher. One of the chief differences between polymers produced by PLP and dispersion techniques is their higher molecular weights; PLP polymers are much less than 100,000 $g \cdot mol^{-1}$ whereas dispersion polymers at final conversion have a MW of hundreds of thousands. The use of the PVP surfactant in dispersion may also play a role, although as discussed previously, most non-grafted PVP should be removed by washing in THF and the amount remaining bound to the polymer should be low.

4.3.5 Semibatch vs. Batch Molecular Weight Distributions

The MW of the pMMA homopolymer and of the 25|75 and 50|50 MeMBL/MMA semibatch copolymers, which were all THF soluble, was investigated by the same method/equipment as described in Chapter 3. The 75|25 copolymer was not analyzed as it was insoluble in THF as discussed in Chapter 2. SEC results are reported in Table 4-3and shown in Figure 4-8. The MW of the pMMA that was processed was similar to other samples previously analyzed (as in Chapter 3), and the MW of the copolymers decrease with increasing MeMBL fraction (both mass and number). From Figure 4-8, it can be seen that the low MW fraction is more significant with increased levels of MeMBL and continues below the SEC's limit of detection. The increased fraction of smaller chains and lower MW values are indicative of more solution-like polymerization of MeMBL, as was discussed in Chapter 3. The results reported are for the same samples that were investigated for physical testing, discussed in Section 4 of this chapter.

Table 4-3 - Molecular Weight distribution data for MeMBL/MMA semibatch copolymers near final conversion

Sample	Time (min)	Conversion (%)	Mn ($g \cdot mol^{-1}$)	Mw ($g \cdot mol^{-1}$)	PDI
MMA	480	88	119,000	412,000	3.45
25-75	480	88	65,000	234,000	3.60
50-50	480	88	52,000	197,000	3.77

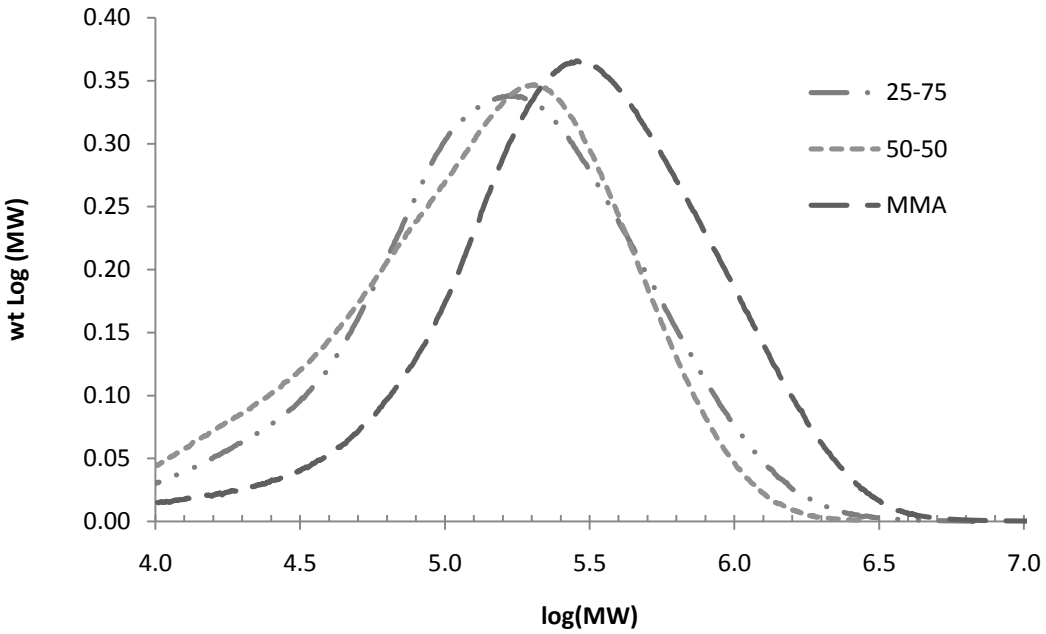

Figure 4-8 – Molecular Weight Distributions for MeMBL/MMA semibatch copolymers near final conversion. MMA (batch, ——), 25|75 (– •• –), 50-50 (– – –)

Analysis of the molecular weight evolution with conversion is also interesting. Figure 4-9 plots MW measurements for pMMA homopolymer (batch) and 25|75 MeMBL/MMA batch and semibatch copolymers at a number of time/conversions individually and Figure 4-10 compares the distributions at selected time/conversions on the same plots. The 25|75 copolymer was examined since all samples from all timepoints were soluble for the batch reaction, which was not the case for higher MeMBL content copolymerizations. It can be seen that MW grows with conversion. At final conversion, the highest MW is obtained for MMA homopolymer dispersions, followed by batch and then semibatch copolymerizations. It is interesting to note that initially (at lower conversion as in Figure 4-9), there is a greater fraction of low MW chains produced by the batch copolymerization than the semibatch copolymerization, which is consistent with greater MeMBL incorporation in the early stages of the reaction. However, ultimately (even by only 27%

conversion as in Figure 4-10), the semibatch copolymerization has more small chains, which is consistent with its better overall control of MeMBL incorporation.

4.4 Physical Properties Testing

4.4.1 Processing

Attempts were made to test the physical properties of the polymers prepared by dispersion polymerization but were largely unsuccessful. The dried polymer prepared as described was milled into a powder with mortar and pestle, and 0.25 wt% of the antioxidant Irganox 1010 was added in order to protect the polymer from degradation during processing at high temperatures. Prior to using injection moulding to form specimens for physical properties testing, attempts were made to homogenize the polymer via extrusion with a co-rotating conical twin screw extruder (Haake Minilab Microcompounder). First attempts were made using the homopolymer MMA at 200^{o}C and 50rpm, which is in a typical range for acrylics and below 250^{o}C where decomposition starts to occur. Surprisingly, the pMMA homopolymer, which has a T_g of approximately 122^{o}C (unwashed samples were used, as total volumes of polymers taken for testing was on the order of 100-150g) would not flow through the extruder at these conditions. Temperature was slowly ramped up to 250^{o}C and at this point, and only with significant force applied at the feeding end, some polymer slowly was extruded. However, the extrudate was white-yellow, indicating signs of thermal decomposition, despite the presence of an antioxidant. Extrusion of the 75|25 MeMBL|MMA copolymer was also attempted at the same conditions and proved even more difficult. The polymer that could eventually be extruded was much thicker in diameter compared to the pMMA and the size of the dye it was extruded from, indicating significant die swell and poor fluid processing. The polymers that were extruded are shown in Figure 4-11. Note the much

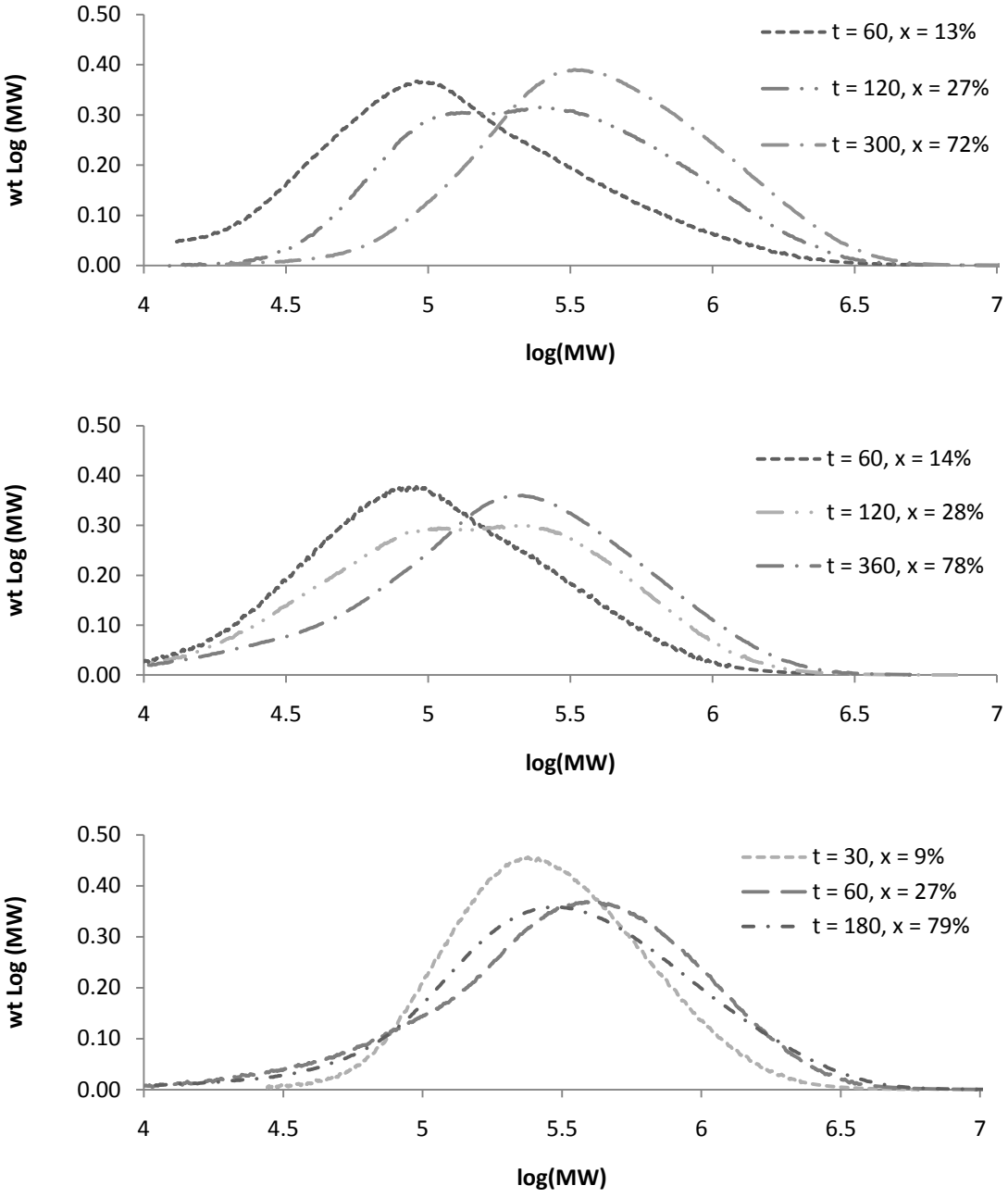

Figure 4-9 – Molecular Weight Distributions for MeMBL/MMA copolymers produced by batch (top) and semibatch (middle) methods and pMMA homopolymer (bottom) at varying conversion (x). See figure for legend.

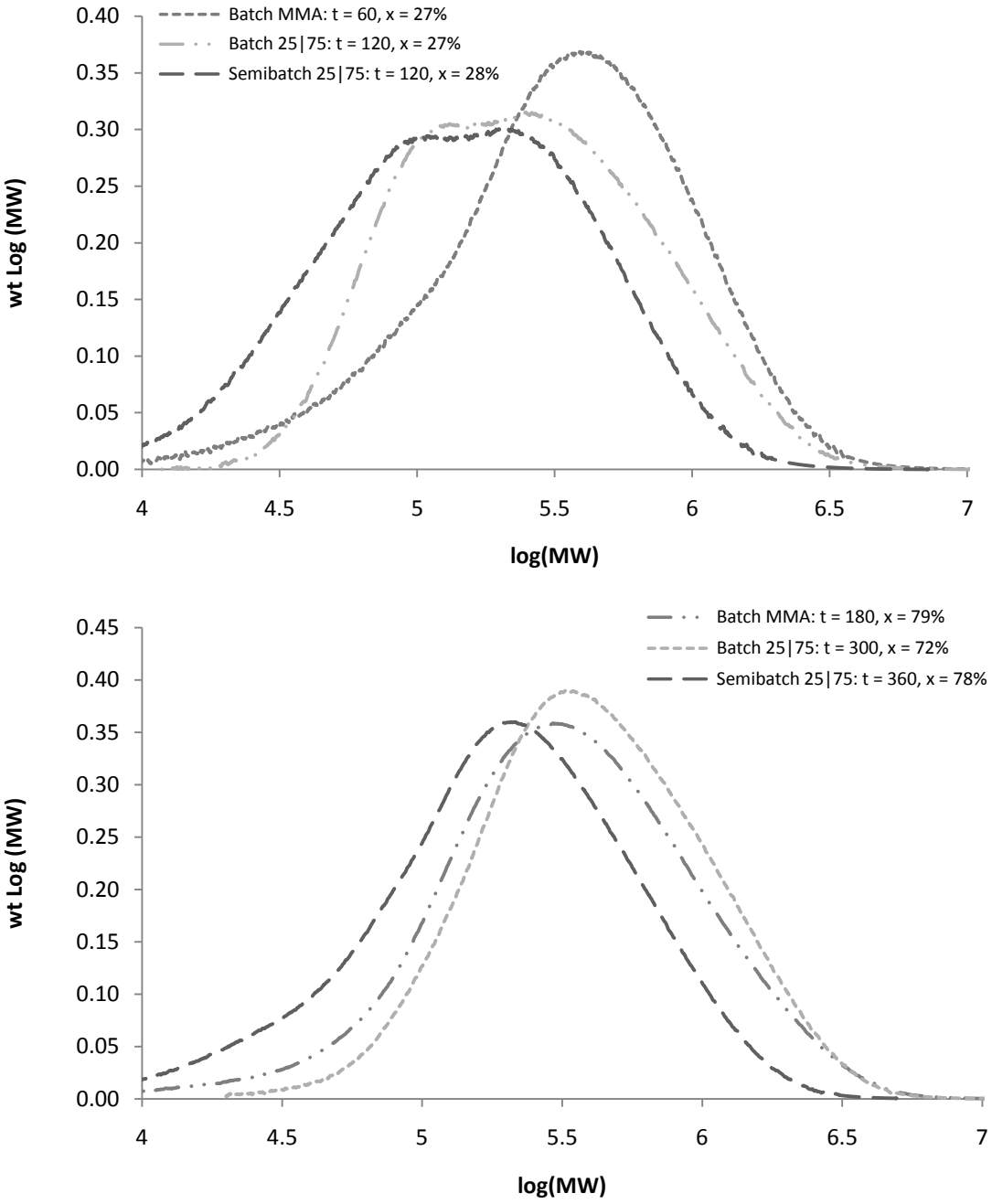

Figure 4-10 – Molecular Weight Distributions for MeMBL/MMA copolymers and pMMA homopolymer produced by batch and semibatch methods at low (top) and final (bottom) conversion (x). See figure for legend.

larger diameter of the 75|25 copolymer compared to the homopolymers; the pMMA diameter was approximately 1/16 of an inch (comparable to the extruder die) while the copolymer was more than 1/8 of an inch. The darker colour of the copolymer also shows more evidence of degradation due to the longer residence time in the extruder as a result of its poor flow.

Figure 4-11 – Image of extruded polymers. pMMA top left and p(MeMBL-co-MMA) (75|25) top right with direct comparison at bottom.

Since the extruder was unable to process the polymers, injection moulding was not attempted; The Ray-ran injection moulder requires polymer to flow easily and can only inject at a maximum of 100psi. Because of the difficulties encountered with achieving polymer flow, the melt flow index (MFI) of the pMMA homopolymers was investigated using a Dynisco Polymer Test MFI device. Usually, the MFI of acrylics is measured at 230^{o}C with a 1.2 or 3.8 kg weight (ASTM D1238). However, at those conditions, the polymer would not flow through the MFI die. In order to achieve any flow, the temperature was increased to 300^{o}C and a 5kg weight was used. The

MFI achieved was 1.18±0.06 (/10 min, 300^{o}C, 5kg ASTM D1238). Comparatively, most commercial acrylics have an MFI higher than 2 (/10 min, 230^{o}C, 3.8kg, ASTM D1238 – dependant on a range of polymer properties) – i.e., they flow more easily at less extreme conditions. An attempt was made to quantify the MFI of a commercial pMMA homopolymer (Scientific Polymer Products Inc., 35,000 weight Avg. MW, suspension polymerization product); however, it was so fluid at the conditions that it could not be measured.

Since injection moulding of physical testing specimens was unsuccessful, compression moulding of the same polymers was investigated. Again, similar issues appeared, most notably the need to use temperatures in excess of 250^{o}C and long holding times (15+ minutes) to form the appropriate shapes in metal moulds. The high temperatures and decomposition of the polymers releases volatile gasses that also compromise the integrity of the specimens by forming voids in the shapes. The process of removing the polymers from the metal moulds is extremely difficult owing to the brittle nature of the polymer and especially the small sizes associated with the neck section of typical dog bone shapes used for tensile testing. Figure 4-12 shows the physical testing specimens that were formed by compression moulding of pMMA at 280^{o}C with a holding time of 15 minutes. The tensile "dogbone" shapes were extremely difficult to remove with only 1 out of 8 specimens removed without snapping. The one complete dogbone (shown) would not actually be suitable for testing as there was a small chip in the neck (the thin section of the sample) that would compromise results. Removing the polymer samples carefully while still above their T_g was determined to be the best way to obtain good specimens. All samples displayed some signs of incomplete melting as pieces of the polymer added to the moulds are still visible (as in the flexural sample, at left). The thicker flexural samples would also not be suitable for testing because void spaces were formed in the sample, either by decomposition gasses or the inability of the polymer to flow well or a combination of both.

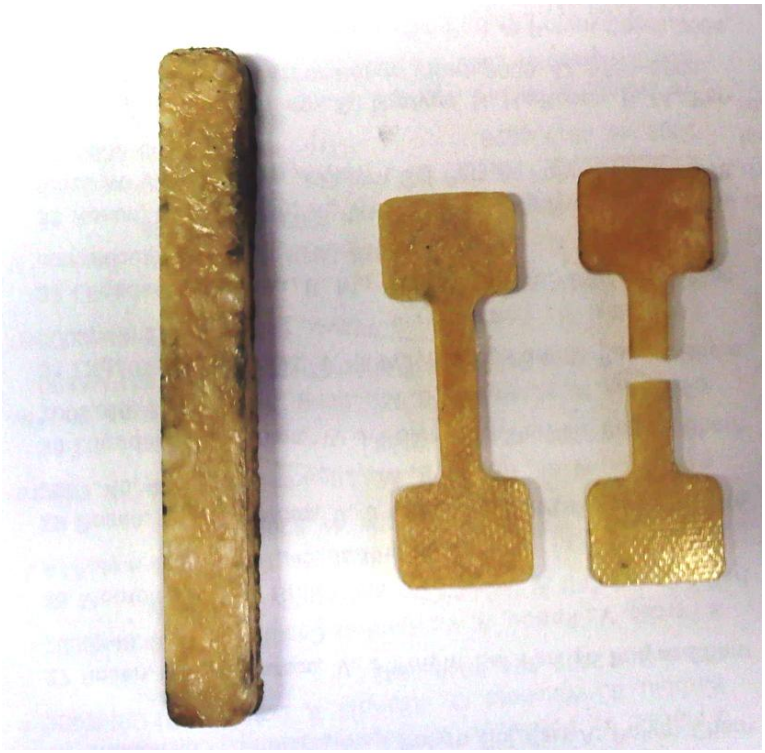

Figure 4-12 – Image of compression moulded pMMA flexural (ASTM D638, left) and tensile (ASTM D790, right) sample specimens.

4.4.2 Investigation of Parameters affecting Physical Processing

The factors that make the polymers created by dispersion polymerization so difficult to process are worth investigation. The high T_g values and relatively narrow temperature window until decomposition occurs is one challenging aspect. The MW of the polymers also bears investigation. Jiang et al. explored the effects of MW differences between precipitation and dispersion polymerization, but are quite unspecific when reporting what MW value is associated with a particular condition.[43, 44] Additionally, in their works, the amount of surfactant and volume of the continuous phase was not scaled to monomer loading; rather, the same quantities of initiator, surfactant and MeOH and water were used in all cases and monomer loading was changed, which will affect the solubility of growing polymer chains as discussed in Chapter 3 and

make the results not directly comparable to those determined here. The molecular weights measured are however in a similar range to those determined in this work.

The issues encountered thus far with physical processing of the polymer made by dispersion polymerization appear to affect all polymerizations and since MMA polymers should be the easiest to work with and understand (due to their lower T_g and as the subject of a great deal of study) thus, further investigation considers only MMA homopolymers. From Chapter 3, Table 2 we know that the pMMA homopolymer produced via dispersion in an 80|20 MeOH|Water continuous phase has a MW of about half that of the 70|30 polymer. This lower MW polymer was more easily compression moulded at lower temperatures (200^{o}C) and displayed accordingly less degradation than the higher MW polymers. The MW of the 80|20 polymer was likely still higher than desirable for processing as the dogbones did not become transparent as expected; some of the individual polymer pieces placed in the mould were still identifiable, indicating incomplete melting in the mould. To investigate the effect of MW still further, pMMA produced by emulsion and suspension polymerization[96] and commercially sourced pMMA (as described earlier in this chapter) were also analyzed. When processed at the same conditions as the lower MW 80|20 pMMA, specimens were formed that were transparent and homogenous, as had been expected for all polymers, and showed no observable signs of degradation and incomplete melting, also seen in Figure 4-14. The commercial pMMA seemed especially brittle and was actually the most difficult polymer to work with, being very sticky with the lowest viscosity in the mould. The T_g's measured for the samples (washed) were not greatly different from that of the dispersion polymer, at 112^{o}C, 118^{o}C and 118^{o}C for suspension, commercial suspension and emulsion pMMA, respectively. The molecular weights of the polymer did varied greatly as summarized in Table 4-4. The emulsion product had a MW of well over 2,000,000 g·mol^{-1} yet presented no issues when processed by compression moulding. The only real difference in the MW of the various polymers

that may affect processing is that the PDI of the dispersion product is much narrower than the other polymers produced in the lab. A broad MWD is known to make processing easier as the range of chain lengths help promote melting over a wider temperature range. It is not suspected that the dispersion polymers are crosslinked as they are soluble in THF, as is expected for pMMA and low MeMBL content polymers. The other primary difference between the polymers created by the various recipes is the use of the PVP surfactant in dispersion polymerization. PVP, as discussed in Chapter 3, functions much differently to and is very much larger than surfactants commonly employed in aqueous systems. To investigate the potential role of the surfactant in processing, a precipitation polymerization of MMA was carried out by the same recipe as presented in Chapter 3, Table 1, omitting the use of surfactant.

The precipitate pMMA polymer was also analyzed by DSC and SEC and found to have a T_g of 125^{o}C and a weight average MW of 392,000 g·mol^{-1}. Processing of the pMMA formed by precipitation produced was unsuccessful, like that of dispersion polymerization polymers. Although the MW of the precipitate pMMA was slightly lower than that of the dispersion product and had a broader PDI and lacked PVP surfactant, it still would not flow in the mould under temperature and pressure. The dogbone samples produced (not shown) were similar to those of dispersion polymers but did appear somewhat less yellowed than even the 80|20 specimens and had a more uniform surface, indicating some melting.

While emulsion polymerization had been ruled out as a method for polymerizing MeMBL homopolymers previously,[96] attempts had never been made to try and produce copolymers of MeMBL and MMA by that method. Since the emulsion pMMA could be processed easily, copolymerization of 25% and 50% MeMBL were attempted by the same recipe[96] and proved successful. The copolymers had similar T_g's to the batch MeMBL/MMA dispersion copolymers

but displayed the processability of the emulsion pMMA homopolymer. The MW of the copolymers was also seen to decrease with the addition of MeMBL, as was observed with dispersion polymerizations. Further information on emulsion copolymers is contained in Appendix C.

Because PVP content did not appear to alter the properties of the dispersion and precipitate polymers and since it was possible to process polymers of both much higher and lower MW, another property must be different among the samples. DSC was used again, but measurements were taken over a larger temperature range to see where and how the melting profiles of the various polymers appeared. Samples were taken above their T_g and cooled to erase any thermal history and subsequently were heated to above 300^{o}C on the third and final cycle. Figure 4-13 shows the DSC curve for the polymers produced by emulsion, precipitation and dispersion polymerization. The T_g's of the polymers are all approximately the same, however the profiles of the polymers at higher temperatures are very different. The emulsion product, which was the most easily processed of all polymers, has a very gradual melting profile that basically extends from the T_g to 280^{o}C, also seen with emulsion copolymers whose T_g's increase with increasing MeMBL content in line with batch dispersion copolymerizations. The dispersion and precipitation products do not begin to melt at all until 260^{o}C, although curiously, the suspension polymer, which was processable, displays a similar profile to the dispersion polymers which were not. It is likely this difference in melting that causes the issues with processing of polymers formed by dispersion and precipitation polymerization. All pMMA homopolymers show a steep rise in heat flow above 320^{o}C, indicative of the degradation that goes on at that temperature. The copolymers made by emulsion show greater thermal stability to higher temperatures, as expected based on TGA results. The use of a non-aqueous continuous phase may be causing a difference in the way that monomer units orient themselves in polymer chains, which is an unexpected result

that bears further investigation. When the same experiment as shown in Figure 4-13 is repeated with an additional cooling cycle after the high temperature heating phase, there is some evidence of cyrstallinity in the polymer, exhibited by a broad crystallization peak observed. However, repeat tests have proved inconclusive in reproducing crystallization peaks in the DSC traces and further investigation is required to prove that the polymers produced are crystalline.. If the polymers are crystalline, it is likely this aspect combined with their high melting temperatures that prevents their processing. A high degree of ordering of the polymer chains, as observed in the literature with syndiotactic polymers[125] is known to increase the melting temperature of the polymers such that they occur in the range where thermal degradation also occurs. Testing polymers via ^{13}C NMR to quantify tacticity and conducting DSC experiments with varied rates of cooling may be able to confirm these suspicions.

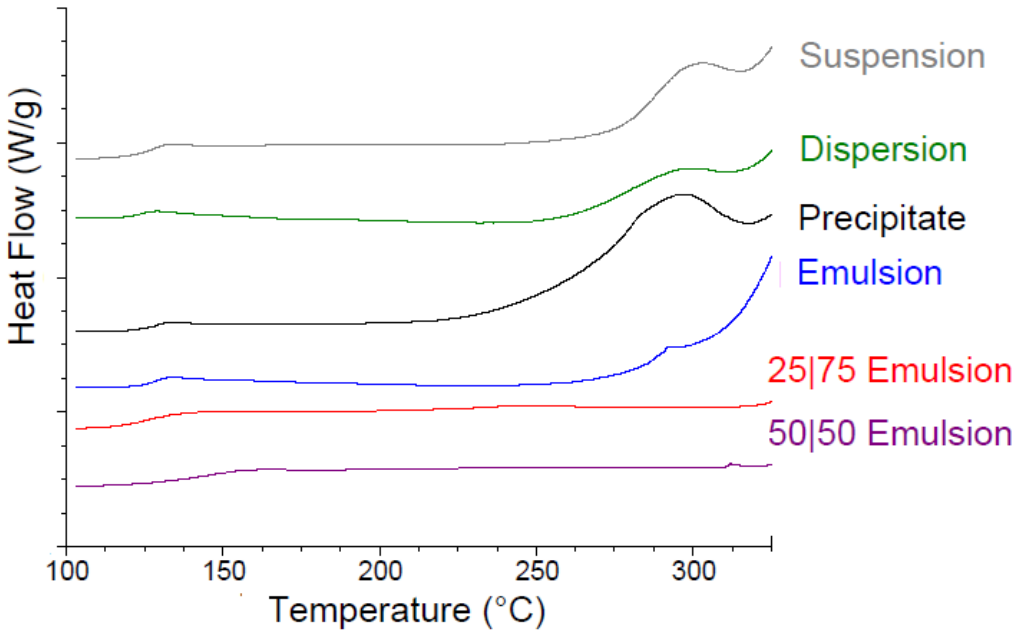

Figure 4-13 – Differential Scanning Calorimetry curves for pMMA produced by dispersion, precipitation , suspension and emulsion techniques and p(MMA/MeMBL) copolymers produced by emulsion.

Table 4-4 – Molecular Weights of pMMA from various sources

Sample	Mn ($g \cdot mol^{-1}$)	Mw ($g \cdot mol^{-1}$)	PDI
Commerial Suspension pMMA	16,000	31,000	1.92
Suspension pMMA	42,000	571,000	13.54
Emulsion pMMA	309,000	2,040,000	6.60
Dispersion pMMA	119,000	412,000	3.45
Precipitation pMMA	93,000	392,000	4.26

4.5 Conclusion

Although the mechanical properties of MeMBL containing copolymers were unable to be tested, a great deal was discovered about the characteristics of these polymers. Semibatch polymerization techniques were successfully applied to control and mitigate the compositional drift seen in polymers produced by batch methods. The semibatch polymers displayed glass transition temperatures that were accordingly more consistent than those of batch polymers, and confirmed that, as was seen with polymers produced via PLP, it is possible to modify the T_g of a pMMA based polymer to a higher, desired value by incorporating MeMBL. Analysis of molecular weight distributions of the polymers show that the incorporation of MeMBL tends to decrease the ultimate MW and increase the fraction of short chain polymer, consistent with the observations made in Chapter 3 on MeMBL polymerizing at a slower rate to a greater extent by solution-like polymerization mechanisms. Semibatch polymerization keeps the ultimate MW lower than in batch due to the steady addition of MeMBL, rather than the uncontrolled incorporation encountered with the batch polymerization methods whose MW distribution becomes more like those seen in MMA homopolymerizations as increasing fraction of MMA is incorporated later in the reaction.

The ultimate issue that prevented the processing of the polymers produced by dispersion polymerization appears to be a combination of both high T_g and high melting temperatures. The potential issue of polymer tacticity caused by non-aqueous polymerization affecting processing was unforeseen; subsequent analysis of pMMA homopolymers produced by other methods shows that those polymers could be processed by compression moulding and have lower molecular weights, melting temperatures and glass transition temperatures than the dispersion and precipitation pMMA polymers. The high T_g of MeMBL and its close proximity to the range of temperatures where polymer decomposition occurs (yet are necessary for processing) is a property that, while desirable for some applications, may ultimately limit the utility and fraction of this monomer that can be incorporated with petroleum sourced monomers.

Figure 4-14 - Image of compression moulded pMMA tensile sample specimens. Left, for polymer of 200,000 $g \cdot mol^{-1}$ (right) and 400,000 $g \cdot mol^{-1}$ (left) produced by dispersion polymerization. Right, for polymer of 2,000,000 $g \cdot mol^{-1}$ (left) 570,000 $g \cdot mol^{-1}$ (center) and 31,000 $g \cdot mol^{-1}$ (right) produced by emulsion, suspension and suspension (commercial) polymerization, respectively. ASTM D790 tensile samples shown.

Chapter 5

Conclusions and Recommendations concerning the study of MeMBL

5.1 Concluding Summary

This Chapter summarizes the key discoveries of the prior chapters and details a path forwards for future research endeavours related to the study of this monomer. Since MeMBL has been the subject of relatively little study in the open literature,[8, 24] a great opportunity existed (and still does) to determine the important properties, polymerization characteristics, and potential applications of the monomer/polymer. The initial work completed in this thesis lays the groundwork and will be a resource for further studies of MeMBL-containing polymers.

The first part of this thesis (Chapter 2) examined the reaction kinetics of MeMBL copolymerizations with petroleum based monomers commonly used in industry. In order to be able to produce copolymers of MeMBL with well-defined characteristics and tailored physical properties, an improved understanding of its free radical polymerization kinetics is essential. The PLP/SEC technique was successfully employed to systematically investigate free radical bulk copolymerization of MeMBL with Styrene, Methyl Methacrylate and Butyl Acrylate. Because MeMBL is insoluble in many common organic solvents such as THF, analysis was conducted using both THF and DMAc as eluents for SEC. Initial measurements from THF SEC were investigated to the solubility limits of the copolymer systems, which vary with MeMBL mol fraction. These results were later confirmed and extended by analysis in DMAc where all polymers studied are fully soluble. Analysis of pMeMBL produced by PLP in DMAc has provided an Arrhenius expression for the k_p of MeMBL for the first time, which allows for more detailed study and fitting of kinetic models to the copolymerization data.

Investigation of the complete copolymer composition range for each system and of the MeMBL homopolymer has provided insight into the reactivity of lactone monomers relative to other common monomers. The homopolymer propagation rate coefficient of MeMBL has been found to be quite similar to that of MMA (approximately 15% higher). However, MeMBL is preferentially incorporated into ST, BA and MMA copolymers far more so than when MMA is copolymerized with the same monomers. Thus, compositional drift will occur in all systems studied, as the fraction of MeMBL in a copolymerization will be depleted at a faster rate than its comonomer in batch polymerizations. While the terminal model adequately describes polymer composition for all cases, as measured using proton NMR, experimental $k_{p,cop}$ data suggests that it does not sufficiently represent the copolymerization kinetics of any of the systems studied. Copolymerization kinetics were better described by the implicit penultimate unit effect (IPUE) model for all systems investigated.

Having investigated the kinetics of MeMBL copolymerizations, a method of easily producing polymers was required. Of the three comonomer systems investigated in Chapter 2, polymerizations of MeMBL and MMA were chosen for further study to differentiate from previous work with gamma lactones that focused on Styrene copolymerizations[24, 89] and because of the great similarity in monomer structures between MeMBL and MMA.[6, 7] We developed a dispersion method capable of producing MeMBL copolymers based on polymerization techniques known to be successful for MMA.[43-45, 53, 97] In the process, we thoroughly investigated the mechanism of dispersion polymerization, paying particular attention to particle nucleation (Chapter 3). We identified a distinct population of small precursor particles detectable throughout the entire polymerization, a case not previously reported in the literature. The results support Paine's assertation[54] that there are aggregates of nuclei generated in a reaction that are typically one tenth as large as mature particles and it is these smaller aggregates that are captured by the

mature particles in order to grow. The principle distinction from previous literature is the finding that the small particles are stable and observable by laser light scattering detectors long after polymerization has been stopped and under a variety of conditions including different surfactant concentrations and reaction media compositions. The small particle populations appear to be most affected by changes that alter the critical chain length of the precipitating polymer, such as changes to the composition of the continuous phase, the addition of other monomers with different critical chain lengths, and changes in CCTA concentration.

The kinetic values determined by PLP in Chapter 2 and the dispersion polymerization process investigated in Chapter 3 have been used together to design a polymerization system to produce MeMBL copolymers with controlled composition, as described in Chapter 4, which also examined the effect of MeMBL incorporation on copolymer physical properties. Although the mechanical properties of MeMBL containing copolymers were unable to be tested, a great deal was discovered about the characteristics of these polymers. The compositional drift seen in polymers produced by batch methods was controlled and mitigated by the successful application of semibatch polymerization techniques, as also seen by the evolution of copolymer T_g. As was seen with polymers produced via PLP, it is possible to increase the T_g of a pMMA based polymer to a higher, desired value. The incorporation of MeMBL tends to decrease the ultimate MW and increase the fraction of short chain polymer, consistent with the observations made in Chapter 3 on MeMBL polymerizing at a slower rate to a greater extent by solution-like polymerization mechanisms. Semibatch polymerization keeps the ultimate MW lower than in batch due to the steady addition of MeMBL.

One of the goals of this thesis that was not accomplished was to quantify the effect of MeMBL incorporation on the mechanical properties of copolymers. The ultimate issue that prevented the

processing of the semibatch polymers produced by the dispersion polymerization method appears to be a combination of both high T_g and high melting temperatures which required that extrusion and compression moulding use temperatures that cause the thermal degradation of the polymer. The polymers made in dispersion polymerizations appear to have a higher degree of ordering, likely a high degree of syndiotacticity, compared to typical polymers, showing an unexpected crystallization temperature in some DSC traces. Analyses of pMMA homopolymers produced by methods other than dispersion polymerization shows that those polymers could be processed by compression moulding and have lower molecular weights, melting temperatures and glass transition temperatures than the dispersion and precipitation pMMA polymers. Despite the setbacks encountered with polymer physical testing, this thesis has been largely successful in discovering much about the polymerization characteristics of MeMBL and about the dispersion polymerization technique in general. This effort may be useful to future researchers if MeMBL is determined to be a practical alternative to petroleum sourced monomers like MMA. The discovery that highly ordered polymers can be produced by the dispersion polymerization technique is an interesting result in its own right and may also be of interest to future researchers.

5.2 Path Forwards and Recommendations

The successes and failures encountered in this thesis point to new questions about MeMBL. Further PLP studies of MeMBL with many other monomers are possible, but our understanding of its polymerization behaviour may benefit more from investigation into batch solution polymerization kinetics with monomers such as MMA, as the discoveries in Chapter 3 tend to show a solution-like polymerization rate and behaviour. Testing the polymerization of MeMBL in a solvent capable of being heated to more than 100^{o}C may also be of interest as it could help determine whether or not the solution-like rate observed is due to the reaction temperature being so much less than the T_g of the homopolymer. Determining how the MeMBL monomer is

partitioned in polymerization systems would also be of great interest and is necessary to attempt to model the system.

In Chapter 3, only one stabilizer was investigated. An examination of the effects of stabilizer type on the time taken to form the initial large particles and changes in the characteristics of the small and large particle populations may be of interest to further understand the nucleation mechanisms of dispersion polymerization. Much has been attributed in Chapter 3 to differences in the critical chain length of MeMBL compared to MMA and it has been supposed but not quantified that the former is shorter given the results of experiments. Future tests have been envisioned to create MeMBL and MMA polymers of very low MW and narrow PDI by methods such as ATRP to test their solubility in the continuous phase or use online turbidity monitoring of the reaction to detect the first signs of particle formation and confirm the critical chain lengths of the polymers. This would be of benefit to our own work and also to the larger scientific community, especially for those with interests in modeling dispersion polymerization.

The most disappointing aspect of this thesis is being unable to quantify the effect of MeMBL incorporation on polymer physical properties. This is the area that most needs to be investigated in future as it will test and answer whether or not MeMBL is a bio-renewable monomer that may displace some volume of and extend the operating range and utility of MMA based polymers such as Lucite® and Plexiglas® with potential applications in medical technologies including implants as well as an impact resistant substitute for glass.[12, 13] Until those results are known, further analysis of other aspects of MeMBL may be pointless if there is no potential application for the polymer. The high T_g of pMeMBL and its close proximity to the range of temperatures where polymer decomposition occurs (yet are necessary for processing) is a property that, while desirable for some applications, may ultimately limit the utility and fraction of this monomer that

can be incorporated with petroleum sourced monomers. Emulsion based copolymers appear to have promise and further investigation and refining of the polymerization method may yield polymers whose mechanical properties can be tested.

To produce MeMBL copolymers that can be processed successfully for mechanical testing, future work could perhaps first investigate the use of a chain transfer agent to significantly reduce the average MW of polymer produced by the dispersion technique in order to obtain more processable polymers before exploring other polymerization techniques in more detail. However, because of the unexpected melting characteristics of the polymer chains produced by dispersion polymerization, it is likely that this technique may not be suitable for the production of MeMBL based copolymers. Determining polymer tacticity by ^{13}C NMR will help clarify if there is a great difference between dispersion and aqueous based polymers. Further DSC analysis that quantifies the crystallinity of these polymers as well would provide yet more useful information on potential reasons for the unexpected properties of the dispersed phase polymers. Investigating how and why the more ordered polymer structures are obtained by this technique would be another important addition to the understanding of the dispersion technique. Future work may wish to develop a polymerization method for copolymers based on the initial, successful tests with emulsion copolymerization or investigate solution based polymerization of MeMBL and MMA.

References

[1] C. K. Williams, M. A. Hillmyer, *Polymer Reviews* **2008**, *48*, 1.
[2] P. B. Weisz, *Physics Today* **2004**, *57*, 47.
[3] M. A. R. Meier, J. O. Metzger, U. S. Schubert, *Chemical Society Reviews* **2007**, *36*, 1788.
[4] J. Mosnacek, K. Matyjaszewski, *Macromolecules* **2008**, *41*, 5509.
[5] L. E. Manzer, *Applied Catalysis A-General* **2004**, *272*, 249.
[6] M. K. Akkapeddi, *Macromolecules* **1979**, *12*, 546.
[7] M. K. Akkapeddi, *Polymer* **1979**, *20*, 1215.
[8] J. Suenaga, D. M. Sutherlin, J. K. Stille, *Macromolecules* **1984**, *17*, 2913.
[9] M. Ueda, M. Takahashi, Y. Imai, C. U. Pittman, *Macromolecules* **1983**, *16*, 1300.
[10] M. Ueda, T. Suzuki, M. Takahashi, Z. B. Li, K. Koyama, C. U. Pittman, *Macromolecules* **1986**, *19*, 558.
[11] M. Ueda, M. Takahashi, Y. Imai, C. U. Pittman, *J. Polym. Sci. Pol. Chem.* **1982**, *20*, 2819.
[12] J. W. Stansbury, J. M. Antonucci, *Dental Materials* **1992**, *8*, 270.
[13] E. N. Peters, "Plastics: Thermoplastics, Thermosets and Elastomers", in *Handbook of Materials Selection*, M. Kutz, Ed., John Wiley & Sons, New York, 2002, p. 335.
[14] S. M. Kupchan, *Pure Appl. Chem* **1970**, *21*, 227.
[15] S. M. Kupchan, M. A. Eakin, A. M. Thomas, *Journal of Medicinal Chemistry* **1971**, *14*, 1147.
[16] E. Rodriguez, G. H. N. Towers, J. C. Mitchell, *Phytochemistry* **1976**, *15*, 1573.
[17] A. Rosowsky, N. Papathanasopoulos, H. Lazarus, G. E. Foley, E. J. Modest, *Journal of Medicinal Chemistry* **1974**, *17*, 672.
[18] J. March, "*March's Advanced Organic Chemistry: Reactions, Mechanisms, and Structure"*, 5 edition, Wiley-Interscience, 2001.
[19] C. J. Cavallito, T. H. Haskell, *Journal of the American Chemical Society* **1946**, *68*, 2332.
[20] J. L. Hartwell, B. J. Abbott, *Adomr. Pharmucol. Chemother.* **1969**, *7*, 117.
[21] R. L. Hanson, H. A. Lardy, S. M. Kupchan, *Science* **1970**, *168*, 378.
[22] G. M. Ksander, J. E. McMurry, M. Johnson, *The Journal of Organic Chemistry* **1977**, *42*, 1180.
[23] L. D. Martin, J. K. Stille, *The Journal of Organic Chemistry* **1982**, *47*, 3630.
[24] G. G. Qi, M. Nolan, F. J. Schork, C. W. Jones, *J. Polym. Sci. Pol. Chem.* **2008**, *46*, 5929.
[25] J. Martin, Watts, PC, Johnson, Francis, *Journal of the Chemical Society D: Chemical Communications* **1970**, 27.
[26] United States. 2,624,723 (1953), Allied Chemical and Die Corporation, inv. W. J. McGraw;
[27] B. J. Nikolau, M. A. D. N. Perera, L. Brachova, B. Shanks, *The Plant Journal* **2008**, *54*, 536.
[28] A. J. Ragauskas, C. K. Williams, B. H. Davison, G. Britovsek, J. Cairney, C. A. Eckert, W. J. Frederick, J. P. Hallett, D. J. Leak, C. L. Liotta, J. R. Mielenz, R. Murphy, R. Templer, T. Tschaplinski, *Science* **2006**, *311*, 484.
[29] T. Werpy, G. Peterson, "Top Value Added Chemicals from Biomass", U.D.o. Energy, Ed., Washington DC, 2004, p. 1/.
[30] A. Heberer, *Journal of the American Oil Chemists' Society* **1937**, *14*, 15.
[31] F. D. Gunstone, "*The Lipid Handbook 3ed"*, CRC Press, London, 2007.
[32] J. Metzger, U. Bornscheuer, *Applied Microbiology and Biotechnology* **2006**, *71*, 13.
[33] L. C. Meher, D. Vidya Sagar, S. N. Naik, *Renewable and Sustainable Energy Reviews* **2006**, *10*, 248.
[34] J. C. de la Cal, Leiza, J.R., Asua, J. M. Butte, A. Sorti, G., Morbidelli, M., "Emulsion Polymerization", in *Handbook of Polymer Reaction Engineering*, T. Meyer, Kuerentjes, J., Ed., Wiley-VCH Verlag GmbH & Co., Weinheim, 2005, p. 249.

[35] M. J. Barandiaran, J. C. de la Cal, J. M. Asua, "Emulsion Polymerization", in *Polymer Reaction Engineering*, J.M. Asua, Ed., Blackwell, Oxford, 2007, p. 233.
[36] M. Taylor, "Synthesis of Polymer Dispersions", in *Polymer Dispersions and their Industrial Applications*, D. Urban, Takamura, K.. Ed., Wiley-VCH Verlag GmbH & Co., Weinheim, 2002, p. 15.
[37] B. W. Brooks, "Free-radical Polymerization:Suspension", in *Handbook of Polymer Reaction Engineering*, T. Meyer, Kuerentjes, J., Ed., Wiley-VCH Verlag GmbH & Co., Weinheim, 2005, p. 213.
[38] G. Kalfas, W. H. Ray, *Industrial & Engineering Chemistry Research* **1993**, *32*, 1822.
[39] G. Kalfas, H. Yuan, W. H. Ray, *Industrial & Engineering Chemistry Research* **1993**, *32*, 1831.
[40] S. X. Zhang, W. H. Ray, *Industrial & Engineering Chemistry Research* **1997**, *36*, 1310.
[41] K. E. J. Barrett, "*Dispersion Polymerization in Organic Media"*, Wiley, London, 1975.
[42] K. E. J. Barrett, H. R. Thomas, *Journal of Polymer Science Part A-1: Polymer Chemistry* **1969**, *7*, 2621.
[43] S. Jiang, E. D. Sudol, V. L. Dimonie, M. S. El-Aasser, *Journal Of Applied Polymer Science* **2008**, *107*, 2453.
[44] S. Jiang, E. D. Sudol, V. L. Dimonie, M. S. El-Aasser, *J. Polym. Sci. Pol. Chem.* **2008**, *46*, 3638.
[45] S. Jiang, E. D. Sudol, V. L. Dimonie, M. S. El-Aasser, *Journal Of Applied Polymer Science* **2008**, *109*, 2979.
[46] Y. Almog, S. Reich, M. Levy, *British Polymer Journal* **1982**, *14*, 131.
[47] S. Grandhee, "Applications for Automotive Coatings", in *Polymer Dispersions and their Industrial Applications*, D. Urban, Takamura, K.. Ed., Wiley-VCH Verlag GmbH & Co., Weinheim, 2002, p. 163.
[48] W. J. Priest, *The Journal of Physical Chemistry* **1952**, *56*, 1077.
[49] S. Shen, E. D. Sudol, M. S. Elaasser, *J. Polym. Sci. Pol. Chem.* **1994**, *32*, 1087.
[50] P. J. Feeney, D. H. Napper, R. G. Gilbert, *Macromolecules* **1984**, *17*, 2520.
[51] A. J. Paine, W. Luymes, J. McNulty, *Macromolecules* **1990**, *23*, 3104.
[52] C. M. Tseng, Y. Y. Lu, M. S. El-Aasser, J. W. Vanderhoff, *Journal of Polymer Science Part A: Polymer Chemistry* **1986**, *24*, 2995.
[53] K. Cao, B.-G. Li, Z.-R. Pan, *Colloids and Surfaces A: Physicochemical and Engineering Aspects* **1999**, *153*, 179.
[54] A. J. Paine, *Macromolecules* **1990**, *23*, 3109.
[55] D. Wang, V. L. Dimonie, E. D. Sudol, M. S. El-Aasser, *Journal of Applied Polymer Science* **2002**, *84*, 2721.
[56] J. Wieme, D. R. D'Hooge, M.-F. Reyniers, G. B. Marin, *Macromolecular Reaction Engineering* **2009**, *3*, 16.
[57] P. A. Mueller, G. Storti, M. Morbidelli, *Chem. Eng. Sci.* **2005**, *60*, 377.
[58] P. A. Mueller, G. Storti, M. Morbidelli, *Chem. Eng. Sci.* **2005**, *60*, 1911.
[59] P. A. Mueller, G. Storti, M. Morbidelli, I. Costa, A. Galia, O. Scialdone, G. Filardo, *Macromolecules* **2006**, *39*, 6483.
[60] C. Bunyakan, L. Armanet, D. Hunkeler, *Polymer* **1999**, *40*, 6225.
[61] C. Bunyakan, D. Hunkeler, *Polymer* **1999**, *40*, 6213.
[62] A. Crosato-Arnaldi, P. Gasparini, G. Talamini, *Die Makromolekulare Chemie* **1968**, *117*, 140.
[63] G. Talamini, G. Vidotto, *Die Makromolekulare Chemie* **1967**, *100*, 48.
[64] Y. E. Kirsch, "*Water Soluble Poly-N-Vinylamides"*, Wiley, London, 1998.

[65] T. Sato, R. Ruch, "*Stabilization of Colloidal Dispersion by Polymer Adsorption"*, Marcel Dekker, New York, 1980.
[66] J. Shi, "Steric Stabilization Literature Review", in *Department Materials Science & Engineering*, Ohio State University, Columbus, 200245.
[67] D. H. Napper, *J. Colloid Interface Sci.* **1977**, *58*, 390.
[68] R. Evans, D. H. Napper, *Colloid & Polymer Science* **1973**, *251*, 409.
[69] R. Evans, D. H. Napper, *Colloid & Polymer Science* **1973**, *251*, 329.
[70] Inkline.gr, "Dispersion Processes", 2011, p. 2011/.
[71] S. Beuermann, M. Buback, T. P. Davis, R. G. Gilbert, R. A. Hutchinson, A. Kajiwara, B. Klumperman, G. T. Russell, *Macromolecular Chemistry and Physics* **2000**, *201*, 1355.
[72] S. Beuermann, M. Buback, T. P. Davis, R. G. Gilbert, R. A. Hutchinson, O. F. Olaj, G. T. Russell, J. Schweer, A. M. van Herk, *Macromolecular Chemistry and Physics* **1997**, *198*, 1545.
[73] M. Buback, R. G. Gilbert, R. A. Hutchinson, B. Klumperman, F.-D. Kuchta, B. G. Manders, K. F. O'Driscoll, G. T. Russell, J. Schweer, *Macromolecular Chemistry and Physics* **1995**, *196*, 3267.
[74] M. L. Coote, L. P. M. Johnston, T. P. Davis, *Macromolecules* **1997**, *30*, 8191.
[75] T. P. Davis, K. F. Odriscoll, M. C. Piton, M. A. Winnik, *Journal of Polymer Science Part C-Polymer Letters* **1989**, *27*, 181.
[76] T. P. Davis, K. F. Odriscoll, M. C. Piton, M. A. Winnik, *Macromolecules* **1990**, *23*, 2113.
[77] D. Li, N. Li, R. A. Hutchinson, *Macromolecules* **2006**, *39*, 4366.
[78] K. Liang, M. Dossi, D. Moscatelli, R. A. Hutchinson, *Macromolecules* **2009**.
[79] W. Wang, R. A. Hutchinson, *Macromolecules* **2008**, *41*, 9011.
[80] S. Beuermann, M. Buback, *Progress in Polymer Science* **2002**, *27*, 191.
[81] E. Merz, T. Alfrey, G. Goldfinger, *Journal of Polymer Science* **1946**, *1*, 75.
[82] T. Fukuda, Y. D. Ma, H. Inagaki, *Macromolecules* **1985**, *18*, 17.
[83] R. A. Cockburn, T. F. L. McKenna, R. A. Hutchinson, **2011**.
[84] R. A. Cockburn, T. F. L. McKenna, R. A. Hutchinson, *Macromolecular Chemistry and Physics* **2010**, *211*, 501.
[85] R. A. Hutchinson, J. H. McMinn, D. A. Paquet, S. Beuermann, C. Jackson, *Industrial & Engineering Chemistry Research* **1997**, *36*, 1103.
[86] R. A. Hutchinson, M. T. Aronson, J. R. Richards, *Macromolecules* **1993**, *26*, 6410.
[87] R. A. Hutchinson, D. A. Paquet, Jr., J. H. McMinn, S. Beuermann, R. E. Fuller and C. Jackson, "The Application of Pulsed-Laser Methods for the Determination of Free-Radical Polymerization Rate Coefficients", in *5th International Workshop on Polymer Reaction Engineering*, K.H. Reichert, Moritz, H.U., Ed., VCH Verlags, Berlin, 1995, p. 131/467.
[88] M. Buback, A. Feldermann, C. Barner-Kowollik, I. Lacík, *Macromolecules* **2001**, *34*, 5439.
[89] C. U. Pittman, H. Lee, *J. Polym. Sci. Pol. Chem.* **2003**, *41*, 1759.
[90] P. R. Couchman, F. E. Karasz, *Macromolecules* **1978**, *11*, 117.
[91] T. G. Fox, P. J. Flory, *J. Appl. Phys.* **1950**, *21*, 581.
[92] M. Gordon, J. S. Taylor, *Journal of Applied Chemistry* **1952**, *2*, 493.
[93] J. M. Asua, S. Beuermann, M. Buback, P. Castignolles, B. Charleux, R. G. Gilbert, R. A. Hutchinson, J. R. Leiza, A. N. Nikitin, J.-P. Vairon, A. M. van Herk, *Macromolecular Chemistry and Physics* **2004**, *205*, 2151.
[94] M. Wulkow, "Predici", Computing In Technology GMbH, Rastede, Germany, 2003, p. 6.37.8/.
[95] M. Wulkow, *Macromolecular Reaction Engineering* **2008**, *2*, 461.

[96] R. A. Cockburn, "Investigation of the Polymerization Behaviours of a Bio-Renewable Monomer: MeMBL", in *Department of Chemical Engineering*, Queen's University, Kingston, 2009, p. BSc Eng/44.
[97] K. Cao, J. Yu, B.-G. Li, B.-F. Li, Z.-R. Pan, *Chemical Engineering Journal* **2000**, *78*, 211.
[98] Y. Y. Lu, M. S. El-Aasser, J. W. Vanderhoff, *Journal of Polymer Science Part B: Polymer Physics* **1988**, *26*, 1187.
[99] S. Shen, E. D. Sudol, M. S. Elaasser, *J. Polym. Sci. Pol. Chem.* **1993**, *31*, 1393.
[100] A. J. Paine, Y. Deslandes, P. Gerroir, B. Henrissat, *J. Colloid Interface Sci.* **1990**, *138*, 170.
[101] A. J. Paine, J. McNulty, *J. Polym. Sci. Pol. Chem.* **1990**, *28*, 2569.
[102] K. P Lok, C. K. Ober, *Can. J. Chem.* **1985**, 63, 209.
[103] T. K. Mandal, B. M. Mandal, *Langmuir* **1997**, *13*, 2421.
[104] C. K. Ober, K. P. Lok, *Macromolecules* **1987**, *20*, 268.
[105] A. J. Paine, *J. Polym. Sci. Pol. Chem.* **1990**, *28*, 2485.
[106] A. Gridnev, *Journal of Polymer Science Part A: Polymer Chemistry* **2000**, *38*, 1753.
[107] A. A. Gridnev, S. D. Ittel, *Chemical Reviews* **2001**, *101*, 3611.
[108] J. P. A. Heuts, G. E. Roberts, J. D. Biasutti, *Australian Journal of Chemistry* **2002**, *55*, 381.
[109] D. C. Sundberg, D. R. James, *Journal of Polymer Science: Polymer Chemistry Edition* **1978**, *16*, 523.
[110] U. El Jaby, "ADVANCED APPLICATIONS OF MINIEMULSION TECHNOLOGY: DEVELOPMENT OF A VIABLE EMULSIFICATION PROCESS", in *Department of Chemical Engineering*, Queen's University, Kingston, 2010, p. PhD/159.
[111] R. P. Moraes, T. F. L. McKenna, **2011**.
[112] N. M. B. Smeets, U. S. Meda, J. P. A. Heuts, J. T. F. Keurentjes, A. M. van Herk, J. Meuldijk, *Macromolecular Symposia* **2007**, *259*, 406.
[113] A. Bakac, M. E. Brynildson, J. H. Espenson, *Inorganic Chemistry* **1986**, *25*, 4108.
[114] N. M. B. Smeets, T. G. T. Jansen, T. J. J. Sciarone, J. P. A. Heuts, J. Meuldijk, A. M. Van Herk, *Journal of Polymer Science Part A: Polymer Chemistry* **2010**, *48*, 1038.
[115] N. P. Cheremisinoff, "*Polymer Characterization: Laboratory techniques and analysis"*, Noyes Publications, Westwood, 1996, p. 254.
[116] R. Brown, "Handbook of Polymer Testing", Marcel Dekker, New York, 1999860.
[117] T. Hatakeyama, Quinn, F.X., "*Thermal Analysis: Fundamentals and Applications to Polymer Science"*, 2 edition, John Wiley & Sons, New York, 1999, p. 190.
[118] L. E. Manring, *Macromolecules* **1988**, *21*, 528.
[119] L. E. Manring, *Macromolecules* **1989**, *22*, 2673.
[120] L. E. Manring, *Macromolecules* **1991**, *24*, 3304.
[121] L. E. Manring, W. R. Hertler, *Abstracts of Papers of the American Chemical Society* **1993**, *206*, 19.
[122] L. E. Manring, D. Y. Sogah, G. M. Cohen, *Macromolecules* **1989**, *22*, 4652.
[123] R. A. Hutchinson, "Free Radical Polymerization: Homogeneous", in *Handbook of Polymer Reaction Engineering*, T. Meyer, Kuerentjes, J., Ed., Wiley-VCH Verlag GmbH & Co., Weinheim, 2005, p. 153.
[124] Y. Dan, Y. H. Yang, S. Y. Chen, *Journal Of Applied Polymer Science* **2002**, *85*, 2839.
[125] E. V. Thompson, *Journal of Polymer Science Part A-2: Polymer Physics* **1966**, *4*, 199.
[126] B. Jiang, J. Tsavalas, D. Sundberg, *Langmuir* **2010**, *26*, 9408.
[127] R. L. Holmes, R. P. Burford, C. D. Bertram, *Journal Of Applied Polymer Science* **2008**, *109*, 1814.

Appendix A

Supporting Information for Chapter 2; *"*A study of the free radical copolymerization kinetics of a bio-renewable monomer γ-methyl-α-methylene-γ-butyrolactone (MeMBL) with Butyl Acrylate, Methyl Metacrylate and Styrene"

N/A = not applicable, No SEC = sample was not able to be analyzed due to solubility constraints, Not Analyzed = sample was not analyzed by SEC where analysis was possible, No Data = data not recorded, No Result = sample analyzed by SEC but could not be processed. *Where M_2/M_1 is equal to zero, a second peak was not able to be resolved from SEC

Table A1. 22-90 °C MeMBL/ST PLP experimental conditions and results with [DMPA]=5 mmol·L^{-1}, with conversion less than 3%

Temp (°C)	Pulse Repetition Rate (Hz)	Monomer Mole Fraction MeMBL f_{MeMBL}	Polymer Mole Fraction MeMBL F_{MeMBL}	Density (g mL^{-1})	SEC Result						
					LS			RI			$k_{p\ cop,LS}$ / $k_{p\ cop,RI}$
					M_1 g mol^{-1}	M_2/M_1	$k_{p,cop}$ from M_1 (L·mol^{-1}·s^{-1})	M_1 $g$mol^{-1}	M_2/M_1	$k_{p,cop}$ from M_1 (L·mol^{-1}·s^{-1})	
22	33	0	-	0.905	3005	1.64	110	2203	2.13	80	1.36
					2386	1.89	87	2228	2.12	81	1.07
22	33	0.1	0.22	0.929	3513	1.61	125	3534	1.74	126	0.99
					3517	1.59	125	3554	1.73	126	0.99
22	33	0.2	0.34	0.955	4366	1.54	151	4291	1.74	148	1.02
					4377	1.55	151	4290	1.75	148	1.02
22	33	0.3	0.43	0.981	5129	1.56	173	5097	1.74	172	1.01
					4854	1.64	163	5114	1.73	172	0.95
22	33	0.4	0.48	1.008	5914	1.70	194	6006	1.78	197	0.99
					5699	1.70	187	6074	1.76	199	0.94
22	33	0.5	0.56	1.037	7782	1.69	248	6866	1.92	219	1.13
					6717	1.83	214	6901	1.93	220	0.97
22	33	0.6	0.64	1.066	7746	1.85	240	7736	1.96	240	1.00
					7932	1.84	246	7725	1.97	239	1.03
22	33	0.7	0.69	1.097	8295	1.91	250	8559	1.97	258	0.97
					8576	1.89	258	8636	1.96	260	0.99
22	33	0.8	0.82	1.129	9727	1.87	284	9320	1.95	273	1.04
					9434	1.92	276	9277	1.94	271	1.02
22	33	0.9	0.88	1.162	No SEC	No SEC	No SEC	No SEC	No SEC	No SEC	N/A
					No SEC	No SEC	No SEC	No SEC	No SEC	No SEC	N/A

Table A1 (cont'd). 22-90 °C MeMBL/ST PLP experimental conditions and results with [DMPA]=5mmol·L^{-1}, with conversion less than 3%

Temp (°C)	Pulse Repetition Rate (Hz)	Monomer Mole Fraction MeMBL f_{MeMBL}	Polymer Mole Fraction MeMBL F_{MeMBL}	Density (g mL^{-1})	SEC Result						
					LS			RI			$k_{p\ cop,LS}$ / $k_{p\ cop,RI}$
					M_1 g mol^{-1}	M_2/M_1	$k_{p,cop}$ from M_1 (L·mol^{-1}·s^{-1})	M_1 $g$mol^{-1}	M_2/M_1	$k_{p,cop}$ from M_1 (L·mol^{-1}·s^{-1})	
50	33	0	-	0.886	6866	1.86	256	6762	2.03	252	1.01
					7725	1.80	288	6762	2.03	252	1.14
50	33	0.1	0.21	0.910	8972	1.87	325	8603	2.03	252	1.04
					8766	1.90	318	8603	2.03	252	1.02
50	33	0.2	0.32	0.934	10423	1.87	368	10507	2.01	312	1.00
					10615	1.86	375	10507	1.98	312	1.01
50	33	0.3	0.42	0.959	13653	1.75	470	12852	1.90	370	1.07
					12383	1.85	426	12684	1.90	370	0.98
50	33	0.4	0.51	0.986	15579	1.77	521	15290	1.82	439	1.03
					15089	1.83	505	15290	1.80	433	1.00
50	33	0.5	0.58	1.013	17391	1.79	567	17235	1.80	507	1.02
					18068	1.76	587	17235	1.80	507	1.06
50	33	0.6	0.65	1.041	19981	1.80	633	19303	1.79	555	1.05
50	33	0.7	0.73	1.071	21586	1.81	665	21080	1.78	555	1.04
50	33	0.8	0.81	1.102	24030	1.84	720	22218	1.75	603	1.10
50	33	0.9	0.90	1.134	No SEC	No SEC	No SEC	No SEC	No SEC	No SEC	N/A
					No SEC	No SEC	No SEC	No SEC	No SEC	No SEC	N/A

Table A1 (cont'd). 22-90 °C MeMBL/ST PLP experimental conditions and results with [DMPA]=5mmol·L^{-1}, with conversion less than 3%

Temp (°C)	Pulse Repetition Rate (Hz)	Monomer Mole Fraction MeMBL f_{MeMBL}	Polymer Mole Fraction MeMBL F_{MeMBL}	Density (g mL^{-1})	SEC Result						
					LS			RI			$k_{p\,cop,LS}$ / $k_{p\,cop,RI}$
					M_1 g mol^{-1}	M_2/M_1	$k_{p,cop}$ from M_1 (L·mol^{-1}·s^{-1})	M_1 $g$mol^{-1}	M_2/M_1	$k_{p,cop}$ from M_1 (L·mol^{-1}·s^{-1})	
70	33	0	-	0.873	12067	1.92	456	12457	1.87	471	0.97
					12020	1.90	455	12323	1.86	466	0.97
70	33	0.1	0.22	0.896	14585	1.87	537	15492	1.85	571	0.94
					14747	1.69	543	15492	1.88	571	0.95
70	33	0.2	0.33	0.920	17527	1.92	629	19200	1.82	689	0.91
					17406	1.92	625	18923	1.85	679	0.92
70	33	0.3	0.43	0.945	20597	1.95	720	21928	1.85	766	0.94
					20807	1.91	727	21928	1.85	766	0.95
70	33	0.4	No Data	0.971	24350	1.93	828	25410	1.85	864	0.96
					24194	1.94	823	25078	1.85	853	0.96
70	33	0.5	0.58	0.997	27823	1.93	921	28268	1.83	935	0.98
					27855	1.95	922	27900	1.83	923	1.00
70	33	0.6	0.66	1.026	31031	1.97	999	30627	1.83	986	1.01
					30584	1.97	984	30634	1.83	986	1.00
70	33	0.7	0.71	1.055	34850	1.96	1090	32757	1.83	1025	1.06
					34166	1.97	1069	32757	1.80	1025	1.04
70	33	0.8	0.81	1.085	36923	2.00	1123	33791	1.15	1028	1.09
					37368	2.00	1136	34127	1.75	1038	1.10
70	33	0.9	0.89	1.117	No SEC	No SEC	No SEC	No SEC	No SEC	No SEC	N/A
					No SEC	No SEC	No SEC	No SEC	No SEC	No SEC	N/A

Table A1 (cont'd). 22-90 °C MeMBL/ST PLP experimental conditions and results with [DMPA]=5mmol·L^{-1}, with conversion less than 3%

Temp (°C)	Pulse Repetition Rate (Hz)	Monomer Mole Fraction MeMBL f_{MeMBL}	Polymer Mole Fraction MeMBL F_{MeMBL}	Density (g mL^{-1})	SEC Result						
					LS			RI			$k_{p\,cop,LS}$ / $k_{p\,cop,RI}$
					M_1 g mol^{-1}	M_2/M_1	$k_{p,cop}$ from M_1 (L·mol^{-1}·s^{-1})	M_1 $g$mol^{-1}	M_2/M_1	$k_{p,cop}$ from M_1 (L·mol^{-1}·s^{-1})	
90	33	0	-	0.860	22269	1.87	855	21164	1.87	813	1.052
					21647	1.89	831	20644	1.88	793	1.049
90	33	0.1	0.22	0.882	30248	1.76	1131	25476	1.89	953	1.187
					25248	1.91	944	25225	1.88	944	1.001
90	33	0.2	0.34	0.906	30123	1.98	1097	30931	1.90	1127	0.974
					29607	2.00	1078	30988	1.91	1129	0.955
90	33	0.3	0.43	0.931	35746	2.06	1267	35681	1.95	1265	1.002
					34437	2.05	1221	35705	1.95	1266	0.964
90	33	0.4	0.50	0.957	40577	2.09	1400	40298	1.98	1390	1.007
					40076	2.09	1383	39745	1.96	1371	1.008
90	33	0.5	0.58	0.983	45310	2.13	1521	43581	1.97	1463	1.040
					45614	2.13	1531	43461	1.97	1459	1.050
90	33	0.6	0.64	1.011	50214	2.12	1639	46380	1.95	1514	1.083
					47318	2.19	1544	46337	1.96	1512	1.021
90	33	0.7	0.72	1.040	52713	2.13	1672	47788	1.94	1516	1.103
					55798	2.11	1770	48230	1.93	1530	1.157
90	33	0.8	0.80	1.071	55671	2.16	1716	49400	1.93	1523	1.127
					56523	2.12	1742	49823	1.92	1536	1.134
90	33	0.9	0.89	1.102	No SEC	No SEC	No SEC	No SEC	No SEC	No SEC	N/A
					No SEC	No SEC	No SEC	No SEC	No SEC	No SEC	N/A

Table A1 (cont'd). 22-90 °C MeMBL/ST PLP experimental conditions and results with [DMPA]=5mmol·L^{-1}, with conversion less than 3%

Temp (°C)	Pulse Repetition Rate (Hz)	Monomer Mole Fraction MeMBL f_{MeMBL}	Polymer Mole Fraction MeMBL F_{MeMBL}	Density (g mL^{-1})	SEC Result						
					LS			RI			$k_{p\ cop,LS}$ / $k_{p\ cop,RI}$
					M_1 g mol^{-1}	M_2/M_1	$k_{p,cop}$ from M_1 (L·mol^{-1}·s^{-1})	M_1 $g$mol^{-1}	M_2/M_1	$k_{p,cop}$ from M_1 (L·mol^{-1}·s^{-1})	
90	50	0	-	0.860	14914	1.91	868	15396	1.92	896	0.97
					14993	1.85	872	15090	1.90	878	0.99
90	50	0.1	0.23	0.882	18893	1.89	1071	19449	1.95	1102	0.97
					18711	1.90	1060	19399	1.94	1099	0.96
90	50	0.2	0.32	0.906	20678	1.97	1141	22851	1.93	1261	0.90
					20483	1.97	1130	22740	1.93	1255	0.90
90	50	0.3	0.41	0.931	24820	1.99	1333	26571	1.93	1427	0.93
					27334	1.89	1468	26479	1.93	1422	1.03
90	50	0.4	0.51	0.957	27644	2.04	1445	30019	1.91	1569	0.92
					27511	2.04	1438	29526	1.92	1543	0.93
90	50	0.5	0.59	0.983	32203	2.05	1638	32181	1.92	1637	1.00
					31081	2.08	1581	31705	1.91	1612	0.98
90	50	0.6	No Data	1.011	34770	2.09	1719	34802	1.90	1721	1.00
					35156	2.07	1739	34762	1.91	1719	1.01
90	50	0.7	No Data	1.040	38397	2.08	1846	36283	1.91	1744	1.06
					37888	2.09	1821	36116	1.89	1736	1.05
90	50	0.8	0.87	1.071	38098	2.16	1779	36966	1.85	1727	1.03
					39774	2.14	1858	37592	1.87	1756	1.06
90	50	0.9	0.92	1.102	No SEC	No SEC	No SEC	No SEC	No SEC	No SEC	N/A
					No SEC	No SEC	No SEC	No SEC	No SEC	No SEC	N/A

Table A2A. 22-90°C MeMBL/MMA PLP experimental conditions and results with [DMPA]=5mmol·L^{-1} for conversions less than 3% in THF

Temp (°C)	Pulse Repetition Rate (Hz)	Monomer Mole Fraction MeMBL f_{MeMBL}	Polymer Mole Fraction MeMBL F_{MeMBL}	Density (g mL^{1})	SEC Result						
					LS			RI			$k_{p\ cop,LS}$ / $k_{p\ cop,RI}$
					M_1 g mol^{-1}	M_2/M_1	$k_{p,cop}$ from M_1 (L·mol^{-1}·s^{-1})	M_1 $g$mol^{-1}	M_2/M_1	$k_{p,cop}$ from M_1 (L·mol^{-1}·s^{-1})	
22	33	0	-	0.931	9319	1.71	330.3	8540	1.98	303	1.09
					8560	1.77	303.4	8514	0.00	302	1.01
22	33	0.1	0.29	0.955	7389	1.84	255.4	7850	2.04	271	0.94
					6589	1.92	227.7	7850	2.04	271	0.84
22	33	0.2	0.41	0.979	6851	1.92	230.8	8002	2.04	270	0.86
					7958	1.77	268.1	8002	2.01	270	0.99
22	33	0.3	0.57	1.004	6935	2.02	228.0	7845	2.00	258	0.88
					8051	1.81	264.7	7874	2.00	259	1.02
22	33	0.4	0.68	1.029	No Result	No Result	No Result	7978	2.02	256	n/d
					9357	1.81	300.0	8072	1.99	259	1.16
22	33	0.5	0.76	1.055	No Result	No Result	No Result	8219	2.00	257	N/A
					No Result	No Result	No Result	8923	2.00	279	N/A
22	33	0.6	0.82	1.082	No SEC	No SEC	No SEC	No SEC	No SEC	No SEC	N/A
					No SEC	No SEC	No SEC	No SEC	No SEC	No SEC	N/A
22	33	0.7	0.88	1.110	No SEC	No SEC	No SEC	No SEC	No SEC	No SEC	N/A
					No SEC	No SEC	No SEC	No SEC	No SEC	No SEC	N/A
22	33	0.8	0.92	1.138	No SEC	No SEC	No SEC	No SEC	No SEC	No SEC	N/A
					No SEC	No SEC	No SEC	No SEC	No SEC	No SEC	N/A
22	33	0.9	0.96	1.168	No SEC	No SEC	No SEC	No SEC	No SEC	No SEC	N/A
					No SEC	No SEC	No SEC	No SEC	No SEC	No SEC	N/A

Table A2A (cont'd). 22-90°C MeMBL/MMA PLP experimental conditions and results with [DMPA]=5mmol·L^{-1} for conversions less than 3% in THF

Temp (°C)	Pulse Repetition Rate (Hz)	Monomer Mole Fraction MeMBL f_{MeMBL}	Polymer Mole Fraction MeMBL F_{MeMBL}	Density (g mL^{1})	SEC Result						
					LS			RI			$k_{p\ cop,LS}$ / $k_{p\ cop,RI}$
					M_1 g mol^{-1}	M_2/M_1	$k_{p,cop}$ from M_1 (L·mol^{-1}·s^{-1})	M_1 $g$mol^{-1}	M_2/M_1	$k_{p,cop}$ from M_1 (L·mol^{-1}·s^{-1})	
50	20	0	-	0.902	30785	1.81	683	27730	1.91	615	1.11
					30949	1.98	686	28579	1.93	634	1.08
50	20	0.1	0.23	0.925	28834	1.91	623	27190	1.94	588	1.06
					29621	1.97	640	27303	1.94	590	1.08
50	20	0.2	0.43	0.950	30119	1.91	634	27902	1.90	587	1.08
50	20	0.3	0.57	0.974	30345	1.97	623	25055	1.86	514	1.21
50	20	0.4	0.66	0.999	32841	1.96	657	26732	1.82	535	1.22
					30833	2.00	617	26123	1.83	523	1.18
50	20	0.5	0.74	1.025	No SEC	No SEC	No SEC	No SEC	No SEC	No SEC	N/A
					No SEC	No SEC	No SEC	No SEC	No SEC	No SEC	N/A
50	20	0.6	0.80	1.052	No SEC	No SEC	No SEC	No SEC	No SEC	No SEC	N/A
					No SEC	No SEC	No SEC	No SEC	No SEC	No SEC	N/A
50	20	0.7	0.86	1.080	No SEC	No SEC	No SEC	No SEC	No SEC	No SEC	N/A
					No SEC	No SEC	No SEC	No SEC	No SEC	No SEC	N/A
50	20	0.8	0.91	1.108	No SEC	No SEC	No SEC	No SEC	No SEC	No SEC	N/A
					No SEC	No SEC	No SEC	No SEC	No SEC	No SEC	N/A
50	20	0.9	0.93	1.138	No SEC	No SEC	No SEC	No SEC	No SEC	No SEC	N/A
					No SEC	No SEC	No SEC	No SEC	No SEC	No SEC	N/A

Table A2A (cont'd). 22-90°C MeMBL/MMA PLP experimental conditions and results with [DMPA]=5mmol·L^{-1} for conversions less than 3% in THF

Temp (°C)	Pulse Repetition Rate (Hz)	Monomer Mole Fraction MeMBL f_{MeMBL}	Polymer Mole Fraction MeMBL F_{MeMBL}	Density (g mL^{1})	SEC Result						
					LS			RI			$k_{p\ cop,LS}$ / $k_{p\ cop,RI}$
					M_1 g mol^{-1}	M_2/M_1	$k_{p,cop}$ from M_1 (L·mol^{-1}·s^{-1})	M_1 $g$mol^{-1}	M_2/M_1	$k_{p,cop}$ from M_1 (L·mol^{-1}·s^{-1})	
50	33	0	-	0.902	15882	1.91	581	13256	1.77	670	0.87
					15992	1.92	585	16650	1.89	609	0.96
50	33	0.1	0.24	0.925	13677	1.93	488	17869	1.85	637	0.77
					13630	1.91	486	17519	1.87	625	0.78
50	33	0.2	0.46	0.950	14343	1.87	498	17960	1.84	624	0.80
					14573	1.88	506	17914	1.84	623	0.81
50	33	0.3	0.57	0.974	15606	1.87	529	18420	1.81	624	0.85
					15335	1.91	520	18599	1.82	630	0.82
50	33	0.4	0.66	0.999	15882	1.94	524	18845	1.79	622	0.84
					15777	1.90	521	18668	1.79	616	0.85
50	33	0.5	0.74	1.025	No SEC	No SEC	No SEC	No SEC	No SEC	No SEC	N/A
					No SEC	No SEC	No SEC	No SEC	No SEC	No SEC	N/A
50	33	0.6	0.82	1.052	No SEC	No SEC	No SEC	No SEC	No SEC	No SEC	N/A
					No SEC	No SEC	No SEC	No SEC	No SEC	No SEC	N/A
50	33	0.7	0.87	1.080	No SEC	No SEC	No SEC	No SEC	No SEC	No SEC	N/A
					No SEC	No SEC	No SEC	No SEC	No SEC	No SEC	N/A
50	33	0.8	0.92	1.108	No SEC	No SEC	No SEC	No SEC	No SEC	No SEC	N/A
					No SEC	No SEC	No SEC	No SEC	No SEC	No SEC	N/A
50	33	0.9	0.96	1.138	No SEC	No SEC	No SEC	No SEC	No SEC	No SEC	N/A
					No SEC	No SEC	No SEC	No SEC	No SEC	No SEC	N/A

Table A2A (cont'd). 22-90°C MeMBL/MMA PLP experimental conditions and results with [DMPA]=5mmol·L^{-1} for conversions less than 3% in THF

Temp (°C)	Pulse Repetition Rate (Hz)	Monomer Mole Fraction MeMBL f_{MeMBL}	Polymer Mole Fraction MeMBL F_{MeMBL}	Density (g mL^{1})	SEC Result						
					LS			RI			$k_{p\,cop,LS}$ / $k_{p\,cop,RI}$
					M_1 g mol^{-1}	M_2/M_1	$k_{p,cop}$ from M_1 (L·mol^{-1}·s^{-1})	M_1 $g$mol^{-1}	M_2/M_1	$k_{p,cop}$ from M_1 (L·mol^{-1}·s^{-1})	
70	33	0	-	0.884	27539	1.90	1028	26797	1.91	1001	1.03
					25977	1.99	970	26978	1.96	1008	0.96
70	33	0.1	0.24	0.907	23090	1.99	840	26882	1.92	978	0.86
					23219	1.98	845	27136	1.89	987	0.86
70	33	0.2	0.41	0.932	24142	1.99	855	27136	1.89	961	0.89
					24491	1.91	868	27136	1.89	961	0.90
70	33	0.3	0.55	0.956	26081	1.96	901	27397	1.84	946	0.95
					25574	2.04	883	27428	1.84	947	0.93
70	33	0.4	0.67	0.981	27510	2.02	925	27784	1.80	935	0.99
					26825	2.01	902	27447	1.84	923	0.98
70	33	0.5	0.75	1.007	29048	1.98	952	26773	1.79	877	1.08
					28879	1.96	946	27315	1.76	895	1.06
70	33	0.6	0.83	1.034	No SEC	No SEC	No SEC	No SEC	No SEC	No SEC	N/A
					No SEC	No SEC	No SEC	No SEC	No SEC	No SEC	N/A
70	33	0.7	0.88	1.062	No SEC	No SEC	No SEC	No SEC	No SEC	No SEC	N/A
					No SEC	No SEC	No SEC	No SEC	No SEC	No SEC	N/A
70	33	0.8	No Data	1.090	No SEC	No SEC	No SEC	No SEC	No SEC	No SEC	N/A
					No SEC	No SEC	No SEC	No SEC	No SEC	No SEC	N/A
70	33	0.9	0.96	1.120	No SEC	No SEC	No SEC	No SEC	No SEC	No SEC	N/A
					No SEC	No SEC	No SEC	No SEC	No SEC	No SEC	N/A

Table A2A (cont'd). 22-90°C MeMBL/MMA PLP experimental conditions and results with [DMPA]=5mmol·L^{-1} for conversions less than 3% in THF

Temp (°C)	Pulse Repetition Rate (Hz)	Monomer Mole Fraction MeMBL f_{MeMBL}	Polymer Mole Fraction MeMBL F_{MeMBL}	Density (g mL^{1})	SEC Result						
					LS			RI			$k_{p\ cop,LS}$ / $k_{p\ cop,RI}$
					M_1 g mol^{-1}	M_2/M_1	$k_{p,cop}$ from M_1 (L·mol^{-1}·s^{-1})	M_1 $g$mol^{-1}	M_2/M_1	$k_{p,cop}$ from M_1 (L·mol^{-1}·s^{-1})	
90	33	0	-	0.87	43324	2.18	1643	42841	2.05	1625	1.01
					45414	2.14	1723	42841	2.05	1625	1.06
90	33	0.1	0.27	0.89	43260	2.07	1604	43736	2.03	1622	0.99
					45328	1.77	1681	42766	2.08	1586	1.06
90	33	0.2	0.43	0.92	41662	2.11	1494	44606	2.00	1600	0.93
					45013	2.08	1615	44760	2.00	1606	1.01
90	33	0.3	0.54	0.94	49652	2.03	1743	44142	1.97	1550	1.12
					47035	2.08	1651	44142	1.98	1550	1.07
90	33	0.4	0.65	0.97	49635	2.08	1689	43615	1.91	1484	1.14
					48845	2.08	1662	42721	1.90	1453	1.14
90	33	0.5	0.76	0.99	No SEC	No SEC	No SEC	No SEC	No SEC	No SEC	N/A
					No SEC	No SEC	No SEC	No SEC	No SEC	No SEC	N/A
90	33	0.6	0.82	1.02	No SEC	No SEC	No SEC	No SEC	No SEC	No SEC	N/A
					No SEC	No SEC	No SEC	No SEC	No SEC	No SEC	N/A
90	33	0.7	0.88	1.05	No SEC	No SEC	No SEC	No SEC	No SEC	No SEC	N/A
					No SEC	No SEC	No SEC	No SEC	No SEC	No SEC	N/A
90	33	0.8	0.92	1.08	No SEC	No SEC	No SEC	No SEC	No SEC	No SEC	N/A
					No SEC	No SEC	No SEC	No SEC	No SEC	No SEC	N/A
90	33	0.9	0.96	1.11	No SEC	No SEC	No SEC	No SEC	No SEC	No SEC	N/A
					No SEC	No SEC	No SEC	No SEC	No SEC	No SEC	N/A

Table A2B - 22-90°C MeMBL/MMA PLP experimental conditions and results with [DMPA]=5mmol·L^{-1} for conversions less than 3% in DMAc

Temp (°C)	Pulse Repetition Rate (Hz)	Monomer Mole Fraction MeMBL f_{MeMBL}	Polymer Mole Fraction MeMBL F_{MeMBL}	Density (g mL^{1})	SEC Result						
					LS			RI			$k_{p\ cop,LS}$ / $k_{p\ cop,RI}$
					M_1 g mol^{-1}	M_2/M_1	$k_{p,cop}$ from M_1 (L·mol^{-1}·s^{-1})	M_1 $g$mol^{-1}	M_2/M_1	$k_{p,cop}$ from M_1 (L·mol^{-1}·s^{-1})	
50	20	0	-	0.902	No Data	No Data	No Data	26922	2.03	597	N/A
					No Data	No Data	No Data	27695	2.00	614	N/A
50	20	0.2	0.46	0.950	No Data	No Data	No Data	36450	2.01	602	N/A
					No Data	No Data	No Data	27720	2.13	584	N/A
50	20	0.4	0.66	0.999	No Data	No Data	No Data	31696	2.07	635	N/A
					No Data	No Data	No Data	29847	2.09	598	N/A
50	20	0.6	0.82	1.052	No Data	No Data	No Data	34538	2.05	657	N/A
					No Data	No Data	No Data	33551	2.09	638	N/A
50	20	0.8	0.92	1.108	No Data	No Data	No Data	37783	2.09	682	N/A

Table A2B (cont'd). 22-90°C MeMBL/MMA PLP experimental conditions and results with [DMPA]=5mmol·L^{-1} for conversions less than 3% in DMAc

Temp (°C)	Pulse Repetition Rate (Hz)	Monomer Mole Fraction MeMBL f_{MeMBL}	Polymer Mole Fraction MeMBL F_{MeMBL}	Density (g mL^{1})	SEC Result						
					LS			RI			$k_{p\ cop,LS}$ / $k_{p\ cop,RI}$
					M_1 g mol^{-1}	M_2/M_1	$k_{p,cop}$ from M_1 (L·mol^{-1}·s^{-1})	M_1 $g$mol^{-1}	M_2/M_1	$k_{p,cop}$ from M_1 (L·mol^{-1}·s^{-1})	
90	25	0	-	0.87	No Data	No Data	No Data	54450	2.14	1567	N/A
					No Data	No Data	No Data	55911	2.05	1609	N/A
90	25	0.1	0.27	0.89	No Data	No Data	No Data	57003	2.13	1598	N/A
90	25	0.2	0.43	0.92	No Data	No Data	No Data	60173	2.15	1642	N/A
90	25	0.3	0.54	0.94	No Data	No Data	No Data	62460	2.14	1661	N/A
90	25	0.4	0.65	0.97	No Data	No Data	No Data	67375	2.09	1744	N/A
90	25	0.5	0.76	0.99	No Data	No Data	No Data	71138	2.09	1793	N/A
90	25	0.6	0.82	1.02	No Data	No Data	No Data	73807	2.07	1811	N/A
90	25	0.7	0.88	1.05	No Data	No Data	No Data	77822	2.18	1858	N/A
90	25	0.8	0.92	1.08	No Data	No Data	No Data	80742	2.13	1878	N/A
90	25	0.9	0.96	1.11	No Data	No Data	No Data	85842	2.02	1942	N/A

Table A3A. 22-90°C MeMBL/BAA PLP experimental conditions and results with [DMPA]=5mmol·L^{-1} for conversions less than 3% in DMAc

Temp (°C)	Pulse Repetition Rate (Hz)	Monomer Mole Fraction MeMBL f_{MeMBL}	Polymer Mole Fraction MeMBL F_{MeMBL}	Density (g mL^{1})	SEC Result						
					LS			RI			$k_{p\ cop,LS}$ / $k_{p\ cop,RI}$
					M_1 g mol^{-1}	M_2/M_1	$k_{p,cop}$ from M_1 (L·mol^{-1}·s^{-1})	M_1 $g$mol^{-1}	M_2/M_1	$k_{p,cop}$ from M_1 (L·mol^{-1}·s^{-1})	
50	33	10	0.41	0.887	16811	0.00	625	15090	2.17	6501	0.82
					17167	0.00	639	20202	2.09	3192	1.32
50	33	20	0.66	0.909	13095	1.91	475	16077	1.92	561	1.11
					12700	2.01	461	16010	1.89	752	0.85
50	33	30	0.78	0.932	14256	1.86	505	15343	1.85	584	0.81
					13973	2.03	495	15424	1.85	581	0.79
50	33	40	0.85	0.958	13852	1.80	477	15553	1.83	543	0.93
					12159	1.83	419	15639	1.82	546	0.91
50	33	50	0.90	0.985	14269	1.92	478	16561	1.79	536	0.89
					13731	2.08	460	16684	1.78	539	0.78
50	33	60	0.93	1.015	20040	1.92	652	17374	1.76	555	0.86
					15816	1.99	514	16014	1.90	559	0.82
50	33	70	0.96	1.048	No SEC	No SEC	No SEC	No SEC	No SEC	No SEC	N/A
50	33	80	0.97	1.084	No SEC	No SEC	No SEC	No SEC	No SEC	No SEC	N/A
50	33	90	0.99	1.124	No SEC	No SEC	No SEC	No SEC	No SEC	No SEC	N/A

Table A3A(cont'd). 50-90°C MeMBL/BA PLP experimental conditions and results with [DMPA]=5mmol·L^{-1} for conversions less than 3% in DMAc

Temp (°C)	Pulse Repetition Rate (Hz)	Monomer Mole Fraction MeMBL f_{MeMBL}	Polymer Mole Fraction MeMBL F_{MeMBL}	Density (g mL^{1})	SEC Result						
					LS			RI			
					M_1 g mol^{-1}	M_2/M_1	$k_{p,cop}$ from M_1 (L·mol^{-1}·s^{-1})	M_1 $g$mol^{-1}	M_2/M_1	$k_{p,cop}$ from M_1 (L·mol^{-1}·s^{-1})	$k_{p\ cop,LS}$ / $k_{p\ cop,RI}$
50	50	0	No Data	0.867	137436	0.00	7926	17886	0.00	1031	7.68
					52420	0.00	3023	49136	0.00	2834	1.07
50	50	5	0.24	0.877	20114	6.13	1147	20170	0.00	1150	1.00
					26742	0.00	1525	18897	2.21	1077	1.42
50	50	10	0.41	0.887	9458	2.60	533	11003	2.62	620	0.86
					8584	2.82	484	11151	3.39	629	0.77
50	50	15	0.59	0.898	9270	2.68	516	9627	2.81	536	0.96
					8183	2.63	456	9598	2.71	534	0.85
50	50	20	0.69	0.909	10730	2.21	590	9432	2.31	519	1.14
					12434	2.21	684	9491	2.31	522	1.31
50	50	40	0.86	0.958	9911	2.16	517	9307	2.14	486	1.06
					10551	2.00	551	9221	2.17	481	1.14
50	50	60	0.93	1.015	11249	2.01	554	10332	2.01	509	1.09
50	50	70	0.95	1.048	No SEC	No SEC	No SEC	No SEC	No SEC	No SEC	N/A
50	50	80	0.97	1.084	No SEC	No SEC	No SEC	No SEC	No SEC	No SEC	N/A
50	50	90	0.98	1.124	No SEC	No SEC	No SEC	No SEC	No SEC	No SEC	N/A

Table A3A(cont'd). 50-90°C MeMBL/BA PLP experimental conditions and results with [DMPA]=5mmol·L^{-1} for conversions less than 3% in DMAc

Temp (°C)	Pulse Repetition Rate (Hz)	Monomer Mole Fraction MeMBL f_{MeMBL}	Polymer Mole Fraction MeMBL F_{MeMBL}	Density (g mL^{1})	SEC Result						
					LS			RI			$k_{p\ cop,LS}$ / $k_{p\ cop,RI}$
					M_1 g mol^{-1}	M_2/M_1	$k_{p,cop}$ from M_1 (L·mol^{-1}·s^{-1})	M_1 $g$mol^{-1}	M_2/M_1	$k_{p,cop}$ from M_1 (L·mol^{-1}·s^{-1})	
70	50	5	0.35	0.855	24434	0.00	1428.91	31557	0.00	1845	0.77
70	50	15	0.54	0.876	23807	0.00	1358.83	18294	2.11	1044	1.30
					21038	0.00	1200.79	18306	2.16	1045	1.15
70	50	20	0.62	0.887	20314	1.89	1145.11	17179	2.07	968	1.18
					18088	1.96	1019.64	17274	2.06	973	1.05
70	50	40	0.82	0.936	16815	1.92	898.24	16550	1.87	884	1.02
					17159	1.89	916.63	16619	1.86	885	1.03
70	50	60	0.93	0.995	17754	1.93	892.17	17223	1.91	865	1.03
70	33	70	0.94	1.028	No SEC	No SEC	No SEC	No SEC	No SEC	No SEC	N/A
70	33	80	0.95	1.065	No SEC	No SEC	No SEC	No SEC	No SEC	No SEC	N/A
70	33	90	0.99	1.105	No SEC	No SEC	No SEC	No SEC	No SEC	No SEC	N/A

Table A3A(cont'd). 50-90°C MeMBL/BA PLP experimental conditions and results with [DMPA]=5mmol·L^{-1} for conversions less than 3% in DMAc

Temp (°C)	Pulse Repetition Rate (Hz)	Monomer Mole Fraction MeMBL f_{MeMBL}	Polymer Mole Fraction MeMBL F_{MeMBL}	Density (g mL^{1})	SEC Result						
					LS			RI			$k_{p\ cop,LS}$ / $k_{p\ cop,RI}$
					M_1 g mol^{-1}	M_2/M_1	$k_{p,cop}$ from M_1 (L·mol^{-1}·s^{-1})	M_1 $g$mol^{-1}	M_2/M_1	$k_{p,cop}$ from M_1 (L·mol^{-1}·s^{-1})	
90	50	10	0.38	0.823	139380	0.00	8468	17885	0.00	1087	7.79
					111071	0.00	6748	49136	0.00	2985	2.26
90	50	20	0.63	0.843	27372	0.00	1623	31543	2.51	1871	0.87
					27397	0.00	1625	32285	0.00	1915	0.85
90	50	30	0.78	0.865	21822	2.07	1261	25270	2.16	1461	0.86
					21130	2.14	1221	25200	2.14	1457	0.84
90	50	40	0.84	0.889	22756	2.30	1280	24283	2.01	1366	0.94
					22751	2.18	1280	23394	2.04	1316	0.97
90	50	50	No Data	0.916	23807	2.16	1300	24986	1.96	1364	0.95
					23697	2.18	1294	25021	1.66	1366	0.95
90	50	60	0.90	0.975	28563	2.12	1465	25942	1.84	1330	1.10
					27127	2.32	1391	25954	1.84	1331	1.05
90	50	70	0.96	1.009	No SEC	No SEC	No SEC	No SEC	No SEC	No SEC	N/A
90	50	80	0.98	1.047	No SEC	No SEC	No SEC	No SEC	No SEC	No SEC	N/A
90	50	90	0.99	1.089	No SEC	No SEC	No SEC	No SEC	No SEC	No SEC	N/A

Table A3B. 50-90°C MeMBL/BA PLP experimental conditions and results with [DMPA]=5mmol·L^{-1} for conversions less than 3% in DMAc

Temp (°C)	Pulse Repetition Rate (Hz)	Monomer Mole Fraction MeMBL f_{MeMBL}	Polymer Mole Fraction MeMBL F_{MeMBL}	Density (g mL^{1})	SEC Result						
					LS			RI			$k_{p\ cop,LS}$ / $k_{p\ cop,RI}$
					M_1 g mol^{-1}	M_2/M_1	$k_{p,cop}$ from M_1 (L·mol^{-1}·s^{-1})	M_1 $g$mol^{-1}	M_2/M_1	$k_{p,cop}$ from M_1 (L·mol^{-1}·s^{-1})	
90	50	10	0.38	0.823	No Data	No Data	No Data	Not Analyzed	Not Analyzed	Not Analyzed	N/A
90	50	20	0.63	0.843	No Data	No Data	No Data	27403	2.45	1458	N/A
90	50	30	0.78	0.865	No Data	No Data	No Data	Not Analyzed	Not Analyzed	Not Analyzed	N/A
90	50	40	0.84	0.889	No Data	No Data	No Data	28615	2.49	1445	N/A
90	50	50	No Data	0.916	No Data	No Data	No Data	Not Analyzed	Not Analyzed	Not Analyzed	N/A
90	50	60	0.90	0.975	No Data	No Data	No Data	32779	2.19	1564	N/A
90	50	70	0.96	1.009	No Data	No Data	No Data	Not Analyzed	Not Analyzed	Not Analyzed	N/A
90	50	80	0.98	1.047	No Data	No Data	No Data	38833	2.15	1740	N/A
90	50	90	0.99	1.089	No Data	No Data	No Data	Not Analyzed	Not Analyzed	Not Analyzed	N/A

Table A3B(cont'd). 50-90°C MeMBL/BA PLP experimental conditions and results with [DMPA]=5mmol·L^{-1} for conversions less than 3% in DMAc

Temp (°C)	Pulse Repetition Rate (Hz)	Monomer Mole Fraction MeMBL f_{MeMBL}	Polymer Mole Fraction MeMBL F_{MeMBL}	Density (g mL^{1})	SEC Result						
					LS			RI			$k_{p\ cop,LS}$ / $k_{p\ cop,RI}$
					M_1 g mol^{-1}	M_2/M_1	$k_{p,cop}$ from M_1 (L·mol^{-1}·s^{-1})	M_1 $g$mol^{-1}	M_2/M_1	$k_{p,cop}$ from M_1 (L·mol^{-1}·s^{-1})	
50	33	10	0.41	0.887	No Data	No Data	No Data	18937	2.33	681	N/A
50	33	20	0.66	0.909	No Data	No Data	No Data	Not Analyzed	Not Analyzed	Not Analyzed	N/A
50	33	30	0.78	0.932	No Data	No Data	No Data	14319	2.21	490	N/A
50	33	40	0.85	0.958	No Data	No Data	No Data	Not Analyzed	Not Analyzed	Not Analyzed	N/A
50	33	50	0.90	0.985	No Data	No Data	No Data	17187	2.11	558	N/A
50	33	60	0.93	1.015	No Data	No Data	No Data	Not Analyzed	Not Analyzed	Not Analyzed	N/A
50	33	70	0.96	1.048	No Data	No Data	No Data	20342	2.03	622	N/A
50	33	80	0.97	1.084	No Data	No Data	No Data	Not Analyzed	Not Analyzed	Not Analyzed	N/A
50	33	90	0.99	1.124	No Data	No Data	No Data	24541	1.98	701	N/A

Table A4. 22-120°C MeMBL PLP experimental conditions and results with [DMPA]=5mmol·L^{-1} for conversions less than 3% in DMAc

Temp (°C)	Pulse Repetition Rate (Hz)	Monomer Mole Fraction MeMBL f_{MeMBL}	Polymer Mole Fraction MeMBL F_{MeMBL}	Density (g mL^{1})	SEC Result						
					LS			RI			$k_{p\ cop,LS}$ / $k_{p\ cop,RI}$
					M_1 g mol^{-1}	M_2/M_1	$k_{p,cop}$ from M_1 (L·mol^{-1}·s^{-1})	M_1 $g$mol^{-1}	M_2/M_1	$k_{p,cop}$ from M_1 (L·mol^{-1}·s^{-1})	
22	33	1	1	1.200	No Data	No Data	No Data	10802	1.94	297	N/A
50	33	1	1	1.170	No Data	No Data	No Data	25342	2.06	716	N/A
70	33	1	1	1.150	No Data	No Data	No Data	38815	2.05	1114	N/A
90	25	1	1	1.135	No Data	No Data	No Data	87720	2.10	1932	N/A
120	33	1	1	1.120	No Data	No Data	No Data	95258	2.17	2807	N/A

Appendix B

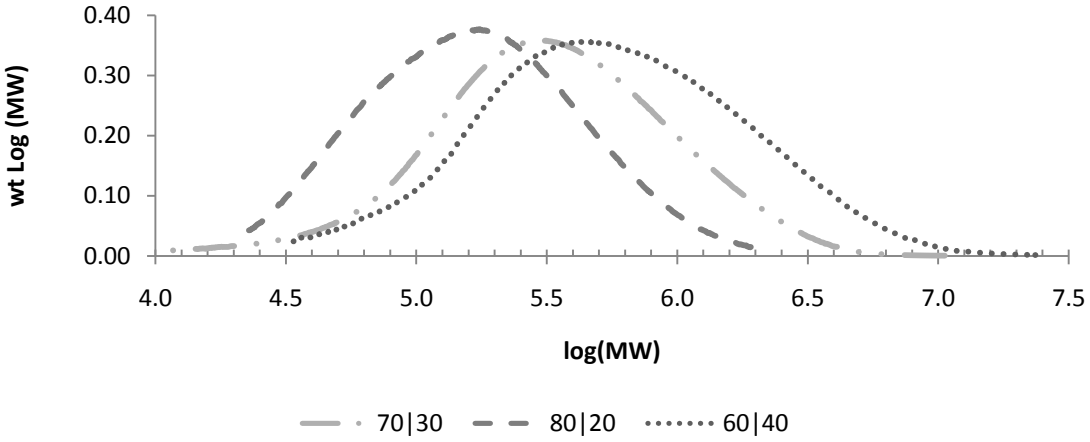

Figure B-1 – Molecular weight distribution of dispersion polymers from different continuous phases. See figure for legend.

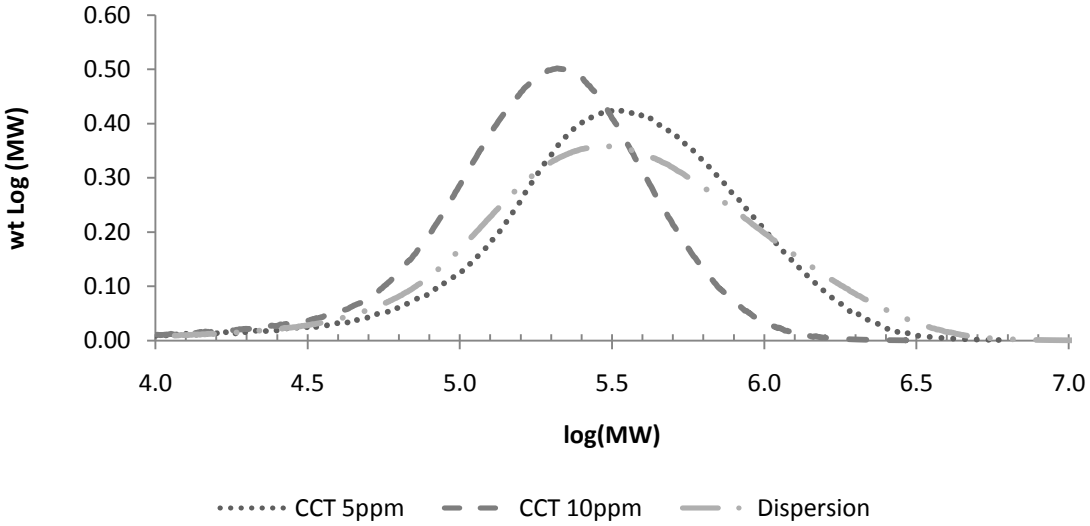

Figure B-2 – Molecular weight distribution of dispersion and CCT polymers. See figure for legend.

Note that no CCT data is presented in the following plots because only single experiments were conducted and thus no other experiments have been recorded to compare that data to.

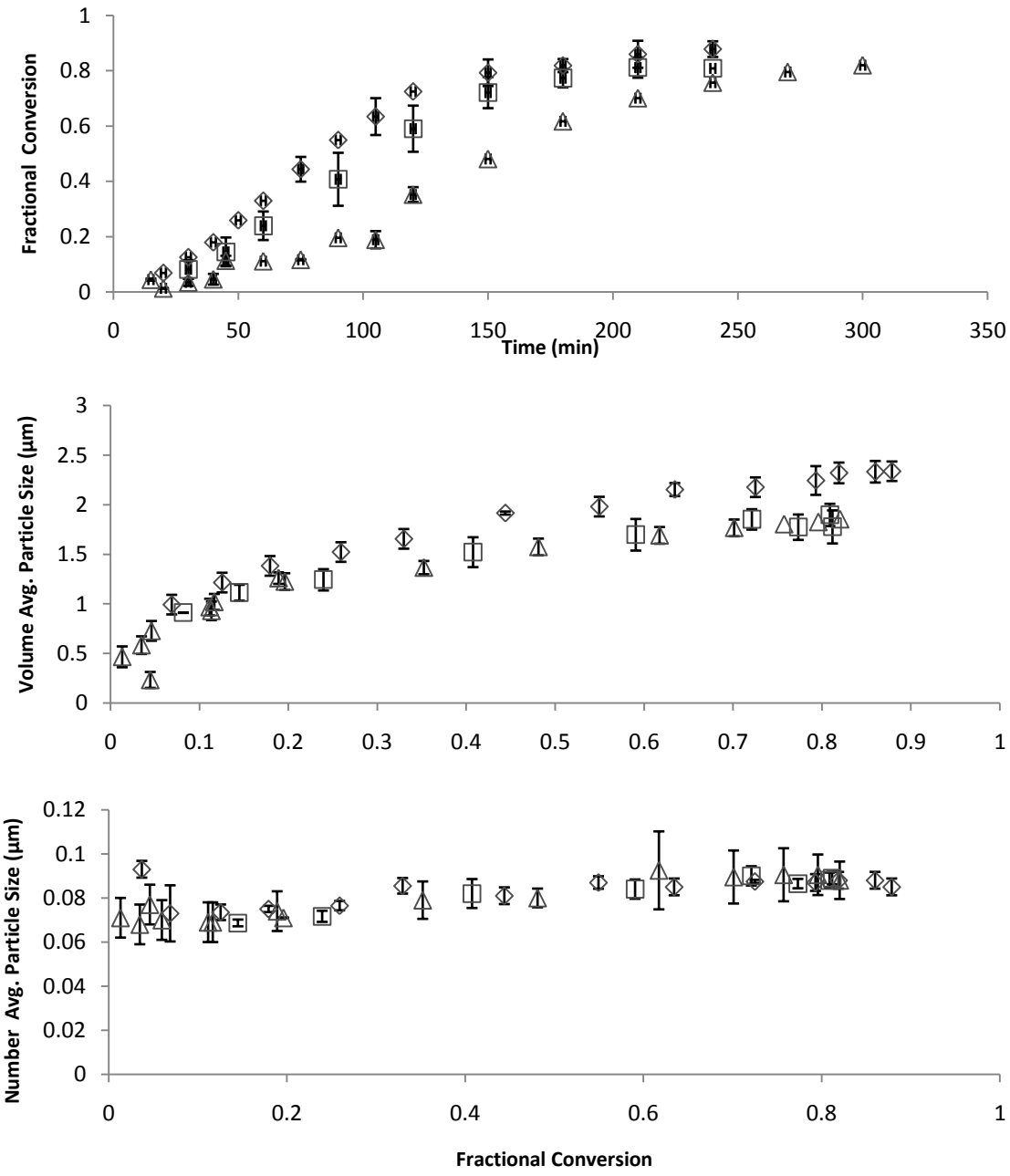

Figure B-3 – Conversion (top), volume-average large particle diameter (middle) and number-average small particle diameter (bottom) for dispersions in a 70|30 MeOH|Water continuous phase with 0.5%(Δ), 2%(□), and 4%(◊) initiator. Error bars represent ±1 standard deviation between measurements. If no error bar is shown replicate measurements were not available.

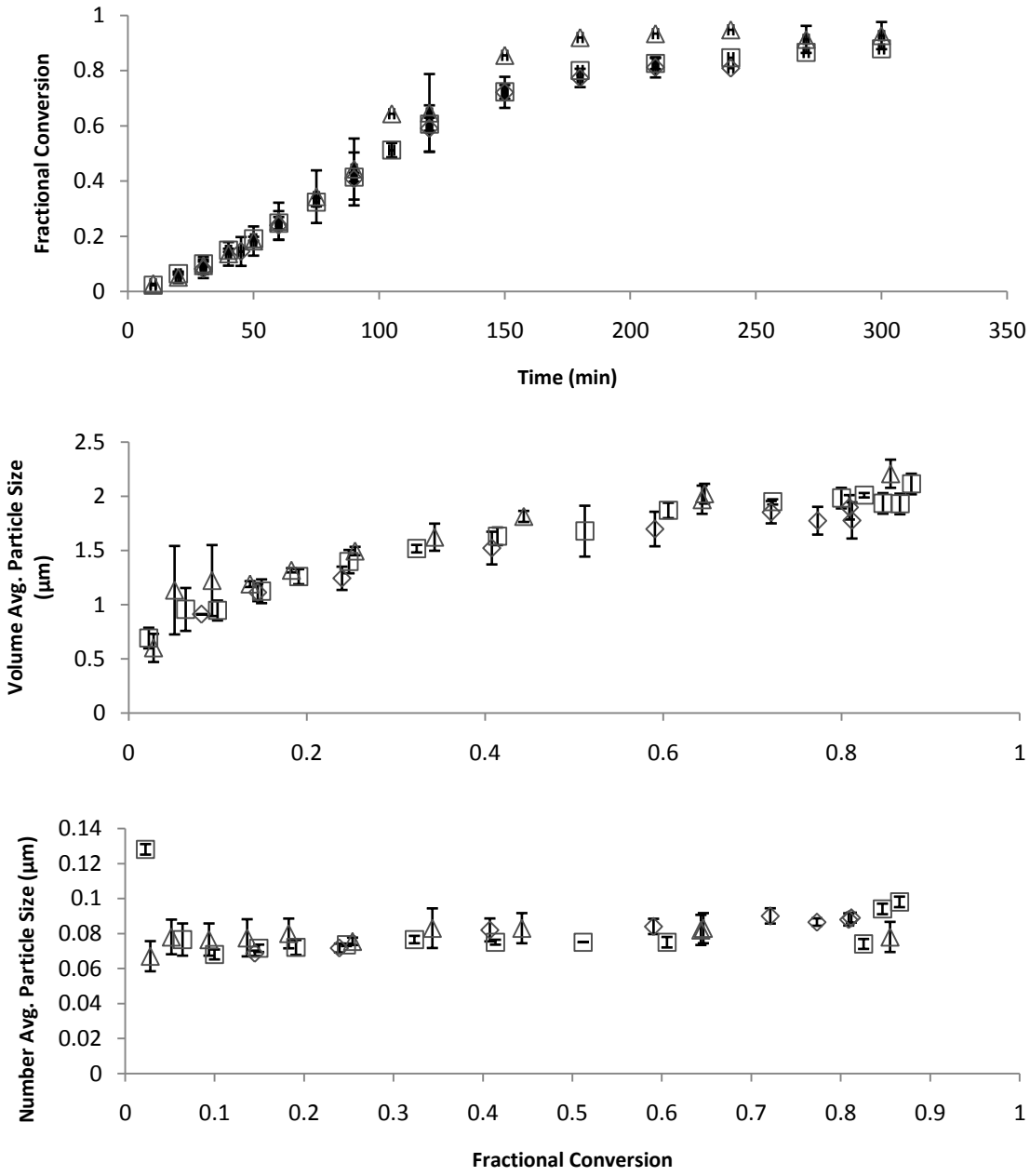

Figure B-4 – Conversion (top), volume-average large particle diameter (middle) and number-average small particle diameter (bottom) for dispersions in a 70|30 MeOH|Water continuous phase with 10%(Δ), 15%(◊) and 20%(□) surfactant. Error bars represent ±1 standard deviation between measurements. If no error bar is shown replicate measurements were not available.

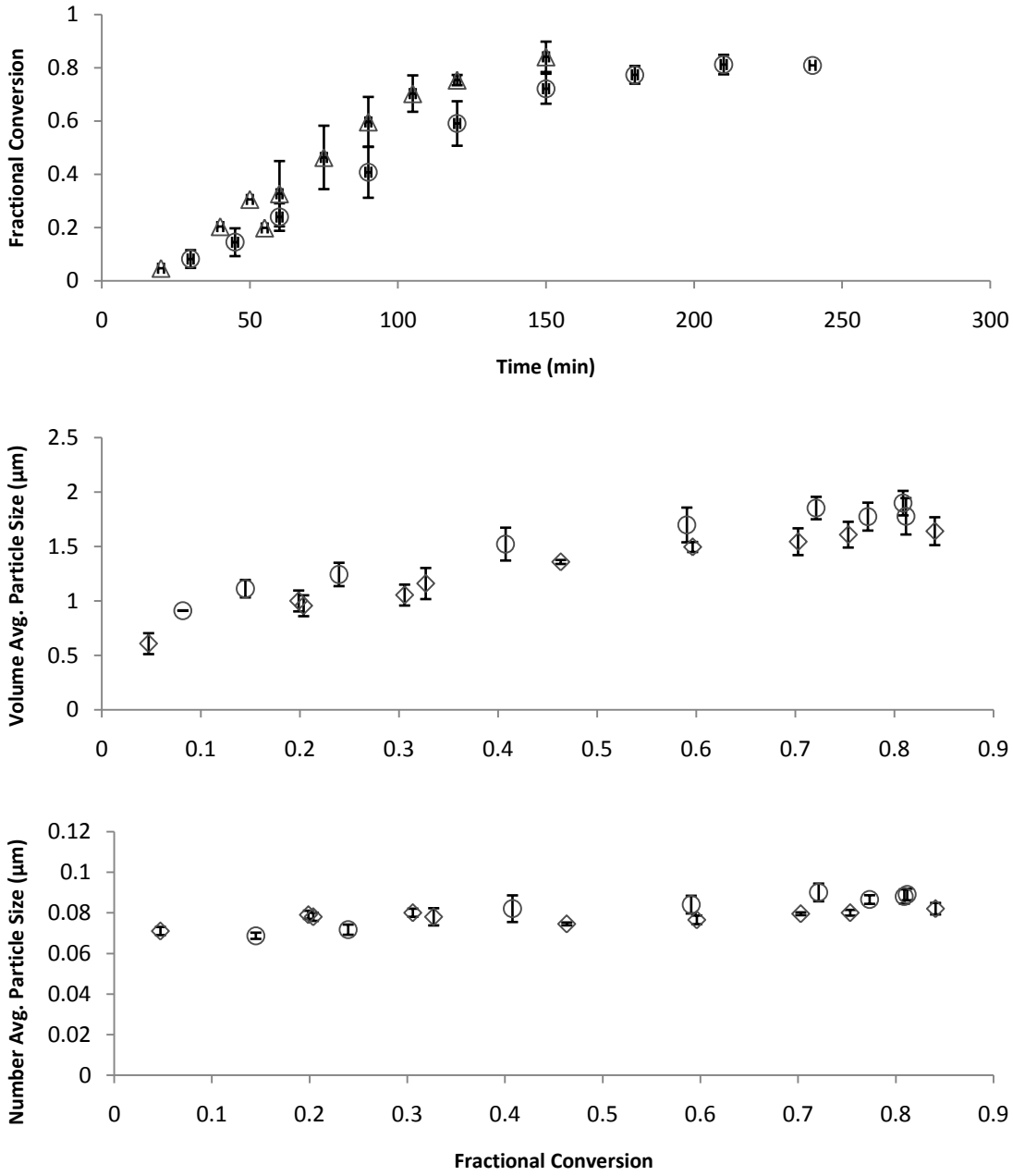

Figure B-5 – Conversion (top), volume-average large particle diameter (middle) and number-average small particle diameter (bottom) for dispersions in a 65|35 (◊) and 70|30(○) MeOH|Water continuous phase. Error bars represent ±1 standard deviation between measurements. If no error bar is shown replicate measurements were not available.

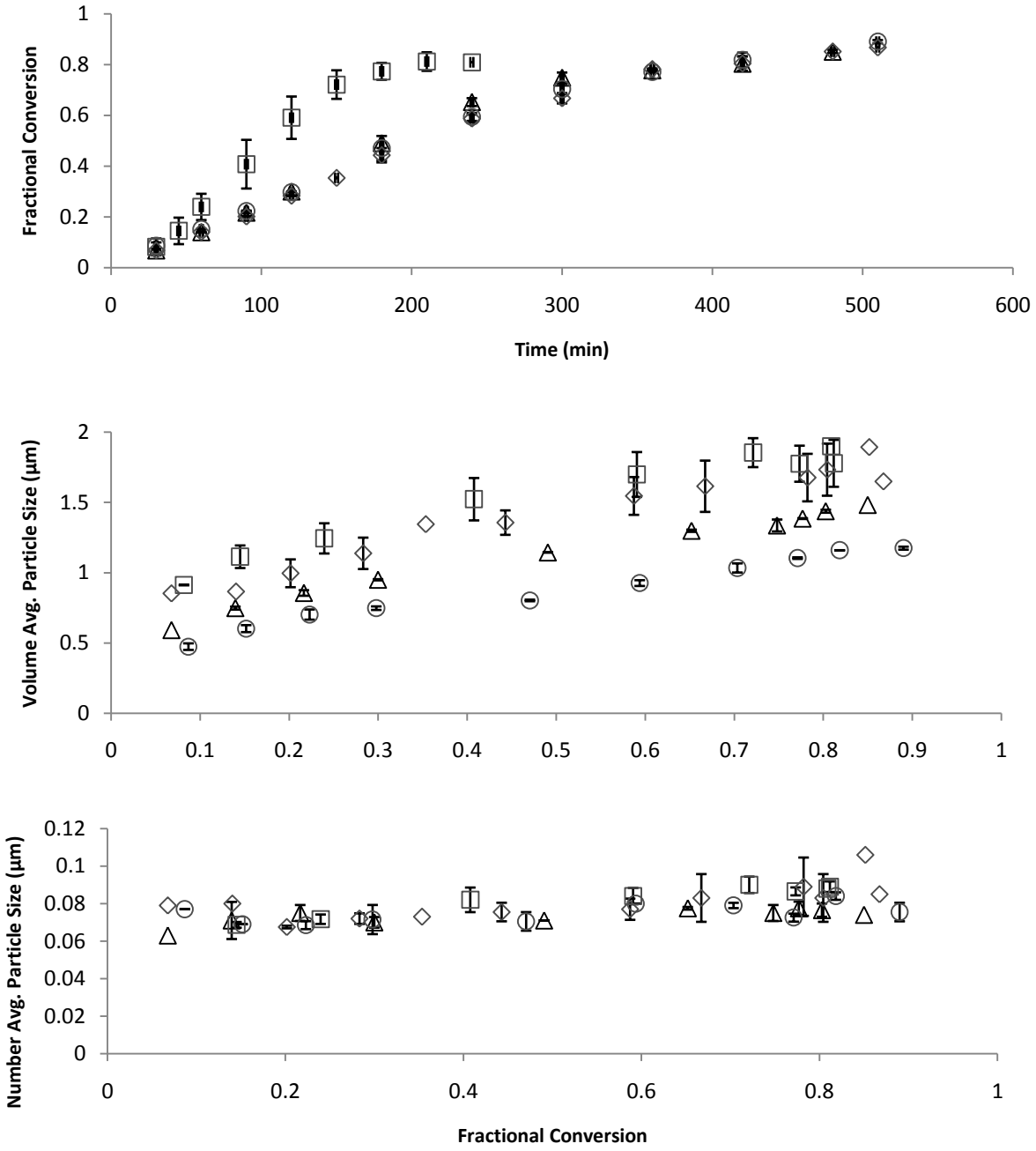

Figure B-6 – Conversion (top), volume-average large particle diameter (middle) and number-average small particle diameter (bottom) for dispersions in a 70|30 MeOH|Water continuous phase with 25%(◊), 50%(Δ), 75%(○) and 0%(□, MMA) MeMBL added. Error bars represent ±1 standard deviation between measurements. If no error bar is shown replicate measurements were not available.

Appendix C

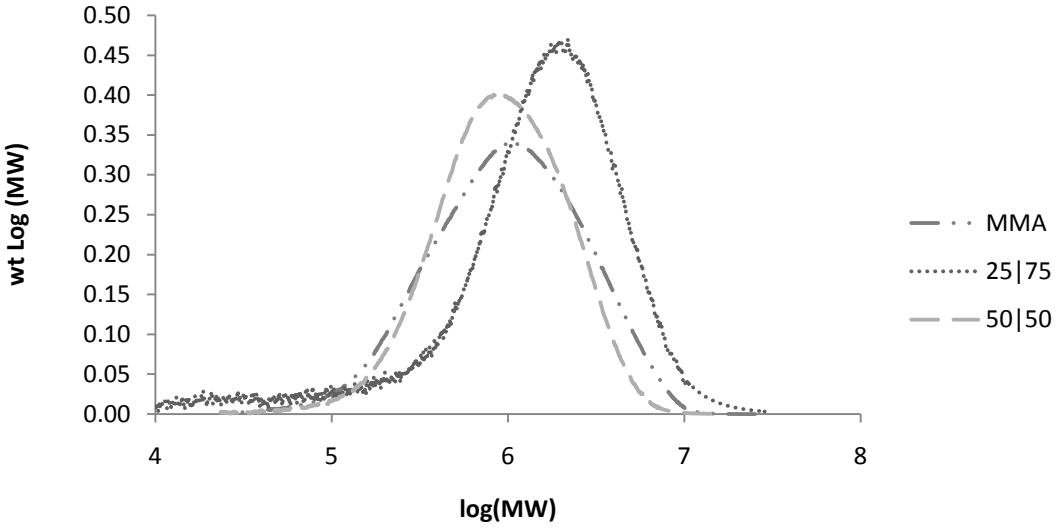

Figure C-1 – Molecular Weight distributions of MMA homopolymer and MeMBL/MMA copolymers produced by emulsion polymerization. See figure for legend.

Table C-1 - Molecular Weight and T_g data for MMA homopolymer and MeMBL/MMA copolymers produced by emulsion polymerization.

Sample	Mn	Mw	PDI	T_g (^oC)
MMA	310,000	2,040,000	6.58	118
25-75	560,000	1,460,000	2.61	124
50-50	577,000	1,177,000	2.04	146

Note that the 50|50 MeMBL|MMA emulsion copolymer was not fully soluble in THF and so the MW data may not be entirely representative of the actual polymer MW. The conversion time profile (Figure C-2) shows that the addition of MeMBL decreases the rate of polymerization and reduces the gel effect seen with MMA homopolymerization, also limiting final conversion. This suggests that the reaction temperature (again 60^oC, as was the case with the dispersion polymerizations) may affect the mobility and partitioning of the MeMBL monomer because it is so far removed from its T_g.

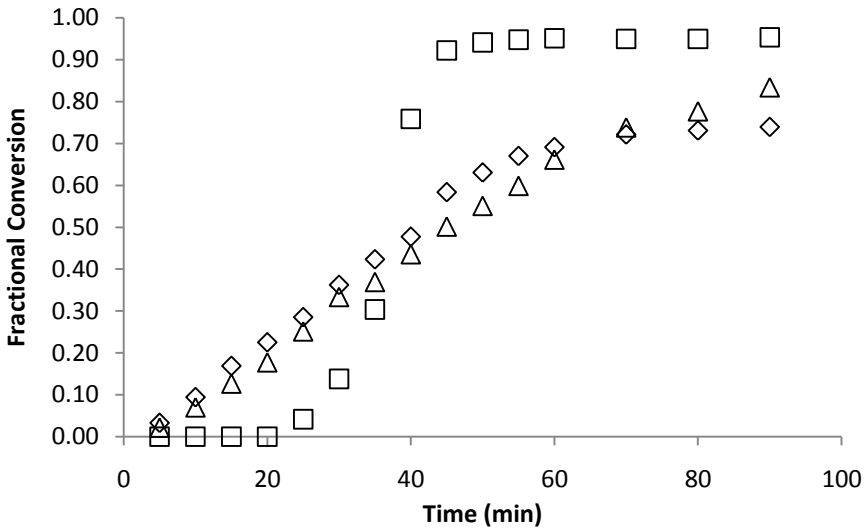

Figure C-2 – Conversion for emulsion polymerizations containing 25%(◊), 50%(Δ) and 0%(□, MMA) MeMBL added.